IDENTIFICATION OF PEPTIDE SEQUENCE TO BLOCK DENGUE VIRUS TRANSMISSION INTO CELLS VIA *In Silico* and *In Vitro* Assays

AATHE CANGAREE A/P ARUMUGAM

FACULTY OF SCIENCE
UNIVERSITI MALAYA
KUALA LUMPUR

2020

Universiti Malaya

IDENTIFICATION OF PEPTIDE SEQUENCE TO BLOCK DENGUE VIRUS TRANSMISSION INTO CELLS VIA *In Silico* and *In Vitro* Assays

AATHE CANGAREE A/P ARUMUGAM

DISSERTATION SUBMITTED IN FULFILMENT OF THE REQUIREMENTS FOR THE DEGREE OF MASTER OF SCIENCE

DEPARTMENT OF CHEMISTRY
FACULTY OF SCIENCE
UNIVERSITI MALAYA
KUALA LUMPUR

2020

Universiti Malaya

UNIVERSITI MALAYA

ORIGINAL LITERARY WORK DECLARATION

Name of Candidate: **AATHE CANGAREE A/P ARUMUGAM**

Matric No: **SMA180008**

Name of Degree: **MASTER OF SCIENCE**

Title of Dissertation ("this Work"):

IDENTIFICATION OF PEPTIDE SEQUENCE TO BLOCK DENGUE VIRUS TRANSMISSION INTO CELLS VIA *In Silico* and *In Vitro* Assays. Field of Study: **ORGANIC CHEMISTRY**

I do solemnly and sincerely declare that:

(1) I am the sole author/writer of this Work;
(2) This Work is original;
(3) Any use of any work in which copyright exists was done by way of fair dealing and for permitted purposes and any excerpt or extract from, or reference to or reproduction of any copyright work has been disclosed expressly and sufficiently and the title of the Work and its authorship have been acknowledged in this Work;
(4) I do not have any actual knowledge nor do I ought reasonably to know that the making of this work constitutes an infringement of any copyright work;
(5) I hereby assign all and every rights in the copyright to this Work to the University Malaya ("UM"), who henceforth shall be owner of the copyright in this Work and that any reproduction or use in any form or by any means whatsoever is prohibited without the written consent of UM having been first had and obtained;
(6) I am fully aware that if in the course of making this Work I have infringed any copyright whether intentionally or otherwise, I may be subject to legal action or any other action as may be determined by UM.

Candidate's Signature Date: 23 August 2021

Subscribed and solemnly declared before,

Witness's Signature Date: 23 Aug 2021

Name:

Designation:

University Malaya

IDENTIFICATION OF PEPTIDE SEQUENCE TO BLOCK DENGUE VIRUS TRANSMISSION INTO CELLS VIA *In Silico* and *In Vitro Assays*

ABSTRACT

Dengue virus (DV) infection has become main public wellbeing concerns, affecting approximately 390 million people worldwide. This fact was reported by the World Health Organization. Yet, there is no commercial antiviral treatment for DV infection. Therefore, the development of potent and non-toxic anti-DV, as a complement for the existing treatment strategies, are urgently needed. Herein, we investigate a series of low molecular weight peptides inhibitors by aiming the cellular entry process as the promising approach to block DV infection. The peptides were designed based on previously reported peptide sequence, DN58opt (TWWCFYFCRRHHPFWFFYRHN), to identify minimal effective inhibitory sequence via molecular docking and molecular dynamics simulation studies. The *in silico* designed peptides were synthesized using conventional FMOC solid-phase peptide synthesis chemistry, purified by RP-HPLC, and characterized using LCMS. Later, they were screened for their antiviral activity. One of the peptides, AC 001, showed the best inhibitory activity towards DV2 with inhibition percentage of 40.34% ± 5.9%. This observation correlates well with the molecular mechanics-Poisson–Boltzmann surface area (MM-PBSA) analysis – AC 001 showed the most favourable binding affinity (-33.51 ± 5.11 kcal/mol) through 60ns simulations. Trough pairwise residue decomposition analysis, it was found that the key residues involved in the binding were mainly, Glu13, Arg350, Leu351, and Ser16 for the protein and F3, Y4, Y5, and R7 for AC 001. Hence, this work identifies the minimal peptide sequence required to inhibit DV replication and explains the behaviour of AC 001 towards DV2.

Keywords: Dengue envelope inhibitors, antiviral peptides, molecular docking, molecular dynamics.

Universiti Malaya

PENGENALPASTIAN URUTAN PEPTIDA UNTUK MENGHALANG PENGHANTARAN VIRUS DENGGI KE DALAM SEL VIA *In* Silico dan *In Vitro*

ABSTRAK

Jangkitan virus denggi (DV) adalah salah satu masalah utama kesihatan awam, yang menjejaskan kira-kira 390 juta orang di seluruh dunia. Ianya dilaporkan oleh Pertubuhan Kesihatan Sedunia. Namun, tiada rawatan komersil antivirus untuk jangkitan DV. Oleh itu, pembangunan anti-DV yang kuat dan tidak toksik, sebagai pelengkap untuk strategi rawatan sedia ada, sangat diperlukan. Di sini, kami menyelidik pelbagai perencat peptida berat molekul rendah dengan menyasarkan proses kemasukan ke dalam sel sebagai strategi untuk menghalang jangkitan DV. Peptida-peptida tersebut direka berdasarkan jujukan peptida yang dilaporkan sebelum ini, DN58opt (TWWCFYFCRRHHPFWFFYRHN), untuk mengenal pasti urutan perencat minimum yang berkesan melalui kajian mengedok (*docking*) dan simulasi dinamik molekul. Peptida yang direka bentuk melalui *in silico,* disintesis menggunakan proses sintesis peptida fasa pepejal (SPPS) FMOC, penulenan oleh RP-HPLC dan dicirikan menggunakan LCMS. Kemudian, peptida tersebut diuji untuk kebolehan sebagai perencat DV (antivirus). Salah satu daripada peptida tersebut, AC 001, menunjukkan aktiviti perencatan terbaik terhadap DV2 dengan peratusan perencatan 40.34% ± 5.9%. Pemerhatian ini berkait rapat dengan simulasi analisis mekanik molekul-Kawasan Poisson-Boltzmann (MM-PBSA) di mana AC 001 menunjukkan afiniti daya tarik yang paling kuat (-33.51 ± 5.11 kcal/mol) melalui simulasi 60 ns. Analisis penguraian residu pasangan telah mendedahkan residu utama yang terlibat dalam pengikatan adalah terutamanya, Glu13, Arg350, Leu351, dan Ser16 untuk protein dan F3, Y4, Y5, dan R7 untuk AC 001. Oleh itu, karya ini mengenal pasti urutan peptida minimum yang diperlukan untuk menghalang replikasi DV dan menjelaskan tingkah laku AC 001 terhadap DV2.

Kata kunci: Inhibitor virus denggi, peptide antiviral, docking molekul, dinamik molekul**.**

Universiti Malaya

ACKNOWLEDGEMENTS

First, my sincere appreciation to my supervisors Professor Dr. Norsaadah Binti Abd Rahman and Dr. Abdullah Al-Hadi bin Ahmad Fuaad for giving me continuous support for my Master study and research. My supervisors have been very much supportive, patience and sincere in guiding me to complete my research project. They guided me a lot throughout my research and brought out the best in me.

Besides that, I also thank my parents who was encouraging me and gave moral and mental support to complete my research work. They have been tolerating my stress level throughout my studies. Also, to my siblings, cousins, relations and my close friend who has been there for me whenever I was mentally vulnerable. My sincere thanks to my laboratory manager, Dr. Lee Yean Kee for being supportive for my research. Sincere gratitude to my fellow lab mates, Dr. Chee Chin Fei, Tamilarasi Muniandy, Sudtha Moorthy, Thy Choon Keng, and Chan Pei Qie. We have been working together for about two years and shared many common things during the research period. They also encouraged me throughout my studies.

Additionally, my special appreciation to my laboratory Postdoctoral fellow, Dr. Fatima Ezzahra Agharbaoui who has been very helpful in completing my Master project. She guided me very well in Molecular Dynamics part for my research paper and project. Also, I would like to thank Dr. Ahmad Suhail bin Khazali who is a Postdoctoral fellow in Department of Molecular Medicine, Universiti Malaya. He guided me in biological part for my research work. My appreciation also extends to our Ministry of Education especially to MyBrainSc Scholarship who offered me scholarship for my graduate studies. Without a financial support for myself this work would not have been possible. Finally, my sincere gratitude to God Almighty for giving me mental strength, calmness and good health to complete this research.

Universiti Malaya

TABLE OF CONTENTS

Universiti Malaya

Universiti Malaya

Universiti Malaya

Universiti Malaya

LIST OF FIGURES

Universiti Malaya

Universiti Malaya

LIST OF TABLES

Universiti Malaya

LIST OF SCHEMES

Universiti Malaya

LIST OF SYMBOLS AND ABBREVIATIONS

E_{bdn}	:	Binding energy
E_{el}	:	Electrostatic interaction energy
S	:	Entropy
G_{np}	:	Non-polar contributions to the solvation free energies
G_{pol}	:	Polar contributions to the solvation free energies
T	:	Temperature
E_{vdW}	:	Van der Waals interactions between ligand and surrounding
ACN	:	Acetonitrile
Arg	:	Arginine
CO_2	:	Carbon dioxide
C	:	Capsid
Cys	:	Cysteine
2-CTC resin	:	2-Chlorotrityl chloride resin
DV2 E protein	:	Dengue virus serotype-2 envelope protein
DF	:	Dengue fever
DV	:	Dengue Virus
Et_2O	:	Diethyl ether
DMF	:	Dimethylformamide
DCM	:	Dichloromethane
DI	:	Domain I
DII	:	Domain II
DIII	:	Domain III

Universiti Malaya

DIPEA	:	Di-isopropylamine
DMEM	:	Dulbecco's Modified Eagle Medium
DBU	:	1,8-Diazabicyclo [5.4.0] undec-7-ene
E protein	:	Envelope protein
eq	:	Equivalent
FBS	:	Fetal bovine serum
Fmoc	:	Fluroenylmethyloxycarbonyl
His	:	Histidine
HPLC	:	High-performance liquid chromatography
LCMS	:	Liquid chromatography-mass spectrometry
µM	:	Micromolar
MeOH	:	Methanol
M protein	:	Membrane protein
Mtr	:	4-methoxy-2,3,6-trimethylbenzenesulfonyl
MEM	:	Modified Eagle's Medium
nM	:	Nanomolar
Phe	:	Phenylalanine
prM	:	Precursor membrane
Boc	:	tert-butyloxycarbonyl
tBu	:	Tert-butyl
Thr	:	Threonine
TIS	:	Triisopropylsilane
TFA	:	Trifluoroacetic acid
Trt	:	Triphenylmethyl

Universiti Malaya

Tyr	:	Tyrosine
Trp	:	Tryptophan
MTS	:	3-(4,5-Dimethylthiazol-2-yl)-5-(3-carboxymethoxyphenyl)-2-(4-sulfophenyl)-2H-tetrazolium
HCTU	:	O-(1H-6-Chloro-benzotriazole-1-yl)-1,1,3,3-tetramethyluronium hexafluorophosphate
H_2O	:	Water

Universiti Malaya

CHAPTER 1 INTRODUCTION

Dengue fever (DF) is caused by dengue virus (DV), is a re-emerging disease in the tropical and subtropical countries where the total amount of victims and geographical extension of the infection have been increasing in the past decade. DF infects approximately 390 million and threatening 3.9 billion people across the region (WHO, 2019). DF is typically debilitating but may progress to lethal dengue hemorrhagic fever (DHF) and dengue shock syndrome (DSS). Until today, there is no approved medication to treat dengue infection, and the only preventive measure, the Dengvaxia®, is limited to individuals with prior exposure (Fatima & Syed, 2018). Globally, the research groups have taken many challenges and different approaches to develop a molecule or inhibitor which can potentially inhibit DV infection by targeting several DV biological components. One attractive approach would be by blocking/inhibiting the viral entry into the target cell.

The DV entry into the host cell's cytoplasm is initiated by dengue envelope protein (E protein). Therefore, it is considered as a promising antiviral target due to its role in dengue replication cycle (*see* **Chapter 2**, sub heading **2.1.3**). Recently, significant efforts have been made to discover inhibitors for E protein of DV and other flaviviruses. Mainly there are two approaches have taken to develop E protein inhibitors. The first approach is through the development of small molecule inhibitors and the alternative is by using peptides as inhibitors (Noble, 2010). Small molecule inhibitors of DV E protein were recently reported (Prusis, 2013); which included anthracene (Tomlinson & Watowich, 2011), phthalazine-based compounds (Bodenreider et al., 2009) and bioflavonoids. More examples of small molecule inhibitors for DV E protein are discussed in Chapter 2 (*see* sub heading **2.2.1**).

The second approach to develop E protein inhibitors is via the use of peptides. Lately, the use of peptides as anti-DV is getting more consideration for their low toxicity, high

Universiti Malaya

specificity to bound target proteins and ease of modification (John et al., 2019). In 2001, Fairlie and his colleagues reported the first application of peptides substrates as inhibitors of NS3pro, one of DV proteases (Leung et al., 2001). Subsequently, a wide range of peptides was designed to target structural and non-structural proteins of DV. The details of peptide inhibitors for DV E protein are discussed in Chapter 2 (*see* sub heading **2.2.2**).

In this project, the optimum condition for peptide synthesis in high humid condition was established, peptides to block the virus-host interaction (entry process) as the strategy to stop the virus's infection/transmission were designed and thereafter a series of DV peptides inhibitors were synthesized. The aim of this project is to identify the effective inhibitory sequence by means of docking and molecular dynamics studies and thereafter connects the *in-silico* information to an *in vitro* experiment. The peptides were designed based on DN58opt (TWWCFYFCRRHHPFWFFYRHN) (Amir-Hassan et al., 2017; Xu et., 2012), a work done by Prof. Dr. Noorsaadah's team. The selected peptides were synthesized using conventional Fmoc-solid phase peptide synthesis chemistry, purified by HPLC, characterized using LCMS and were screened for their antiviral activity using Vero cell plaque formation assay.

1.1 Research objectives

The objectives of research work are shown as below.

1. To design linear peptides for DV E protein.
2. To optimize the solid phase peptide synthesis technique.
3. To synthesize the potential linear peptides.
4. To investigate the cytotoxicity level of the synthesized peptides towards Vero cells.
5. To conduct inhibitory studies of the synthesized peptides towards DV.
6. To validate the correlation between computational and experimental studies.

Universiti Malaya

CHAPTER 2 LITERATURE REVIEW

2.1 Dengue

Dengue is an enormous problem in both local and global. The dengue virus infection is reaching 390 million cases annually (WHO, 2019). Before the 1960s, the infection was regularly found in tropical belt of Asia, Latin America, and the Pacific. However, when the modern civilization started, post-World War 2, the disease has spread to across Africa, and has recently caused sudden occurrence in the USA and parts of the Europe (Katzelnick et al., 2017). The disease is caused by the DV which belongs to the genus *flavivirus* of family *Flaviviridae* (Chen et al., 1997). The DV carriers, infected *Aedes* mosquitoes, primarily *A. aegypti* and *A. albopictus,* are the contributing factor to spread the virus to humans which are distributed in both rural and urban areas in tropical and subtropical regions (Carolina De La Guardia & Ricardo Lleonart, 2014)

2.1.1 Symptoms

Patient infected with DV commonly develop an elevated fever of 39 ºC or more. After an infected *Aedes* mosquito bite, the incubation period of dengue fever would be four to seven days and can last from 3 to 14 days. Rapid breathing, blood vomit, organ impairment, severe headache and body rashes are the other symptoms of a severe DF (Lescar et al., 2008). The symptom may further progress to a more severe DHF which can be characterized by thrombocytopenia, petechiae hemorrhage and signs of plasma leakage. DHF may also lead to DSS, comatose and eventually death if not treated properly (Salazar et al., 2014). The mortality rate can be as high as 10-15% but, they are consistently below 1% in the countries by maintaining a good clinical management for dengue treatment (Ward et al., 2017).

Universiti Malaya

2.1.2 Dengue Virus

The DV has five distinct serotypes known as DV1, DV2, DV3, DV4 and DV5, of which DV5 was discovered in 2015 (Mustafa et al., 2015). The DV particle is a 50 nm in diameter and made up of a lipid bilayer surrounding a capsid-containing positive single-stranded, 11 kilobase RNA genome (Salazar et al., 2014). Upon infection, the RNA is released into the target cell and translated to a single polyprotein which comprised of three structural proteins; the capsid (C), the glycosylated envelope protein (E), the precursor membrane (prM) (Mondotte et al., 2007; Modis et al., 2003) and seven non-structural mature proteins; NS1, NS2A, NS2B, NS3, NS4A, NS4B and NS5 (Salazar et al., 2014). The structural proteins are responsible for host cell fusion and entry (Screaton et al., 2015) while the non-structural proteins are involved in viral replication, virion assemble and prevent the host immune response (Darwish et al., 2015). **Figure 2.1** shows the basic structure of DV while **Figure 2.2** represents the polyprotein of DV.

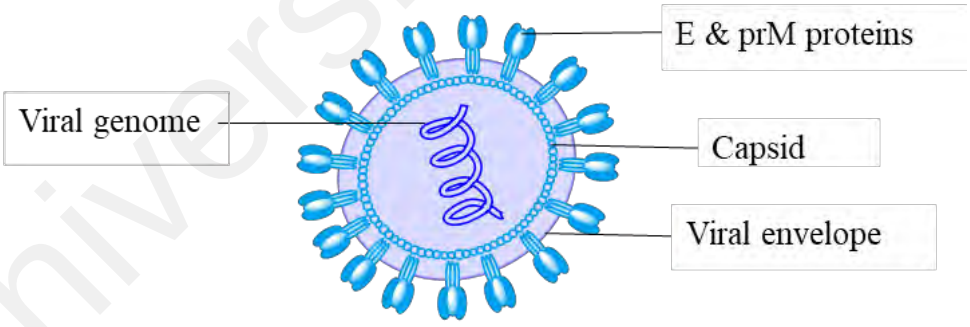

Figure 2.1: Dengue virus. It comprised of viral genome (RNA), capsid (C), envelope protein (E) and precursor membrane (prM).

Universiti Malaya

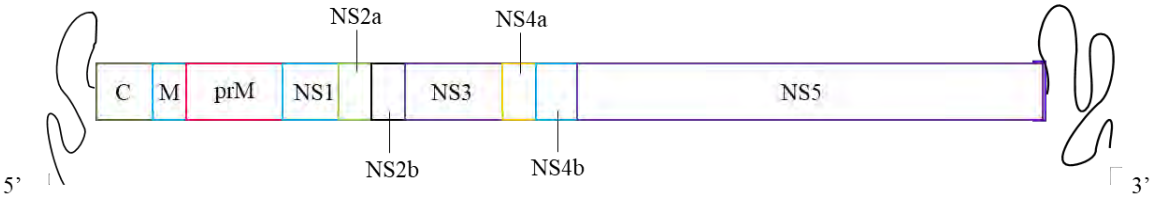

Figure 2.2: Genome and polyprotein of DV. This includes the structural proteins (Capsid, Envelope protein and Precursor membrane) and non-structural proteins (NS1, NS2a, NS2b, NS3, NS4a, NS4b and NS5).

2.1.3 Dengue life cycle and replication cycle in a host cell

DV life cycle (**Figure 2.3**) began from the mosquitoes of the genus *Aedes*, with *Aedes aegypti* serving as the primary vector. The transmission cycle of DV circulates between human and the *Aedes* mosquitoes. After a blood meal from a dengue infected person by a female wild type mosquito (uninfected mosquito), the DV subsequently infect the midgut epithelial cells of the mosquito and spread systemically through the hemocoel and finally reaches the salivary glands (Cheng at al., 2016; Valderrama et al., 2017). Later, the infected mosquito transmits the DV by biting a healthy person and therefore the virus will spread through the host body by undergoing replication cycle (**Figure 2.4**). The viral replication cycle comprised of 3 phases which includes cell entry, translation, and post translation (Screaton et al., 2015).

Universiti Malaya

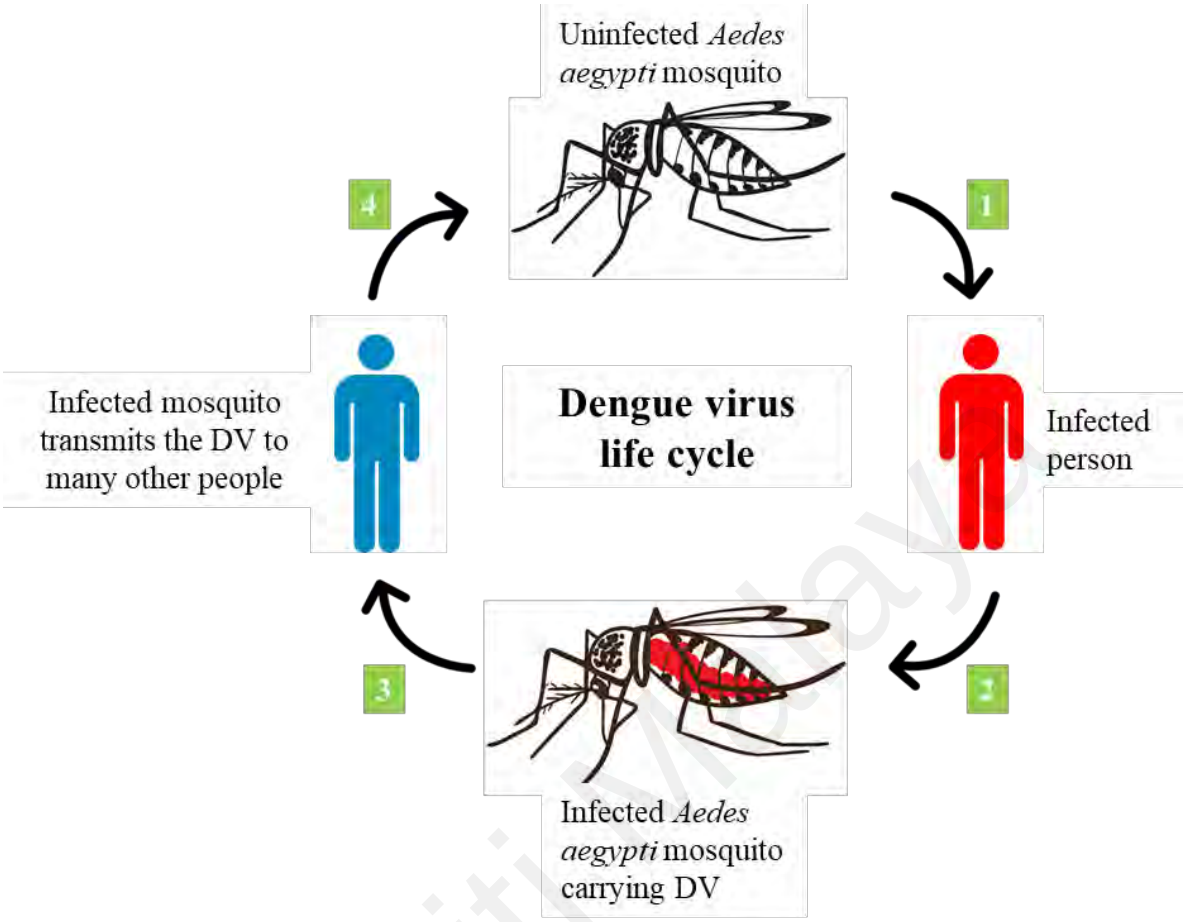

Figure 2.3: Dengue virus life cycle. (1) Uninfected *Aedes aegypti* mosquito feeds on a person infected by DV. (2) The mosquito is now infected by DV. (3) DV will be transmitted into the healthy person's blood when bitten by an infected mosquito, hence, initiates the replication cycle of DV in host body. (4) The cycle will then continue.

Universiti Malaya

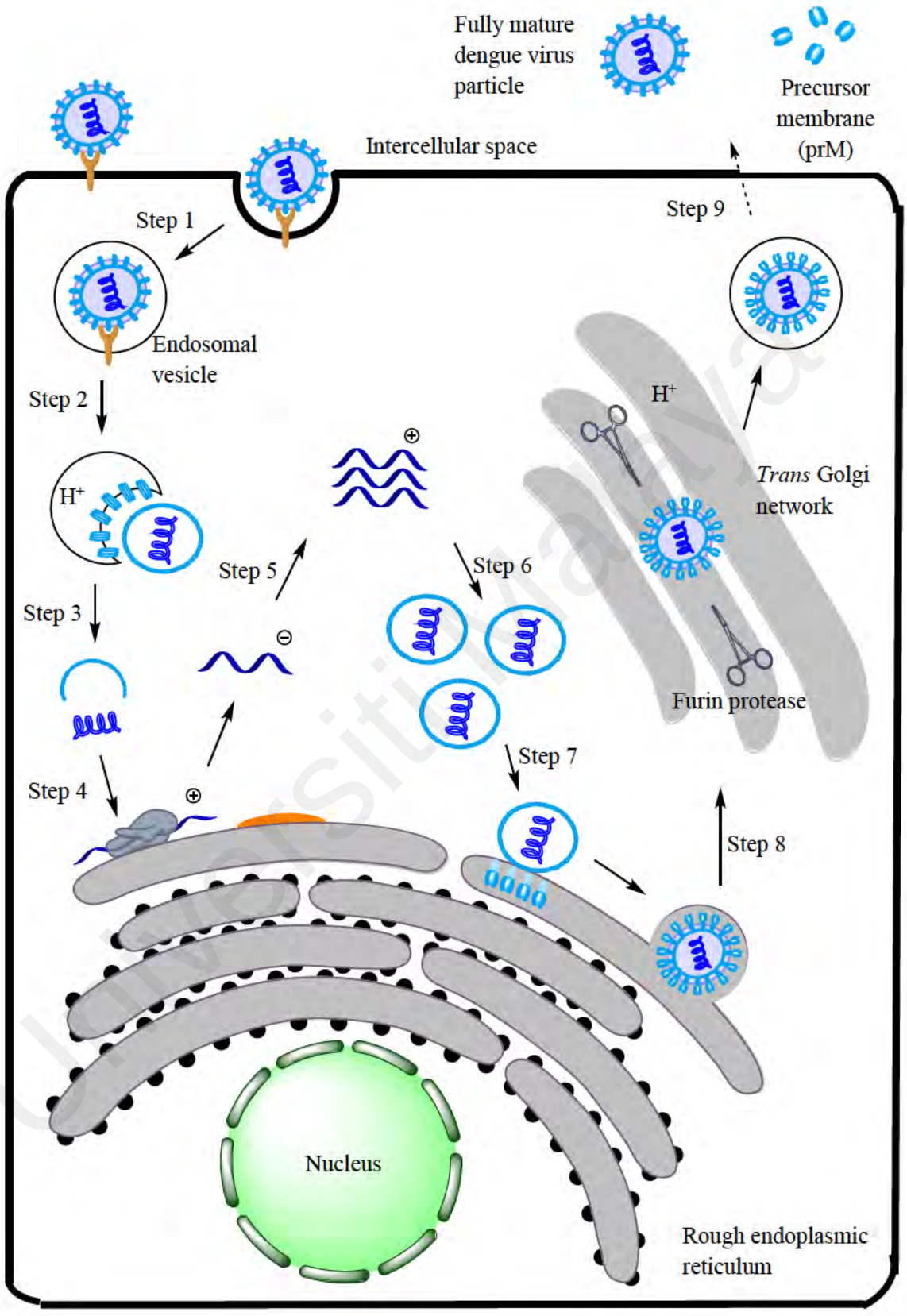
Fully mature dengue virus particle
Precursor membrane (prM)
Intercellular space
Step 1
Step 9
Endosomal vesicle
Step 2
H+
H+
Trans Golgi network
Step 5
Step 6
Step 3
Furin protease
Step 7
Step 4
Step 8
Nucleus
Rough endoplasmic reticulum

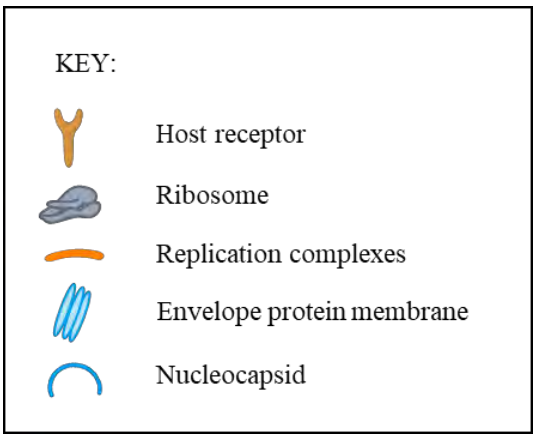

Figure 2.4: Dengue virus replication cycle in host cell. The mature DV enters the cell via CME pathway (Step1), then subsequently enter the endocytic vesicle where due to acidification, the E glycoprotein changes its conformation and leads to viral host membrane fusion (Step 2). This fusion release viral RNA into the cytoplasm (Step 3). At the cytoplasm, the RNA which act as mRNA presented to ER and translated to a single polyprotein which then cleaved by host and viral protease to yield three structural and seven non-structural proteins (Step 4). The transcription of antisense viral RNA occurred followed by RNA replication (Step 5). The C protein molecules incorporate the newly synthesized viral RNA, forming a nucleocapsid (Step 6). These then leads to viral assembly and the immature viral particles buds off from the ER together with E and M proteins and transported into Golgi to the *trans*-Golgi network to be processed. Over there, furin cleaves the M protein (Step 7 and 8) and finally, mature virus particle released to the extracellular space (Step 9).

2.1.3.1 Cell entry

Viral entry into the host cell can be initiated in various ways, by undergoing endocytosis or via direct membrane fusion, a penetration reaction at the plasma membrane (Tourdot, 2013). DV entry is based on a receptor-mediated endocytosis, or also known as the clathrin-mediated endocytosis (CME). According to (Popova et al., 2013), CME is a process where the entry of fragments of the cytoplasmic membrane, along with all of their contents, into the cell in the form of vesicles coated on the outside with a lattice consisting of

Universiti Malaya

polymerized clathrin, although recent data strongly suggest the former as the principal method of DV cellular entry (Chew et al., 2017).

Upon the entry of mature DV into the cell via the CME pathway (**Figure 2.4**, Step 1), the lysosomes, a digestive vesicle containing digestive enzymes such as proteases, merged with the viral endosomes to kick-start what would normally be an intracellular digestion process. Due to the acidification (lowering of pH) at the endosomal vesicles, E glycoprotein is triggered to change its conformation, thus initiating the viral-host endosomal membrane fusion (**Figure 2.4**, Step 2). (The details on mechanism of E protein in facilitating viral-host membrane fusion will be discussed in subheading **2.1.4**). The fusion releases the viral RNA into the cytoplasm of the host's cell following the decapsidation (opening of capsid ring which surround the RNA) process (**Figure 2.4**, Step 3) (Flipse et al., 2013; Screaton et al., 2015).

2.1.3.2 Translation and replication

The viral RNA directly acts as mRNA. Therefore, once the viral RNA enters the cytoplasm, translation process is initiated by having the viral RNA on the endoplasmic reticulum (ER). The viral RNA will be translated to a single polyprotein which comprises about 3000 amino acids (**Figure 2.4**, Step 4). The polyprotein is the then cleaved by host and viral protease to yield three structural and seven non-structural proteins as shown in **Figure 2.2**. The non-structural proteins form a complex on the ER membrane to initiate RNA replication. Then, transcription of antisense viral RNA occurred followed by RNA replication. (**Figure 2.4**, Step 5) (Okamoto et al., 2017).

Universiti Malaya

2.1.3.3 Post translation

The freshly synthesized viral RNA will be surrounded by the C proteins, forming a nucleocapsid (**Figure 2.4**, Step 6). These then leads to virus assembly (**Figure 2.4**, Step 7) and the immature virus particles bud off from the ER together with prM and E protein. Immature virus particles are then transported through Golgi into the *trans*-Golgi network to be processed. Low pH environment in Golgi induces conformational changes on the virion where host protease, furin, cleaves the prM to generate mature M protein (**Figure 2.4**, Step 8). Thus, mature virus particle is subsequently released to the extracellular space by exocytosis (**Figure 2.4**, Step 9) (Okamoto et al., 2017; Screaton et al., 2015). After the mature DV occupied the extracellular space, the person now is infected by DV. This replication cycle will continue until the viral particle is neutralized by the host antibodies or the factories (infected cell) are destroyed by host's immune cells. Meanwhile, if the *Aedes* feeding cycle continues and the DV survives, and these processes repeats.

2.1.4 Dengue envelope protein (E- protein)

The E protein have three domains folded largely based on β sheets out the N-terminus; domain one (DI) the central domain which functions as molecular hinge for the low-pH-catalyzed reorganization; domain two (DII) called the fusion (or dimerization) domain; and domain three (DIII) immunoglobulin (IgG)-like domain which facilitate the viral entry and fusion (Mondotte et al., 2007; Lescar, 2008; Modis et al., 2003). Modis et al. (2003) firstly identified a hydrophobic pocket cavity which was located in between DI and DII back in 2003. This cavity fits N-octyl-β-D-glucoside as a ligand. Therefore, it was named as β-OG hydrophobic pocket cavity (**Figure 2.5**). The mechanism for conformational changes of E-protein is explained in **Figure 2.6**.

Universiti Malaya

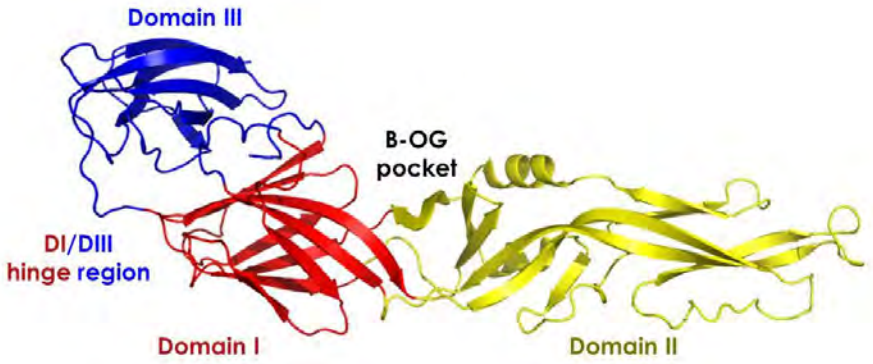

Figure 2.5: Crystal structure of dengue envelope protein for pre-fusion conformation (PDB ID: 1OAN). The E- protein consist of (DI) in red, (DII) in yellow, (DIII) in blue, DI/DIII hinge region and β-OG hydrophobic pocket.

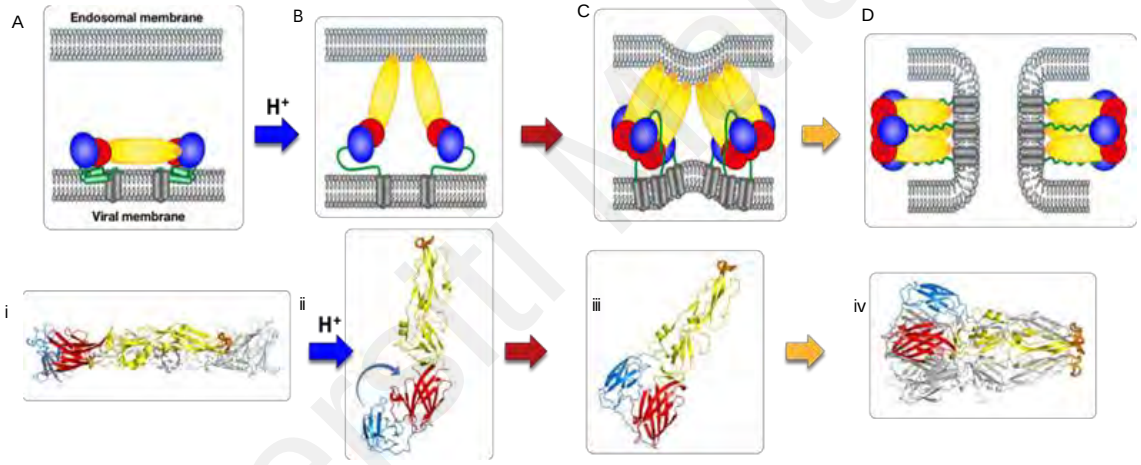

Figure 2.6: Conformational change of E protein during viral entry from endosome into the cytoplasm of the organism. Red represents DI, yellow represents DII and blue shows DIII. (A) At pre-fusion conformation, mature E protein dimer is in its dimer flat conformation; whereby two chains are attached together to form this dimer configuration. (B) Upon acidification, the dimer dissociates in endosome, thus initiates the fusion loop insertion process into the endosomal membrane. (C) Each aligned monomers then trimerize. DIII then flips to the sides of trimer by pulling the TM segments and stem towards the endosomal membrane to initiate both viral and endosomal membrane fusion. (D) At post-fusion conformation, a fusion pore was formed after the first hemi-fusion. This stage was completed together with the aid of TM segments. (i to iv) Shows the 3D structures of DV2 virus E protein matching the steps shown above graphically. (Copyright permission from Rey et al., 2018).

Universiti Malaya

2.2 Inhibitors for dengue envelope protein

The search for a dengue antiviral drug is highly in demand. Therefore, the first approach to discover E protein inhibitors is through the development of small molecule inhibitors and the alternative is by using peptide inhibitors. There are few well known targets which has been rectified for dengue E protein. Those are β-OG hydrophobic pocket, DIII region and DI/DIII hinge region.

2.2.1 Small molecules

According to Kumar & Lukman (2018), the term "small molecule" refers to organic compounds with low molecular weights of lower than 1000 Da (Kumar & Lukman, 2018), for example, derivatives of lipids, flavonoids, and carbohydrates. In the case of dengue virus, flavonoids are one of the commonly tested small molecules *in silico* and *in vitro* against DV particularly on the E protein.

For instance, rolitetracycline and doxycycline had the best activity towards DV E protein with an IC_{50} value of 67.1 μM and 55.6 μM, respectively, compared to other reported tetracyline derivatives. The screening for these lead compounds were made based on computational studies using structural databases of medical compounds and further tested for bioactivity through plaque formation assay (Yang et al., 2007). Besides rolitetracycline and doxycycline, baicalin and baicalein also showed a good binding affinity value of -8.0 kcal/mol and -7.1 kcal/mol, respectively, against DV E protein (Hassandarvish et al., 2016). Other examples of small molecules designed to inhibit DV E protein are listed in **Table 2.1.**

Universiti Malaya

Table 2.1: Small molecules discovered to inhibit DV E protein.

Designation	Compound Structure	Inhibition values*	Binding affinity (kcal/mol)*	Target	References
Rolitetracycline	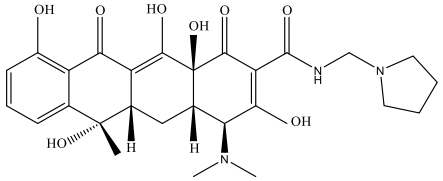	67.1 µM [a]	N.D.	β-OG hydrophobic pocket	(Yang et al., 2007)
Doxycycline	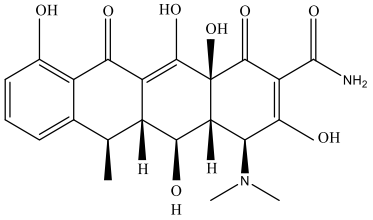	55.6 µM [a]	N.D.	β-OG hydrophobic pocket	(Yang et al., 2007)
Quercetin	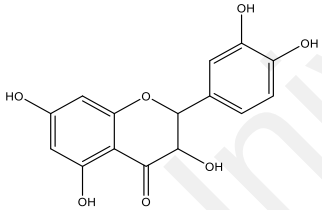	35.7 µg/mL [a]	-7.1	β-OG hydrophobic pocket	(Mir et al., 2016)

Universiti Malaya

Table 2.1, continued.

Designation	Compound Structure	Inhibition values*	Binding affinity (kcal/mol)*	Target	References
Baicalein	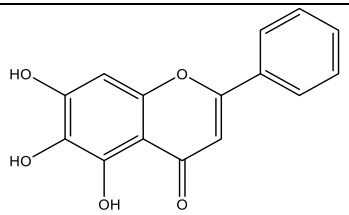	6.46 µg/mL [a]	-7.1	β-OG hydrophobic pocket	(Hassandarvish et al., 2016)
Fisetin	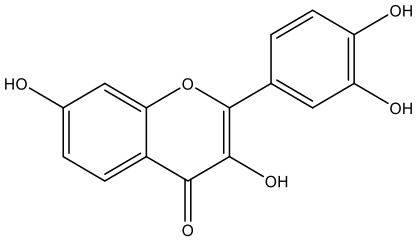	43.12 µg/mL [a]	-7.3	β-OG hydrophobic pocket	(Mir et al., 2016)
Naringenin	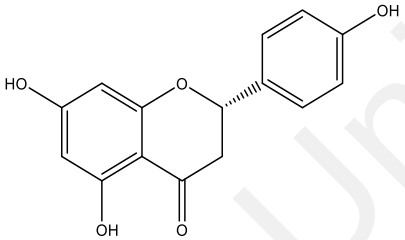	52.64 µg/mL [a]	-8.1	β-OG hydrophobic pocket	(Mir et al., 2016)

Universiti Malaya

Table 2.1, continued.

Designation	Compound Structure	Inhibition values*	Binding affinity (kcal/mol)*	Target	References
5-(3,4-dichlorophenyl)-N-[2-(p-tolyl) benzotriazole-5-yl] furan-2-carboxamide	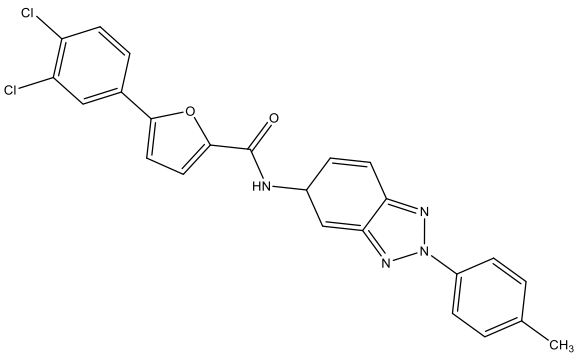	N.D.	ΔG° = -34.46	β-OG hydrophobic pocket	(Tambunan et al., 2015)
Baicalin	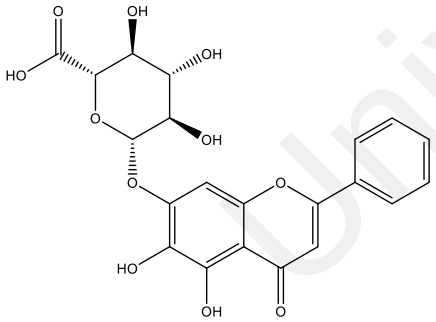	N.D.	-8.0	β-OG hydrophobic pocket	(Hassandarvish et al., 2016)

Universiti Malaya

Table 2.1, continued.

Designation	Compound Structure	Inhibition values*	Binding affinity (kcal/mol)*	Target	References
EGCG	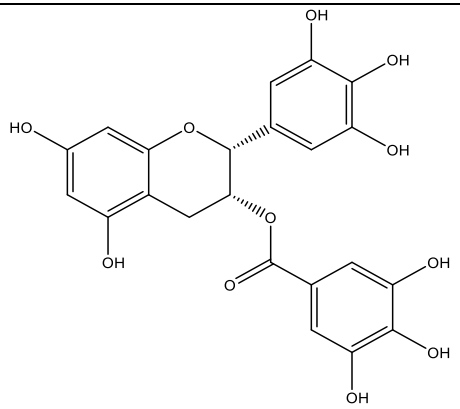	N.D.	-8.4	DV2 E protein	(Ismail & Jusoh, 2017)
Hyperoside	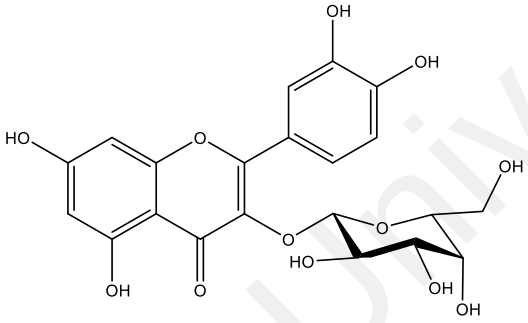	N.D.	-7.7	DV2 E protein	(Ismail & Jusoh, 2017)

Universiti Malaya

Table 2.1, continued.

Designation	Compound Structure	Inhibition values*	Binding affinity (kcal/mol)*	Target	References
Glabranine	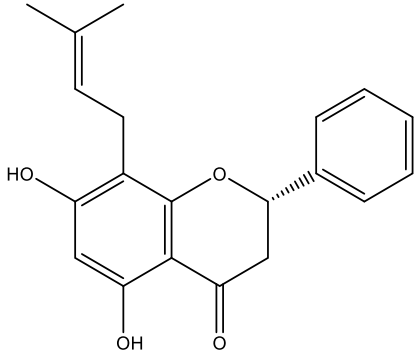	N.D.	-9.0	DV2 E protein	(Ismail & Jusoh, 2017)
Ladanein	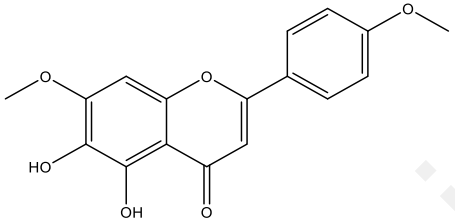	N.D.	-8.2	DV2 E protein	(Ismail & Jusoh, 2017)
FN5Y	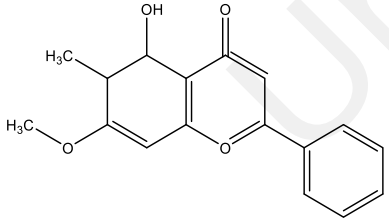	12.31 μM [b]	N.D.	DV2 E protein	(Srivarangkul et al., 2018)

Universiti Malaya

Table 2.1, continued.

Designation	Compound Structure	Inhibition values*	Binding affinity (kcal/mol)*	Target	References
Kaempferol	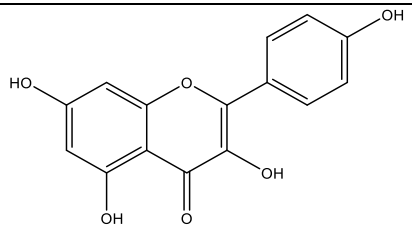	N.D.	-7.2	DV E protein	(Keramagi & Skariyachan, 2018)
Chymopain	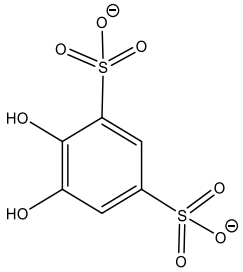	N.D.	-6.5	DV E protein	(Keramagi & Skariyachan, 2018)
Octyl 2-O-sulfo-β-D-GlcA	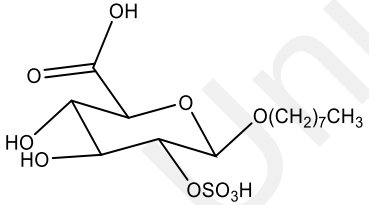	18.4% [c]	N.D.	β-OG hydrophobic pocket	(Abe et al., 2014)

Universiti Malaya

Table 2.1, continued.

Designation	Compound Structure	Inhibition values*	Binding affinity (kcal/mol)*	Target	References
4-(5-(4-chlorophenyl) thiophen-2-yl)-N-(pyridin-3-ylmethyl) quinazolin-2-amine	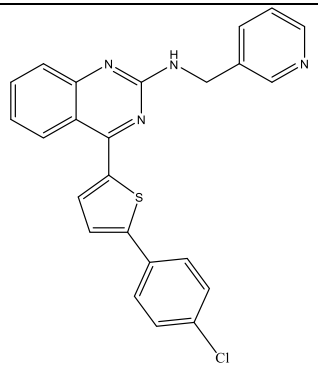	119 nM [b]	N.D.	β-OG hydrophobic pocket	(Wang, 2008)
(*E*)-2-(1-(4-(3-(4-(6-amino-1,4-dihydropyridazin-3-yl) phenyl) ureido) phenyl) ethylidene) hydrazine-1-carboximidamide	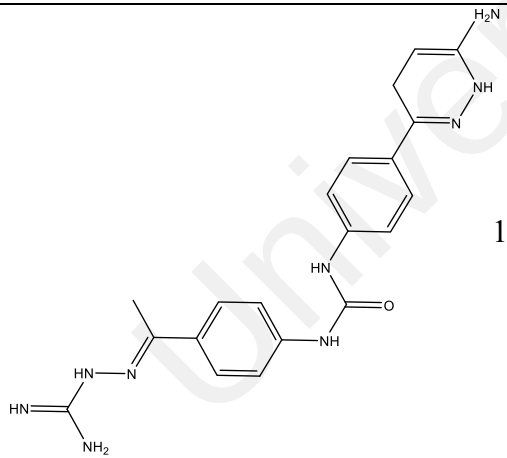	13 μM [a]	N.D.	β-OG hydrophobic pocket	(Zhou et al., 2008)

Universiti Malaya

Table 2.1, continued.

Designation	Compound Structure	Inhibition values*	Binding affinity (kcal/mol)*	Target	References
5-(3-chlorophenyl)-N-(2-phenyl-2H-benzo[d][1,2,3]triazol-6-yl) furan-2-carboxamide	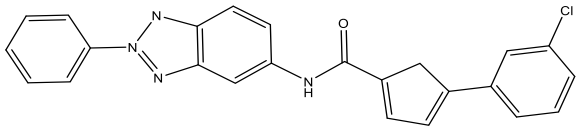	4 µM [a]	ΔG° = -32.43	DI/DIII hinge region of DV2 E protein	(Dubey et al., 2017) (Yennamalli et al., 2009)
NITD448	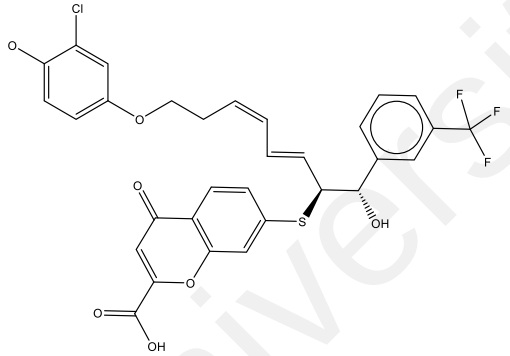	6.8 µM [a] 98 µM [b]	ΔG° = -31.79	β-OG hydrophobic pocket	(Poh et al., 2009)
(*E*)-4-(1-(2-(4-(4-chlorophenyl)thiazol-2-yl)hydrazineylidene)ethyl)phenol	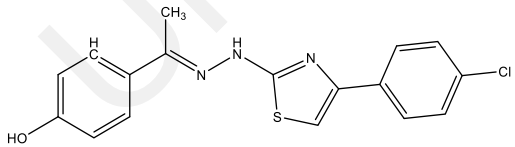	1.32 µM [b]	N.D.	DV2 E protein	(Jadav et al., 2015)

Universiti Malaya

Table 2.1, continued.

Designation	Compound Structure	Inhibition values*	Binding affinity (kcal/mol)*	Target	References
4,5-dichloro-3-((4-(3-(2-chlorophenyl)ureido)thiazol-2-yl)methyl)-4H-imidazol-3-ium	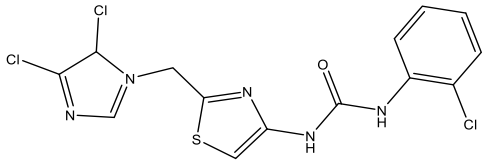	32 μM [a]	N.D.	β-OG hydrophobic pocket	(Kampmann et al., 2009)
(E)-2-(2-chloro-6-(4-chlorophenoxy)pyridin-4-yl)-4-methyl-5-(1-(2-phenylhydrazineylidene)ethyl)thiazole	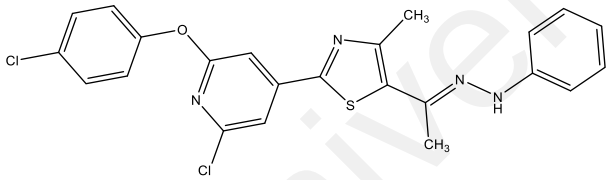	1.2 μM [a]	N.D.	β-OG hydrophobic pocket	(Kampmann et al., 2009)

Universiti Malaya

Table 2.1, continued.

Designation	Compound Structure	Inhibition values*	Binding affinity (kcal/mol)*	Target	References
(*E*)-1-(3-chlorophenyl)-2-(1-cyano-2-(furan-2-yl)-2-oxoethylidene) hydrazin-1-ide	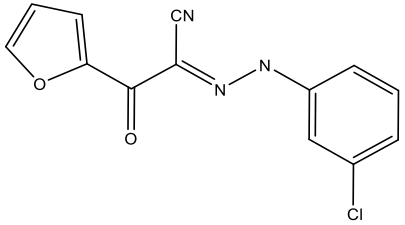	15 µM [a]	N.D.	β-OG hydrophobic pocket	(Schmidt et al., 2012)
2-((2-oxo-2-(2-(phenylcarbamothioyl)hydrazineyl)ethyl)thio)-*N*-(4-(trifluoromethoxy)phenyl)acetamide	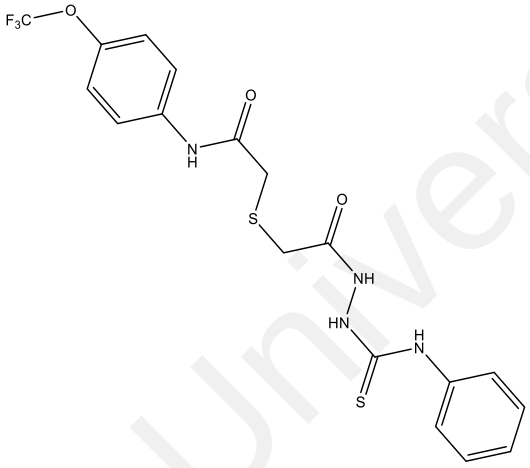	5 µM [b]	N.D.	β-OG hydrophobic pocket	(Leal et al., 2017)

Universiti Malaya

Table 2.1, continued.

Designation	Compound Structure	Inhibition values*	Binding affinity (kcal/mol)*	Target	References
N-(6-((7-chloroquinazolin-4-yl)oxy)pyridin-3-yl)-5-(pyridin-2-yl)thiphene-2-carboxamide	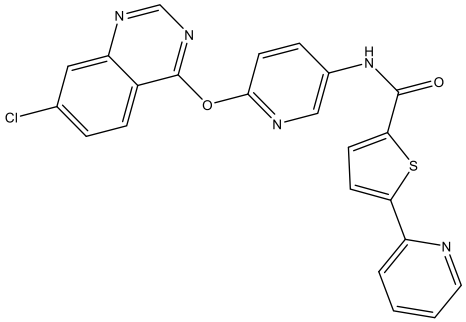	3 μM [b]	N.D.	β-OG hydrophobic pocket	(Leal et al., 2017)

[a] *Half maximal inhibitory concentration (IC_{50})* [b] *Half maximal effective concentration (EC_{50})* [c] *Relative infectivity (%)* * *Experimetal reported values; N.D. – No data*

Universiti Malaya

2.2.2 Peptides

Commonly, peptides comprised of short chains of 2 to 50 amino acids which are linked via amide bond in a straight chain conformation. To date, there are number of examples regarding linear peptides which act as an inhibitor for dengue infections. Peptide possess several advantages over small molecules: they are biologically and chemically diverse, and less toxic as the peptides are easily degraded into amino acids which can be eliminated or recycled from/by the biological system. These advantages make the peptide inhibitors to be an ideal lead for DV E protein inhibition drug.

In 2005, Hrobowski et. al. (2005) developed a series of peptides that mimics regions of DV E protein. these peptides were able to inhibit DV in both *in silico* and *in vitro* studies. Their research was inspired by the human immunodeficiency virus (HIV) T20 drug which mimics part of the HIV's envelope protein to cater inhibition. Then, a peptide called DN59 (MAILGDTAWDFGSLGGVFTSIGKALHQVFGAIY), correspond to the stem domain of DV2 was identified to confer an inhibition percentage of 93 ± 2% and with IC_{50} value of 10 μM in viral plaque reduction assay. Besides that, scrambled DN59 peptides also were screened towards DV E protein fortunately, the scrambled sequence did not show any inhibition against DV E protein (Hrobowski et al., 2005). Other examples of peptides designed to inhibit DV E protein as listed in **Table 2.2.**

Universiti Malaya

Table 2.2: Peptides designed to inhibit DV E protein based on the literature.

Designation	Peptide Sequence*	IC_{50} (μM)**	Mode of Action/Target	References
DN57opt	RWMVWRHWFHRLRLPYNPGKNKQNQQWP	8 ± 1	DV2 E protein, /viral entry	(Costin et al., 2010)
1OAN1	FWFTLIKTQAKQPARYRRFC	7 ± 4	DV2 E protein, /viral entry	(Costin et al., 2010)
$DV2^{419-447}$	ASDHJKAGASDKHASD	0.125	DV2 E protein, /viral entry or fusion	(Schmidt et al., 2010)
DET 2	PWLKPGDLDL	N.D.	DV2 E protein, /viral binding and entry	(Alhoot et al., 2013)
DET 4	AGVKDGKLDF	35	DV2 E protein, *viral binding and entry	(Alhoot et al., 2013)

Universiti Malaya

Table 2.2, continued.

Peptide EF	EF	96.50	DV2 E protein, /binds to hydrophobic pocket	(Panya et al., 2014)
gg-ww	GGARDAGKAEWW	77	DV2 E protein, /viral entry	(Chew et al., 2015)
LL-37	LLGDFFRKSKEKIGKEFKRIVQRIKDFLRNLVPRTES	N.D.	DV2 E protein, /viral entry	(Alagarasu et al., 2017)
P4	CKIPFEIMDLEKRHVL	19.08 ± 2.52	DV2 E protein, /viral entry	(Cui et al., 2018)
P7	VEPGQLKLNWFKK	12.86 ± 5.96	DV2 E protein, /viral entry	(Cui et al., 2018)
Pep1	LEHGSCVTTMAKDKPTL	< 50	DV2, DV3 and DV4, /viral entry	(John et al., 2019)
Pep2	DRGWGNNGCGLFG	< 20	DV1, DV2, DV3, and DV4 entry, /viral entry	(John et al., 2019)
Pep3	GQGKAHNGRLITANP	10 to 33	DV1, DV2, DV3, and DV4 entry, /viral entry	(John et al., 2019)

** Single letter amino acids ** Reported values; N.D. – No data*

Universiti Malaya

2.3 Computational strategies in peptide-based drug discovery

Computational, or *in silico*, methods (i.e. docking and molecular dynamics) have become important tools in peptide-based drug design and development. Before utilizing the computational docking methods, other biophysical methods techniques were used to calculate/estimate the ligand-protein interactions. For instance, X-ray crystallography, NMR spectroscopy, fluorescence spectroscopy, and spectrophotometric assays. However, these techniques can be laborious, time consuming, difficulties in getting crystallized (except for small proteins) or even has a lower resolution (Lee et al., 2019). Therefore, due to these obstacles, computational methods are getting enormous attention as computational power grows and thereafter the prediction of ligand-protein interaction can be done within the order of minutes with accurate predictions (Lee et al., 2019).

Before performing the docking studies, it is a norm to have a knowledge on the binding site of the interested protein structure to elevate the docking efficacy. However, in some cases, the binding site will be unknown. Therefore, cavity prediction detection and other online tools can be used to recognize probable binding sites of the proteins. For peptide-based ligands, DynaRock, Rosetta FlexPepDock and PepCrawler are the most used methods/tools to define the binding sites while for low molecular weight peptides, Gold, Surflex and AutoDock Vina are utilized. Through the docking process, ligand conformations and orientations at the binding site of the protein can be predicted. Additionally, the binding affinities of each ligand conformations and orientations also can be analyzed (Meng et al., 2011). The ligand which indicates a lower binding energy value towards the binding pocket (of the protein) are predicted to be the most stable and obtain higher binding affinities at the binding site. However, this can be further verified using Molecular dynamics (MD) studies.

Molecular dynamics is a powerful stimulation method widely utilized in many fields of molecular modelling in which the stimulation provides flexibility for both

Universiti Malaya

peptide and protein along with stimulation time. AMBER, CHARMM, GROMACS, NAMD, DESMOND and TINKER are some of the commonly used software's to run the MD stimulations. Generally, the docked ligand poses, or conformations will be further refined by MD stimulations to assess the binding free energy of ligand-protein complexes (Antes, 2010). By doing so, electrostatic and van der Waals energies, solvation energy and entropic contributions at the binding interface can be obtained in addition to hydrogen bonding analysis and structural stability of the systems can be monitored/predicted to better understand the nature of the ligand-protein bindings. Not only that, but these in silico methods can also be automated for a high-throughput screen approach – saving time for the researcher. Therefore, the *in-silico* strategies have become helpful for experimental scientist to discover rational designs of new peptide-based drugs of higher effectiveness.

2.4 Peptide chemistry

2.4.1 Amino acids

Amino acid is a type of organic compound consists of a carboxylic functional group (-COOH) and an amine functional group ($-NH_2$). Apart from having two functional groups, it also has a side chain, commonly referred as R, as shown in **Figure 2.7**. The amino acids have carbon, hydrogen, nitrogen, and oxygen atoms in common and R group is significant for each it. Amino acids serve as the building blocks to produce polypeptides and proteins (Nelson et. al., 2005). Therefore, 20 natural amino acids are available which involved in protein production. Amino acids have standard notations which can be abbreviated as three-letter code or single letter. The structure of 20 amino acids is shown in **Table 2.3**.

Universiti Malaya

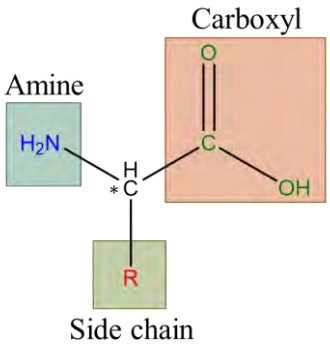

Figure 2.7: Basic structure of amino acid. (* shows the chiral center) which comprised of side chain, amine, and carboxyl group.

Table 2.3: Details of 20 amino acids.

Name	Abbreviation		Structure
	Three-letter code	Single letter symbol	
Alanine	Ala	A	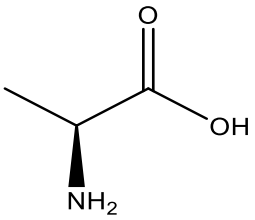
Arginine	Arg	R	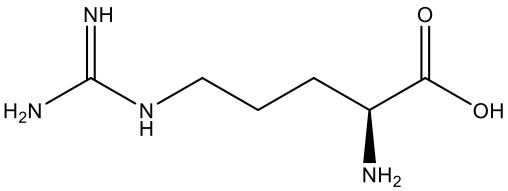
Asparagine	Asn	N	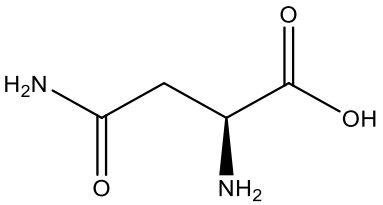
Aspartic Acid	Asp	D	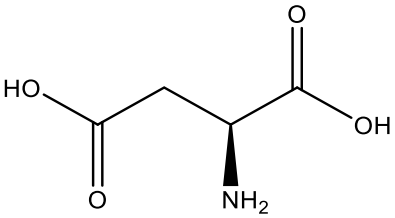

Universiti Malaya

Table 2.3, continued.

Name	Abbreviation		Structure
	Three letter code	Single letter symbol	
Cysteine	Cys	C	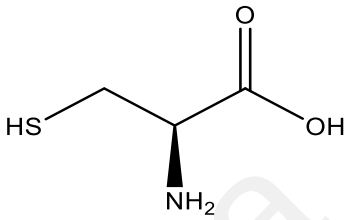
Glutamic Acid	Glu	E	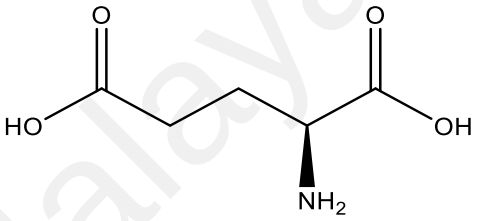
Glutamine	Gln	Q	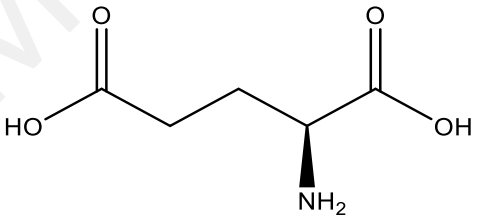
Glycine	Gly	G	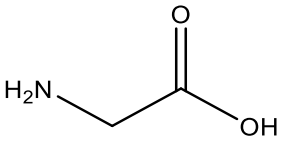
Histidine*	His	H	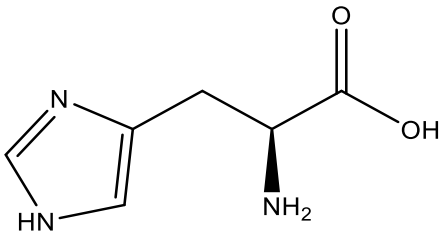
Isoleucine*	Ile	I	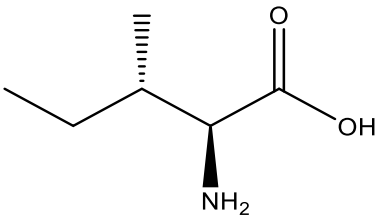

Universiti Malaya

Table 2.3, continued.

Name	Abbreviation		Structure
	Three letter code	Single letter symbol	
Leucine*	Leu	L	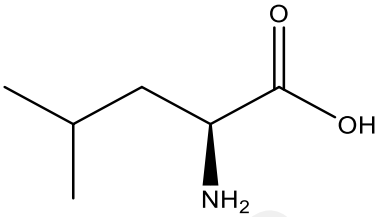
Lysine*	Lys	K	
Methionine*	Met	M	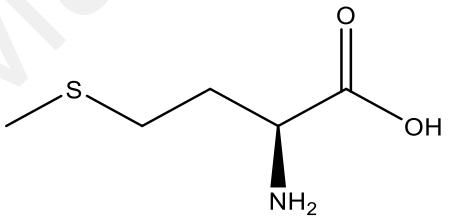
Phenylalanine*	Phe	F	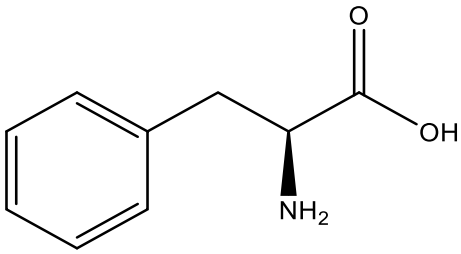
Proline	Pro	P	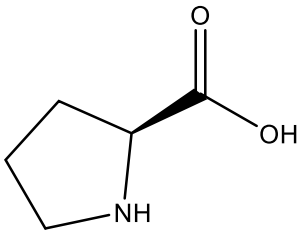
Serine	Ser	S	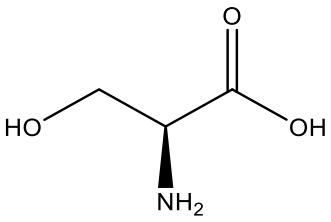

Universiti Malaya

Table 2.3, continued.

Name	Abbreviation		Structure
	Three letter code	Single letter symbol	
Threonine*	Thr	T	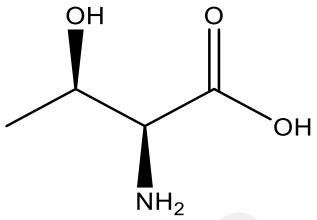
Tryptophan*	Trp	W	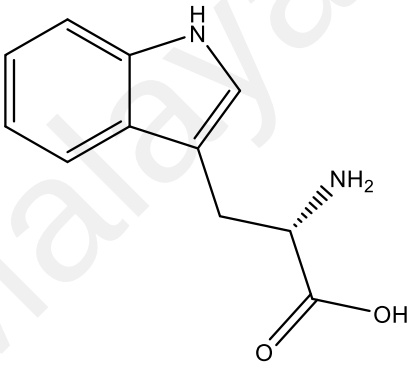
Tyrosine	Tyr	Y	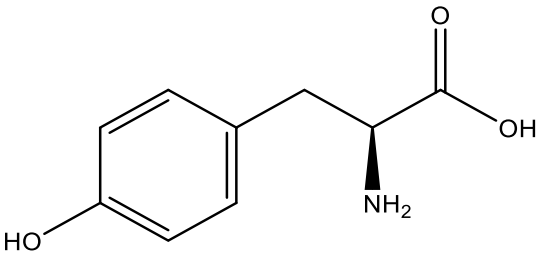
Valine*	Val	V	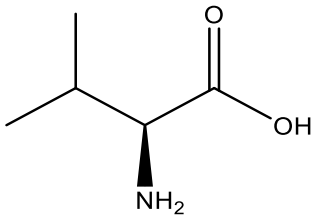

**essential amino acids*

Universiti Malaya

Amino acids are also essential for human growth – as proteins building block. There are nine 'essential' amino acids because they cannot be produced in human body and acquired via digestion only (**Table 2.3**) while the rest of the 20 naturally found amino acids are non-essential amino acids which can be biosynthesized in human body (Young, 2000). Since the amino acids plays a major role in human biological system, they are commonly used in nutritional supplements, drugs, and food technology. The application of amino acids is well discussed in subheading **2.4.1.4**.

Amino acids are capable of chirality. A chiral compound possesses a mirror image (**Figure 2.8**). The alpha-carbon (α-carbon) of all amino acids are optically active as it is bonded to four different atoms or groups with the exception for glycine. Therefore, each of the amino acids (except glycine) can exists in two enantiomers, known as L- or D-amino acids (Creighton, 1993). The L-isomers of amino acids have high abundance over D- isomers of amino acids in living organism however, the reason for such occurrence is still puzzling scientists until today.

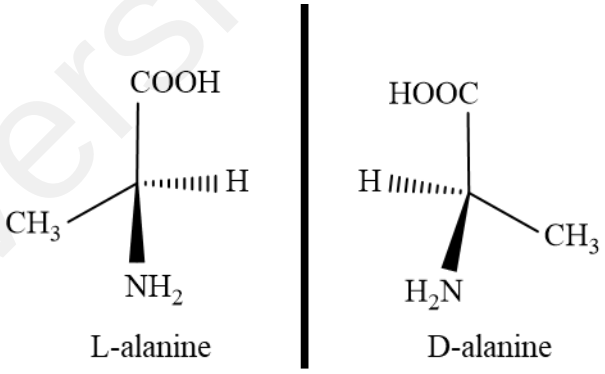

Figure 2.8: Isomers of amino acids (Example: L- and D-alanine).

2.4.1.1 Protecting groups of amino acids

In peptide chemistry, solid phase peptide chemistry (SPPS) plays critical role in. modern peptide-based drug design. This chemistry utilizes protecting groups (PG) at the N-terminal and the R group of an amino group. The purpose is to enhance the coupling

Universiti Malaya

reaction and to obtain the desired product of the best purity. Besides that, the choice of protecting groups must be safely and easily removed in order to proceed with next step of the synthesis. The most common N-terminal α-amino protecting groups in SPPS are 9-fluorenymethoxycarbonyl (Fmoc) and the *tert*-butyloxycarbonyl (Boc) group. **Table 2.5** and **Table 2.6** summarizes the protecting groups that can be used at the N-terminal of an α-amino group and side chain group in an amino acid, respectively.

Table 2.4: The common α-amino protecting groups of amino acids.

Name and structure	Removal conditions
9- Fluorenymethoxycarbonyl Chloride (Fmoc - Cl) 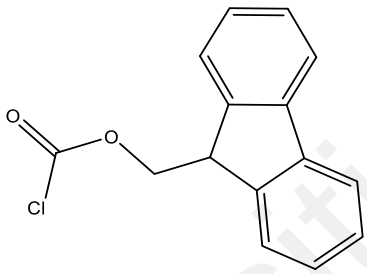	20% piperidine (most common)
tert-butyloxycarbonyl (Boc) 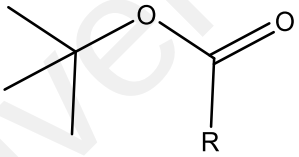	Neat trifluoroacetic acid (TFA)

Universiti Malaya

Table 2.5: The common side chain protecting groups of amino acids.

Name and structure	Reagents for deprotection
Acetamidomethyl (Acm) 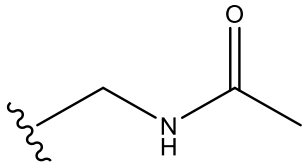	95% TFA
4-methoxy-2,3,6-trimethylbenzenesulphonyl (Mtr) 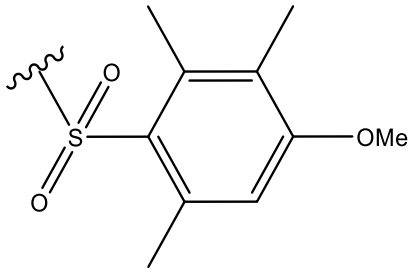	95% TFA
Trityl (Trt) 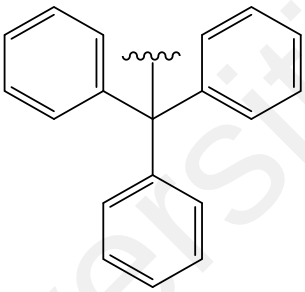	95% TFA
tert-butyloxycarbonyl (t-Bu) 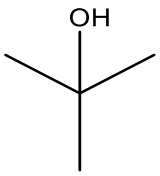	95% TFA
2,2,4,6,7-pentamethyIdlhydrobenzofuran-5-sulfonyl (Pbf) 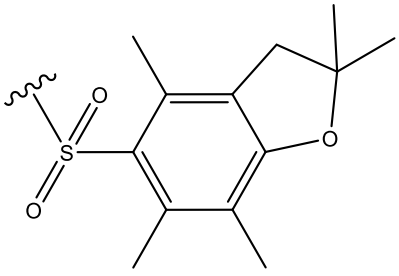	95% TFA

Universiti Malaya

2.4.1.2 Amino acid synthesis

Amino acids can be produced by biochemical processes and chemical synthesis. In human, amino acids will be formed by undergoing three key metabolic pathways. Those are glycolysis, pentose phosphate pathway and citric acid cycle. Serine, Alanine, Valine, Isoleucine and Leucine will be produced through glycolysis process. While Histidine, Phenylalanine, Tyrosine and Tryptophan are gained from pentose phosphate pathway. The remaining Aspartate, Asparagine, Methionine, Threonine, Lysine, Glutamate, Glutamine, Proline and Arginine are formed from citric acid cycle. **Figure 2.9** shows an overview of amino acid biosynthesis.

Universiti Malaya

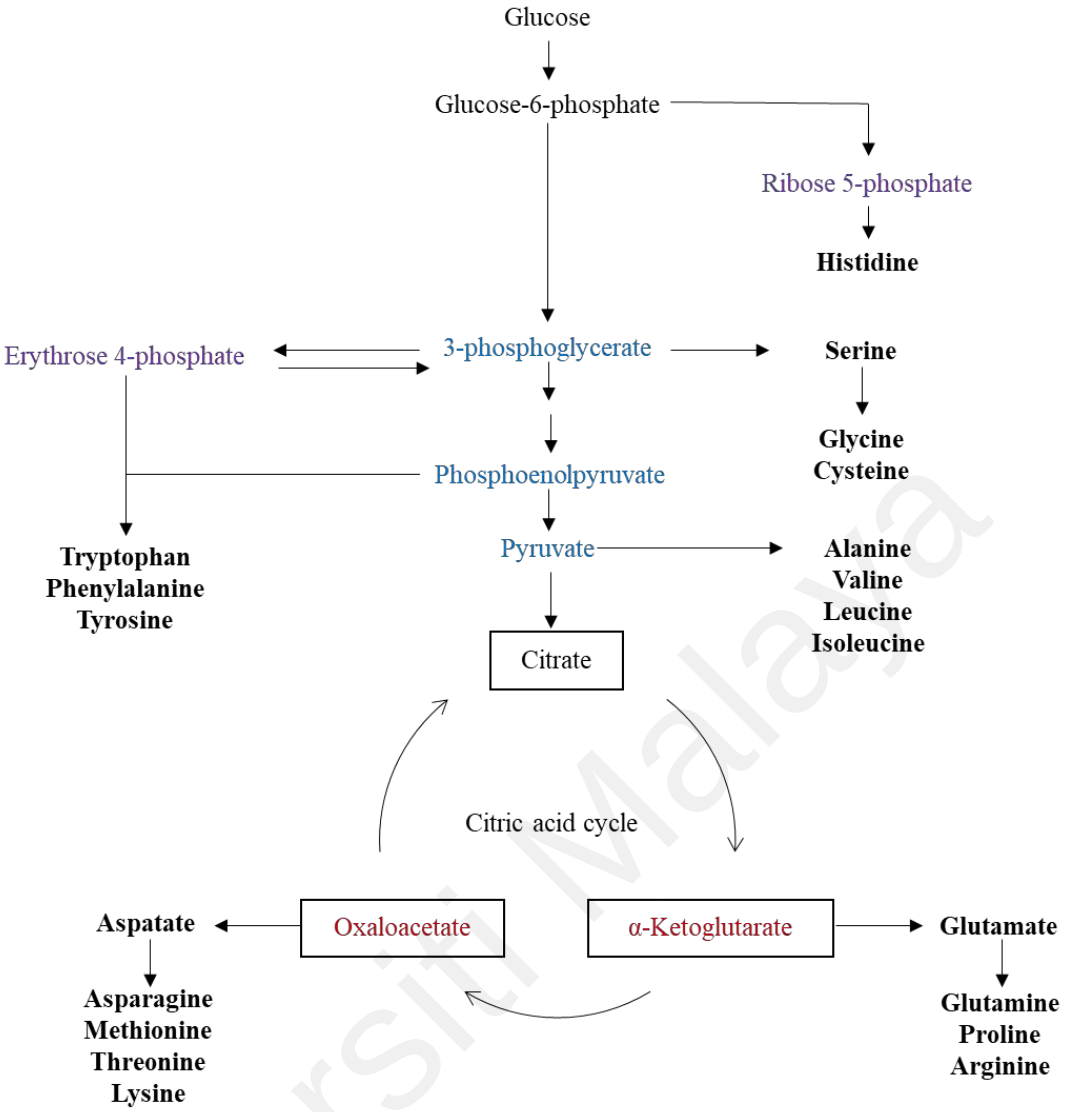

Figure 2.9: Overview of amino acid biosynthesis pathways (Yang et al., 2020). Blue fonts indicate glycolysis process; purple fonts indicate pentose phosphate pathway and dark red fonts represents citric acid cycle. Amino acids are written in black.

Apart from biosynthesis, amino acids are also can be produced through organic synthesis. Strecker synthesis is well known for production of amino acids. During the synthesis, the amino acids are produced by the reaction between an aldehyde and ammonium chloride in the presence of potassium cyanide. Later the condensation reaction yields an α-aminonitrile followed by hydrolysis to obtain the α-amino acid as shown in **Scheme 2.1**. Usually, nucleophilic cyanide ion gives a cyanohydrin by reacting

University Malaya

with an aldehyde. But, in the presence of ammonium chloride, the analogues α-aminonitrile has obtained (Drauz at al., 2006).

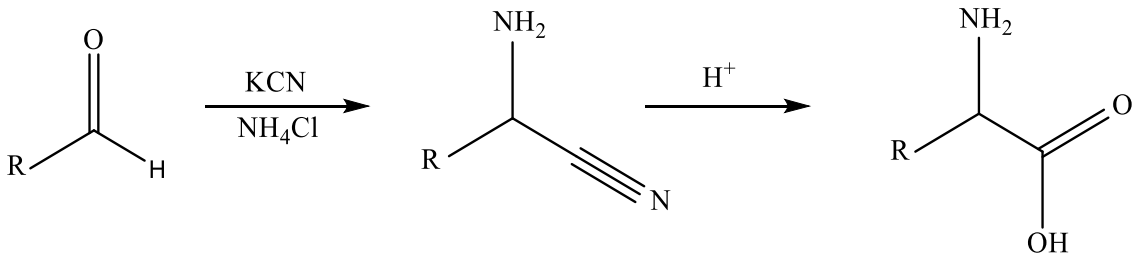

Scheme 2.1: Amino acid production via Strecker synthesis.

Besides that, nucleophilic substitution of α-halocarboxyllic acids by excess ammonia leads to the production of amino acids. This is a simple reaction where halide act as a leaving group while ammonia as a nucleophile (Synthesis of amino acids., 2000). **Scheme 2.2** shows the nucleophilic substitution of α-halocarboxyllic acids.

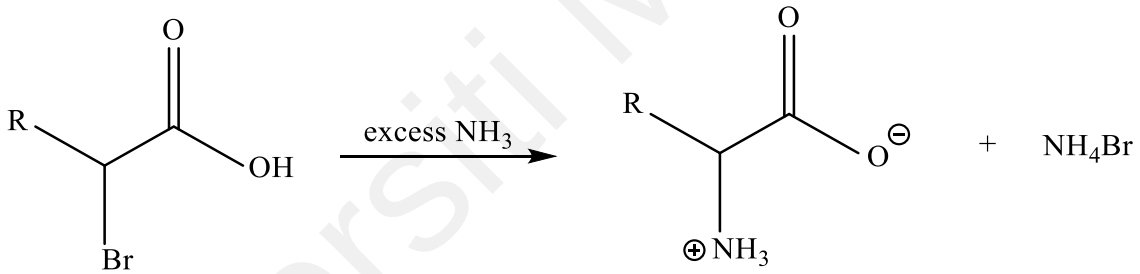

Scheme 2.2: Nucleophilic substitution of α-halocarboxylic acids to produce amino acid.

Moreover, amino acids also can be yielded by alkylation process of an acetamidomalonate (**Scheme 2.3**). This reaction consists of multiple processes which can be occurred stepwise. Sodium ethoxide, a strong base will be added into the acetamidomalonate to form nucleophilic enolate, followed by alkylation of the enolate. Then, hydrolysis of malonate ester and amide bond leads to production of amino dicarboxylic acid. Subsequently, decarboxylation of a β-dicarboxylic acids produces an α-amino acid (Synthesis of amino acids., 2000).

Universiti Malaya

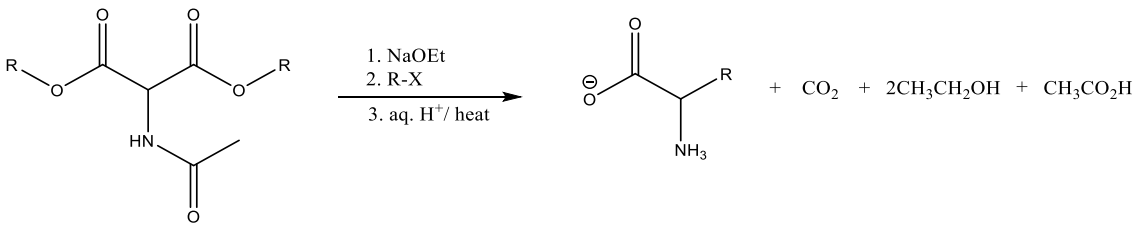

Scheme 2.3: Alkylation process of an acetamidomalonate to yield amino acid.

2.4.1.3 Applications of amino acids

Amino acids have multifunction and plays a major role in many industries. Food industries are making profits over the years. In here, amino acids are also contributing in enhancing the food quality. For instance, glycine and alanine are used to intensify the food taste and flavor while tryptophan and histidine act as an antioxidant for food preservation. Besides that, amino acids are utilized in medical field especially the essential amino acids which has been used in infusion fluids for patients who had operation or treatment. Human are consuming amino acids via dietary supplements. This helps in compensating amino acids deficiencies (Davis, 2018).

Apart from pharmacy industries, amino acids are also utilized for research usage. In chemistry, amino acid has been a starting material for various kind of synthesis. As mentioned earlier, chemists can synthesize peptides, polymers, and oligomers by having amino acids as a starting material based on the research scope. For cell culture processes, amino acids are essential ingredient in cell culture medium as they can promote cell growth and capable of producing antibodies and proteins. Additionally, amino acids have a unique moisturizing effect, pH levels, relative stability, and absorbance. Therefore, they are highly contributing to cosmetics production (Davis, 2018).

Universiti Malaya

2.4.2 Peptide synthesis

Peptide synthesis, a known chemical reaction to produce peptides. There are multiple amino acids are linked together via amide bonds/peptide bonds in the production of peptides (Isidro-Llobet et al., 2009). The peptide bonds are formed by a simple condensation process in which the hydroxyl from carboxylic terminal and hydrogen atom from amino terminal are removed and released as one water molecule as shown in **Figure 2.10**. Chemical peptide synthesis is commonly initiated at carboxyl end of the peptide (C-terminal) and proceeds towards the amino terminal (N-terminal). Peptides can be synthesized using solid-phase methods and solution-phase techniques. Solution phase peptide synthesis is preferred for large scale production of peptides but faces challenge in controlling the side reactions. However, for current research findings, solid phase peptide synthesis is more preferred than the latter one.

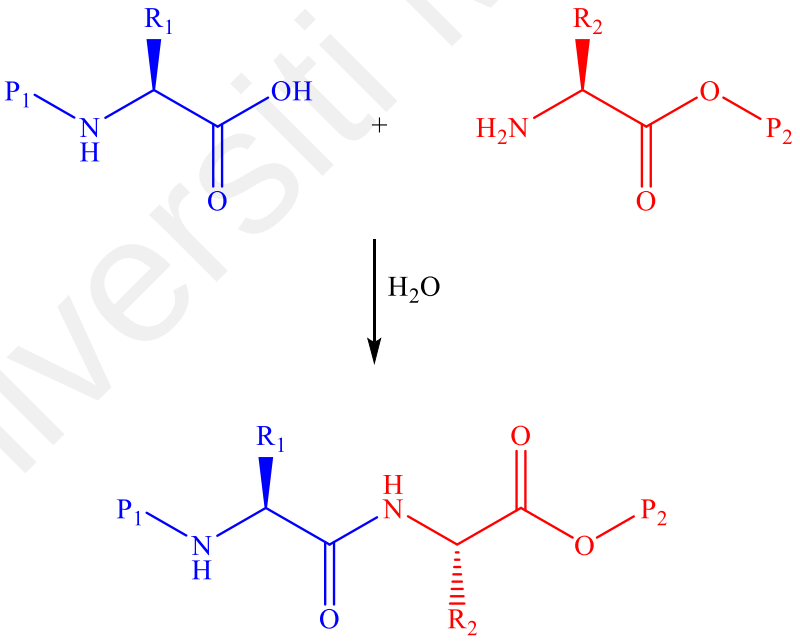

Figure 2.10: Coupling reaction of two amino acids in solution. This involves removal of water molecule.

Universiti Malaya

2.4.2.1 Solid phase peptide synthesis (SPPS)

SPPS is the stepwise assembly of peptides by conservative addition of α-amino acids and side chain protected group amino acids, while the C-terminal is tethered to a solid polymeric support, also known as resin (Merrifield, 1963). The stepwise procedure of SPPS is shown in **Chapter 3, Figure 3.1**. In short, the SPPS involves coupling of first amino acid to the resin and repeat cycle of N-terminal Fmoc-removal using piperidine and double coupling of pre-activated amino acid until sequence completion, and finally peptide removal from solid support using a TFA/TIS/water (95:2.5:2.5% v/v) cocktail (A detailed principle of SPPS are discussed in subheading **3.2**).

With such system, high concentration of excess reagents can lead the coupling reactions to complete. In addition, the used excess reagents and side products from the respective steps in peptide synthesis can be easily separated/removed from the reaction mixtures by only filtrating and washing the solid support, and while the synthesis steps can be repeated in the same vessel without any reallocation of the solid material. Anything which are attached to the solid polymeric support becomes insoluble while, the remaining soluble molecules can be easily washed out from the system. Furthermore, the laborious purification of intermediate peptides, a typical process of the classical solution synthesis, can be circumvented and helps in saving the time (Kim & McAlpine, 2013). **Figure 2.11** shows the basic experimental set up for SPPS.

The SPPS can be conducted either via Fmoc-chemistry or Boc-chemistry. The similarity between both the chemistry is that the peptides will be synthesized from C-terminal to N-terminal. Meanwhile, the lability for Fmoc- and Boc- chemistry are unlike. Fmoc-chemistry is labile to organic bases while the Boc- labile to acids. Therefore, choosing resin for both the chemistries are vital. Herein, Wang resin and Rink amide resin can be utilized for Fmoc-chemistry while for Boc-chemistry, Merrifield resin, PAM resin, MBHA resin and many more can be used. Yet, Boc-chemistry is not practical to be used

Universiti Malaya

as it needs liquid anhydrous hydrofluoric acid (HF), a hazardous chemical. Even though, the use of HF is highly effective, but the cleavage process must be carried out in special HF-resistant apparatus due to the highly corrosive nature of HF.

Figure 2.11: The basic experimental set up for solid phase peptide synthesis (SPPS). It consists of flask (to collect the solvent waster), vacuum trap (contains mild acid to neutralize the piperidine) and reaction vessel (resin will be placed in).

2.4.2.2 Types of resin

Resin selection are very significant in SPPS. The peptide C-terminal functional groups are determined by the resin used. For the synthesis of C-terminal peptide amides, rink amide resin, pal resin and Sieber resin can be used. These resins are compatible with Fmoc-based peptide synthesis and can be cleaved by TFA at final stage. **Figure 2.12** shows the structures of resins used for peptide amide chemistry.

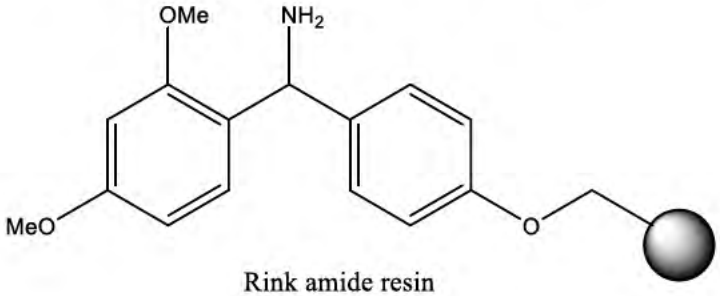

Rink amide resin

Universiti Malaya

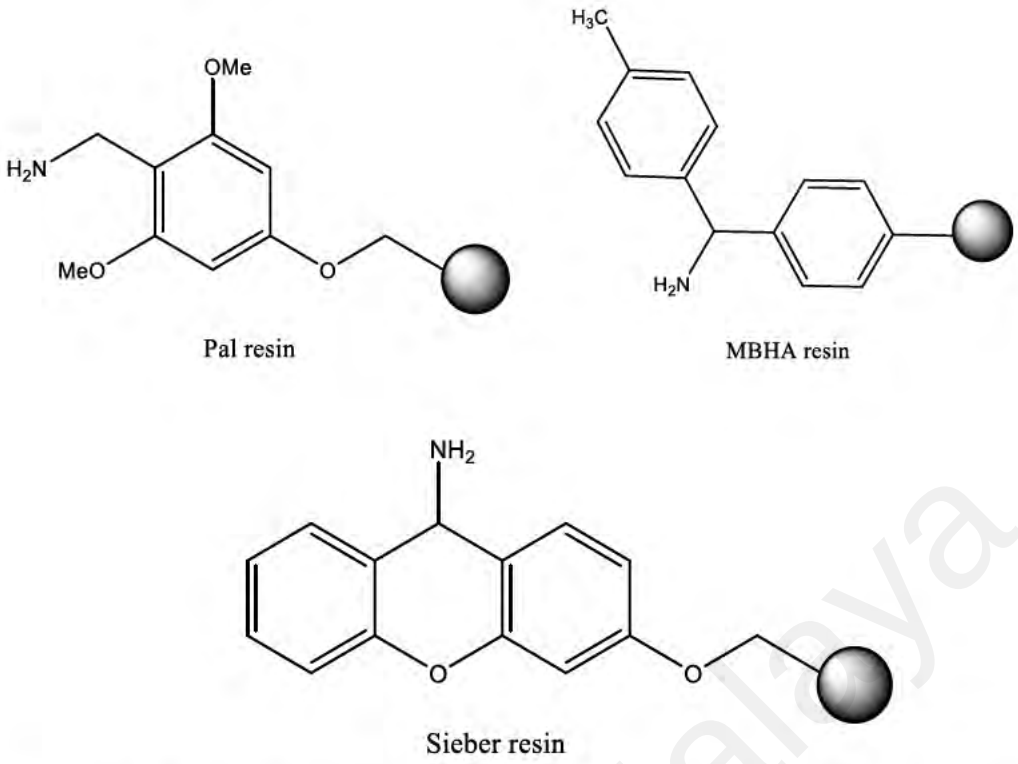

Figure 2.12: Resins for peptide amide chemistry. Silver ball represents the solid support, a place for functionalization.

Peptide acids are commonly used in peptide field where the first amino acids will be anchored to the solid support by esterification process. Wang resin, HMPB resin, trityl chloride resin, chlorotrityl chloride resin, sasrin resin and many more which can be used to produce peptide acids. They are well suited for Fmoc/tBu strategy for the peptide synthesis. **Figure 2.13** shows the structures of resins used for peptide acid chemistry.

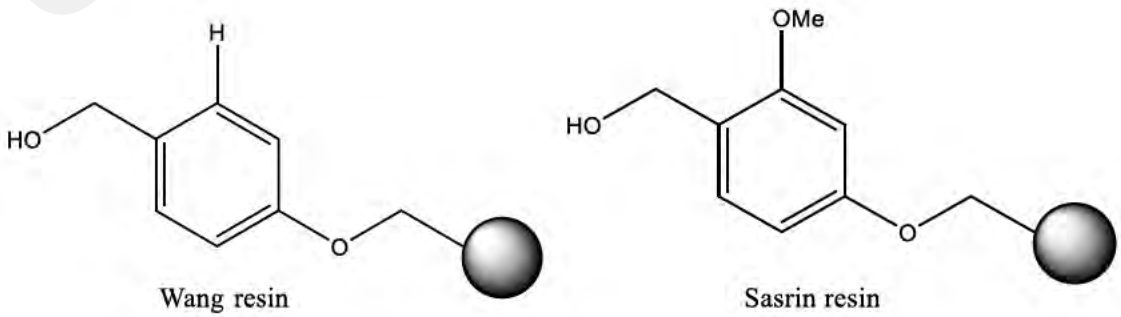

Universiti Malaya

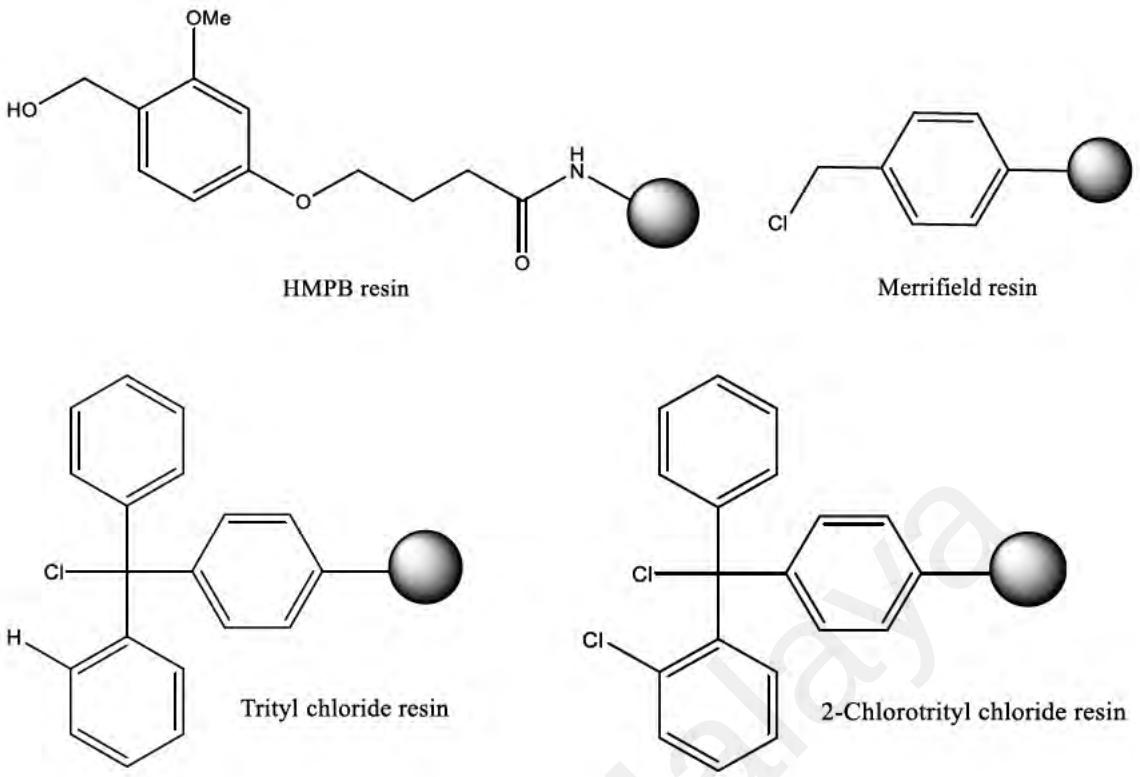

Figure 2.13: Resins for peptide acid synthesis. Silver ball represents the solid support, a place for functionalization.

2.4.2.3 Reagents for peptide synthesis

Generally, for SPPS, there are three major steps to be followed to obtain the desired peptide. Those are deprotection step, coupling step and final cleavage of peptide from the resin. In Fmoc-chemistry, piperidine will be used as deprotection solution while for Boc-chemistry TFA will act as deprotection agent during the deprotection step. For final cleavage, there would be TFA, Tis and water which helps in cleaving the final peptide from the resin.

Meanwhile, for coupling step, few reagents will be used as a mixture. DIPEA act as a base, DMF as solvent and a coupling agent. There are many coupling reagents available for peptide synthesis. These reagents have been categorized according to their chemical structures. **Table 2.6** to **Table 2.9** shows the type of coupling reagents which are currently usable in peptide synthesis (El-Faham & Albericio, 2011). Among all the

Universiti Malaya

coupling agent categories, commonly carbodiimides based coupling reagents are not preferred as the coupling reaction can leads to the production of urea as a byproduct.

Table 2.6: Carbodiimide based coupling reagents in peptide synthesis.

Carbodiimides
Dicyclohexyl carbodiimide (DCC) 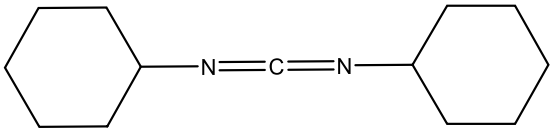 ✓ Gives low racemization when used together with HOBt and HOAt. ✓ Forms insoluble by product.
1,3-Diisocaropropylcarbodiimide (DIC) 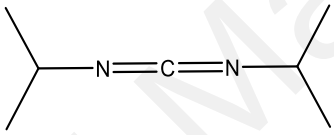 ✓ Gives low racemization when used together with HOBt and HOAt. ✓ Less moisture sensitive. ✓ Works very efficiently at elevated temperature. ✓
1-Ethyl-3-(3-dimethylaminopropyl) carbodiimide (EDC) 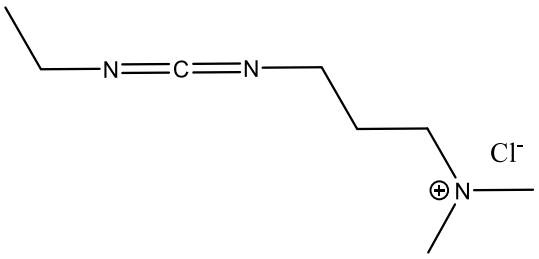 ✓ Used to conjugate proteins with linkers or labels. ✓ The by product and reagent are water soluble

Universiti Malaya

Table 2.7: Phosphonium based coupling reagents in peptide synthesis..

Phosphonium
(benzotriazol-1-yloxytris(dimethylamino)phosphonium hexafluorophosphate), (BOP) 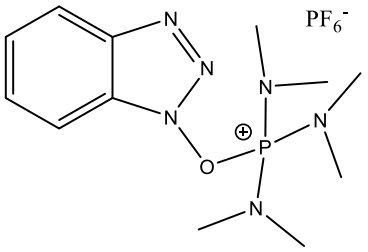 ➢ Minimal racemization ➢ Form esters carcinogenic byproduct.
(benzotriazol-1-yl-oxytripyrrolidinophosphonium hexafluorophosphate), (PyBOP) 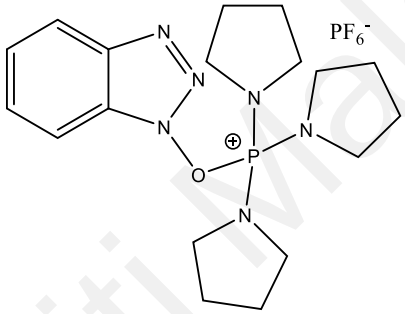 ➢ Takes few minutes to complete the coupling reaction. ➢ The byproducts are less hazardous than BOP.
((7-Azabenzotriazol-1-yloxy) tripyrrolidinophosphonium hexafluorophosphate), (PyAOP) 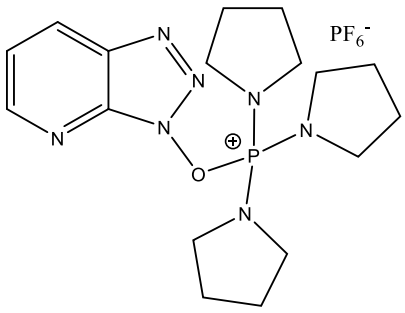 ➢ Highly effective and can cyclize the linear peptides

Universiti Malaya

Table 2.7, continued.

Phosphonium
Bromo-tris(pyrrolidino)- phosphonium hexafluorophosphate (PyBroP) 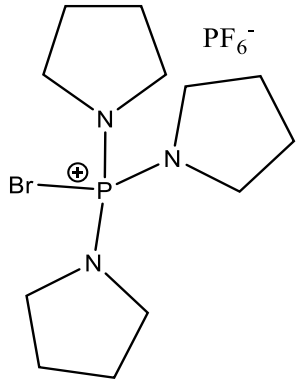   ➢ Very reactive ➢ Couples dialkyl amino acids
Bis (2-oxo-3- oxazolidinyl) phosphinic chloride (BOP-Cl) 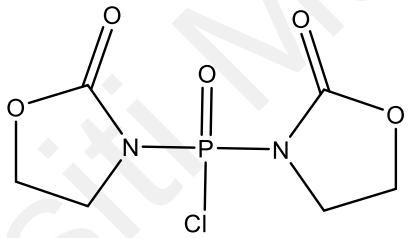   ➢ Can cyclize linear peptides. ➢ Couples dialkyl amino acids also.

University Malaya

Table 2.8: Aminium based coupling reagents in peptide synthesis..

Aminium
(2-(1H-benzotriazol-1-yl)-1,1,3,3-tetramethyluronium hexafluorophosphate (HBTU) 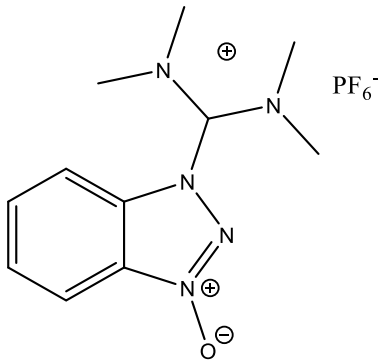 ❖ Highly effective ❖ Leads to little racemization ❖ Can complete the coupling reactions within few minutes. ❖ May cause allergic reactions.
(1-[Bis(dimethylamino)methylene]-1H-1,2,3-triazolo[4,5-b] pyridinium 3-oxide hexafluorophosphate (HATU) 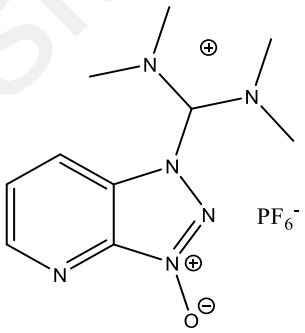 ❖ Expensive ❖ Reacts faster than HBTU. ❖ Produce little racemic products.

Universiti Malaya

Table 2.8, continued.

Aminium
O-(1H-6-Chlorobenzotriazole-1-yl)-1,1,3,3-tetramethyluronium hexafluorophosphate (HCTU) 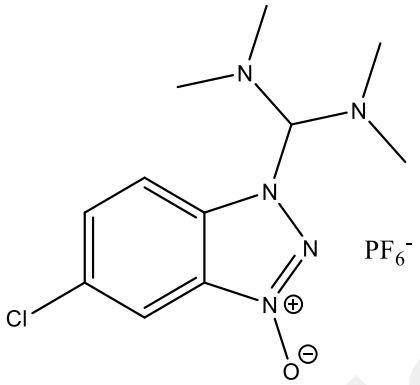 ➢ Has intermediate reactivity between HBTU and HATU. ➢ Less allergic ➢ Reduce racemization compared to BOP.

Universiti Malaya

Table 2.9: Uronium based coupling reagents in peptide synthesis..

Uronium
O-(N-Suc-cinimidyl)-1,1,3,3-tetramethyl-uronium tetrafluoroborate (TSTU) 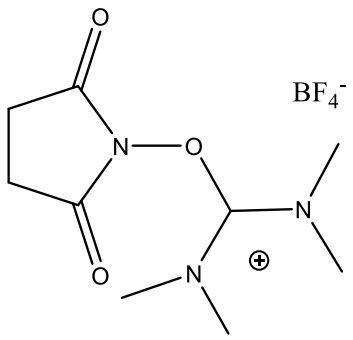   ▪ Used in coupling glycopeptides and conjugating oligosaccharides to proteins. ▪ No racemic product will be formed when used with HOSu and $CuCl_2$.
O-(5-Norbornene-2,3-dicarboximido)-N,N,N',N'-tetramethyluronium tetrafluoroborate (TNTU) 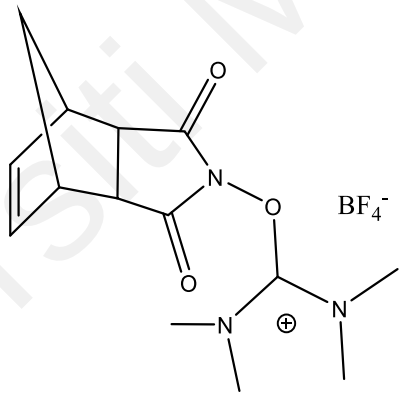   ▪ Used in conjugating biomolecules to linkers.
O-[(Ethoxycarbonyl)cyanomethylenamino]-N,N,NÆ,NÆ-tetramethyluronium tetrafluoroborate (TOTU) 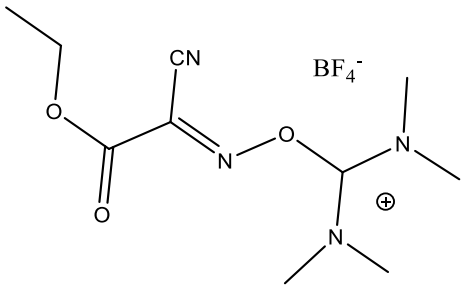   ▪ Couples acid to secondary amines.

Universiti Malaya

Table 2.9, continued.

Uronium O-(1,2-Dihydro-2-oxo-1-pyridyl-N,N,N',N'-tetramethyluronium tetrafluoroborate (TPTU)

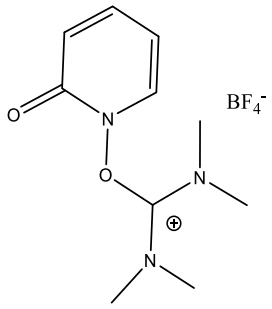

- Produces high coupling yields.
- More racemic products compare to others.

Universiti Malaya

CHAPTER 3 RESEARCH METHODOLOGY

Materials All the Fmoc-amino acids, 2-chlorotrityl chloride resin (2-CTC), rink amide MBHA resin and O-(1H-6-Chloro-benzotriazole-1-yl)-1,1,3,3-tetramethyluronium hexafluorophosphate (HCTU) salt were purchased from Novabiochem (Darmstadt, Germany). Di-isopropylamine (DIPEA), piperidine, trifluoroacetic acid (TFA), acetic anhydride, triisopropylsilane (TIS) and N, N-dimethylformamide (DMF) were obtained from Merck (Darmstadt, Germany). Methanol (MeOH) and diethyl ether (Et2O) was obtained from Friendemann Schmidt (Washington, USA). Dichloromethane (DCM) was from Duksan (Kyungkido, Korea) while acetonitrile (ACN) was from Elite Advanced Materials (Rawang, Malaysia). HPLC grade ACN was obtained from Fulltime (Anhui, China). DMEM (high glucose) was purchased from Nacalai Tesque Inc (Kyoto, Japan).

Instruments HPLC (Model: Shimadzu, SIL-20AHT Prominence UFLC), LCMS (Model: Agilent Technologies, 6650 iFunnel Q-TOF) and Freeze drier (Model: Martin Christ, Alpha 1-2 LDplus)

3.1 Computational studies

3.1.1 Rational design of peptide-based inhibitors

The parent peptide sequence was chosen from DN58opt, TWWCFYFCRRHHPFWFFYRHN. The peptide sequence 'WCFYFC' was selected and served as 'core' for the design of new peptide inhibitors. Peptide length of 7 to 10 monomeric amino acids (7-mer to 10-mer) repeats was designed by manipulating the peptide length from either the N- or C-terminal from the core sequence. For instance, **W**WCFYFC and WCFYFC**R** are the designed 7-mer peptides from the core. Using this technique, a total of 12 peptide sequences were designed and proceed with molecular docking to obtain potential peptide candidates.

Universiti Malaya

3.1.2 Preparation of receptor and ligands for computational studies

The X-ray crystal structure of the DV2 E protein in the pre-fusion form was retrieved from Protein Data Bank (PDB ID: 1OAN) (Berman et al., 2000) and used as an initial structure for the docking studies. After removal of water molecules and non-protein molecules, the initial structure was optimized in Discovery Studio 2.5.5 (Dassault Systèmes BIOVIA, 2017). The 3D structures of the designed peptides were generated from peptide tertiary structure prediction server (Kaur et al., 2007) based on β-turn information together with regular secondary structure states (Kaur et al., 2007). The obtained structures were minimized using Discovery Studio 2.5.5 by means of CHARMm forcefield followed by Smart Minimizer algorithm performing 1000 steps of Steepest Descent with a root mean square (RMS) gradient tolerance of three, followed by Conjugate Gradient minimization, until the RMS gradient for potential energy was less than 0.05 kcal/mol/Å was satisfied.

Auto-DockTools 1.5.4 was used to process the designed 3D structures safeguarding that their atoms were assigned the correct AutoDock atom types, adding Gasteiger charges, merging nonpolar hydrogens, detecting aromatic carbons if any, and setting up the 'torsion tree'. (Isa et al., 2019).

3.1.3 Molecular docking studies

To analyze the binding interactions of the peptides towards DV E protein, docking studies were carried out in two steps via Autodock Vina 1.5.6 software (Trott & Olson, 2010). Firstly, a blind molecular docking strategy, using grid box covering the whole protein, was performed, and permitted the determination of the DI/DIII hinge region of E protein as the potential binding site of the designed peptides that was subsequently validated using the MetaPocket 2.0 server (Huang, 2009). All eight predictors namely, POCASA, ConCavity, GHECOM, Fpocket, SURFNET, Q-SiteFinder, PASS and

Universiti Malaya

LIGSITEcs are ran in parallel by the program and the zscore is calculated for each pocket site from different predictors and thus, made it possible to rank and compare the values to get the final pocket sites (Zhang et al., 2011). Secondly, a focused docking was performed using a smaller grid box with a dimension of 60 x 60 x 60 (Å), centered on the defined potential binding site and accommodating the peptides to move freely. Then automated docking studies were carried out using the empirical free energy function and the Lamarckian Genetic Algorithm (LGA) applying a standard protocol, with an initial population of 150 randomly placed individuals and a maximum number of 2.5 x 10^6 energy evaluations, a maximum number of 27,000 generations, a mutation rate of 0.02, a crossover rate of 0.80 and an elitism value of 1. A total of 50 independent docking runs were carried out for each peptide and the parameters were set using Auto Dock Tools (ADT) . Structures differing by less than 2.0 Å in positional root-mean-square deviation (RMSD) were clustered together and the most favorable free binding energy complex structure was selected. (Miceli et al., 2013).

3.1.4 Molecular dynamics stimulation and binding free energy calculation

Molecular dynamics simulation was performed as mentioned earlier with minor modifications (Isa et al., 2019) using PMEMD.CUDA (Götz et al., 2012; Salomon-Ferrer et al., 2013) from AMBER 14 suite of programs (Case, Darden, & Cheatham, 2008). The structures of peptide–protein complexes from the docking were solvated in a cubic box of TIP3P water. Na+ ions were added to neutralize the complex and the cut-off radius was kept to 15 Å to compute the non-bonded interactions. All simulations were performed under periodic boundary conditions and long range electrostatic were treated based on the particle mesh Ewald (PME) method (Darden, York, & Pedersen, 1993; Essman et al., 1995).

Universiti Malaya

The SHAKE algorithm and Langevin dynamics were applied to constrain bonds that involve hydrogen and to control the temperature. The temperature of each system was gradually increased from 0 to 310.15 K over a period of 60 ps of NVT dynamics, followed by 300ps of NPT equilibration at 310.15 K and 1 atm pressure and finally a total 60 ns of the MD run. Trajectory analyses (root mean square deviation and hydrogen bond) were carried out using CPPTRAJ module from Amber 14 (Roe & Cheatham III, 2013). The binding free energy of each complex was calculated based on Amber molecular mechanics Poisson– Boltzmann surface area (MM-PBSA) (Kollman et al., 2000) protocol. The structural images were generated using PyMOL 1.6 (DeLano, W.L., 2002).

$$G = E_{bdn} + E_{el} + E_{vdW} + G_{pol} + G_{np} - TS \quad (3.1)$$

Where, G refers to binding free energy; E_{bdn} is the binding energy; E_{el} refers the electrostatic interaction energy between the ligand and surrounding; E_{vdW} represents van der Waals interaction between ligand and surrounding; G_{pol} and G_{np} refers to the polar and non-polar contributions to the solvation free energies; T and S are representing temperature and entropy, respectively. This equation implies the calculation of MM-PBSA binding free energy (Genheden & Ryde, 2015) .

3.2 Peptide synthesis

The peptides were synthesized following the conventional Fmoc-SPPS approach as previously reported (Fuaad et., 2015, 2016). The peptides were synthesized manually without the usage of peptide synthesizer. Generally, the synthesis involves removal of N-terminal Fmoc protecting group, amino acid coupling, and peptide cleavage from solid support.

A 0.05mmol scale manual synthesis was performed. The overall peptide synthesis procedure is summarized in **Figure 3.1**. For this research, 2-CTC resin (substituition 1.47

Universiti Malaya

mmol/g) for AC 001 and Rink Amide resin (substituition 0.40 mmol/g) for the peptides which had cysteine at the C-terminal, AC 002, AC 003 and AC 004 were utilized.

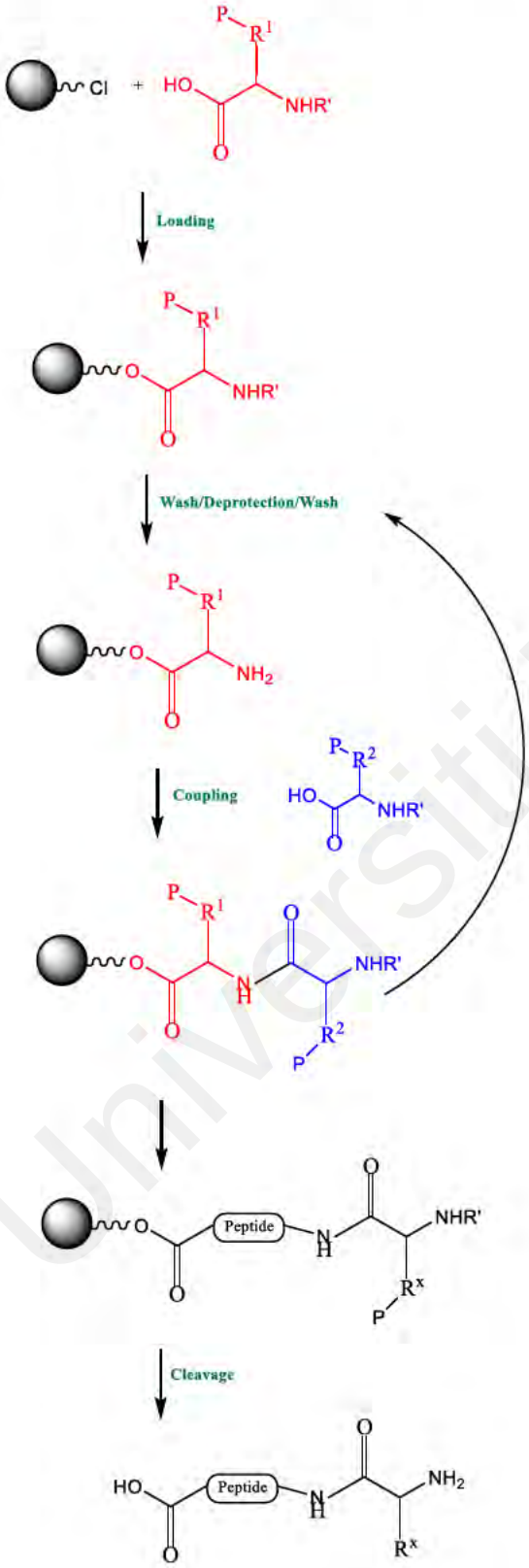

(a) (b)

Universiti Malaya

Figure 3.1: (a) Fmoc- solid phase peptide synthesis for 2-CTC resin (b) Fmoc- solid phase peptide synthesis for rink amide resin. (Key: Silver ball represents the resin; P represents protecting group; R indicates the side chains; R' represents Fmoc)

Resin swelling

a) 2-CTC

The resins (0.034g) were placed in a peptide vessel and suspended in DCM for 5 minutes. DCM then removed by filtration under vacuum. (Ieronymaki et al., 2015)

b) Rink amide resin

Similarly, the resin (0.125g) was placed in a peptide vessel and 5mL of DMF was added into it. Once the DMF was removed, 20% piperidine (2 times × 5mL) was added to remove the protected amino group on the resin for further coupling. Before coupling, the resin was washed with DMF (3 times × 3 mL). (Kreutzer et al., 2018)

Removal of Fmoc protecting group

20% piperidine/DMF (5mL) was added into the peptide vessel and stirred for 5 minutes and rinsed with DMF. Fresh deprotection solution was added again and left for 10 minutes. These steps were done three times. (Kreutzer et al., 2018)

Coupling of amino acids

The resins was pre-swelled in DMF for 5 minutes ans washed throughly with DMF. In a separate flask, 4 equivalent (eq) of amino acids, 4eq of HCTU (0.08g), and 4eq of DIPEA (100µL) was dissolved in DMF, then sonicated for 2 minutes. The activated amino acids then was added into the reaction vessel and allowed to stir for an hour at room temparature. After an hour, the resin was washed 3 times each with DMF, DCM and followed by methanol (each 5mL) (Kreutzer et al., 2018).

Cleavage of peptide from the resin

This cleavage procedure is applicable for both 2-CTC and rink amide resin. The cleaving solution (10mL) was prepared freshly with the ratio of (95:2.5:2.5) =

Universiti Malaya

(TFA:Tis:H_2O). The solution then was added into a container which was pre-filled with resins. The mixture was stirred under room temperature. The cleaving duration will vary according to the amino acid sequences. Our peptides contain Arg(Mtr), therefore 30 minutes will be added for each Arg(Mtr) for the cleaving time. (Palomo, 2014)

Once the reaction complete, the filtrates was transferred into round bottom flask and rinsed with TFA. Cold ether was added into the filtrates with the ratio of 10:1=Et_2O:TFA to precipitate out the peptides. Later, once the peptides precipitate out, it was centrifuged for 10 minutes with 4 rpm. This was done twice to ensure the removal of impurities. Once cold ether was dispensed, 2mL of 50% ACN/H_2O was added into the peptide, lypholized and purified in reversed phase HPLC. (Kreutzer et al., 2018)

Peptide purification and analysis

Peptides crude were purified by analytical reverse phase HPLC at room temperature using Phenomenex Luna C18 column (5 µm, 100 A, 250 x 4.6 mm) with gradients of 0% (ACN, 0.1% TFA) to 100% (ACN, 0.1% TFA) with respect to H_2O over 40 minutes (2.5% ACN/min) with a flow rate of 1 mL/min. The eluent was characterised by monitoning the overlapping of the wavelength of 214 nm and 280 nm. The final products were verified by HPLC and LCMS using m/z value. (Aguilar, 2004). Purity of the peptide sample was detected using UV absorbance in HPLC at 214 nm and 280 nm.

$$\% \, Purity = \frac{\text{Mass of pure compound}}{\text{Total mass of impure sample}} \times 100 \qquad (3.2)$$

Universiti Malaya

3.3 Screening of peptides towards dengue virus using Vero cells

3.3.1 Cells and virus

Vero E6 cells were obtained from ATCC (USA) and maintained in high glucose DMEM (Nacalai Tesque, Japan) supplemented with 10% FBS (Tico Europe, Netherlands) and 100 U/ml penicillin/streptomycin mix (Nacalai Tesque, Japan). DV2 (New Guinea C strain) was a gift from the Department of Medical Microbiology, University of Malaya, Malaysia. The virus was propagated in C6/36 cells using Leibovitz's L-15 medium (Sigma) containing 2% FBS and 100 U/ml of penicillin/streptomycin. The plaque assay was carried out to determine the titre of the stock. In short, Vero cells were seeded in a 6-well plate and incubated at 37ºC in 5% CO_2 for 24 hours. The cells were infected with serially diluted viral inoculums for one hour with gentle mixing after every 15 minutes. After infection, the cells were washed and layered with DMEM supplemented with 2% FBS, 100 U/ml of penicillin/streptomycin, and 0.5% agarose (ACTGene, USA). After 48 hours of culture, the cells were fixed with 4% paraformaldehyde (Merck) for 15 minutes at room temperature, washed with 1x PBS (Sigma), and stained with crystal violet (Sigma). The number of plaques was counted to determine the stock titre.

3.3.2 MTS cytotoxicity assay

Solubility test for the synthesized peptide has been tested prior to conducting bioassays. All the AC 001, AC 002, AC 003, and AC 004 were soluble in DMSO at the concentrations of 100µM and 200µM.

Vero cells were seeded in a 96-well plate and incubated for an overnight. The AC peptides were prepared in four different concentrations (0, 25, 50, and 100 µM) in DMEM

Universiti Malaya

culture medium. The media in the wells were replaced with fresh media containing the peptides or DMSO as a control. After 48 hours, cell viability was measured using Non-Radioactive Cell Proliferation assay (Promega) according to the manufacturer's instructions. The absorbance was recorded using Bio-Rad Model 680 Microplate Reader (USA). The absorbance for each well was corrected against no-cell blank and normalized to their respective DMSO control wells. Each sample was assayed in duplicate and the experiment was repeated three times (n=3).

3.3.3 Plaque formation assay

Vero cells were plated in 12-well plates and incubated for 24 hours at 37 ºC with 5% CO_2. 200 PFU of DV2 were incubated with 100 µM of the peptides at 37ºC for 30 minutes. DMSO (1% v/v) and ribavirin served as the negative and positive control, respectively. The peptide and DV2 mixtures were then removed from the well plates and the cells were washed and layered with DMEM supplemented with 2% FBS, 100 U/ml of penicillin/streptomycin, and 0.5% agarose. After 3 days of culture at 37 ºC with 5% CO_2, the cells were fixed with 4% paraformaldehyde for 15 minutes at room temperature, washed with 1x PBS , and stained with crystal violet (Yang et al., 2007). The number of the plaques in the treated samples was counted and plotted as a percentage of plaque reduction normalized to the DMSO/media control. The assay was repeated at least three times.

3.3.4 Statistical analysis

All statistical analyses were performed using Microsoft Excel and GraphPad Prism 5.0 software (Graph Pad Software, San Diego, CA). The statistical analysis between the treatment and control groups were performed using unequal variance T-test. P values of <0.05 considered to be statistically significant. All the experiments were done in triplicate and error bars were expressed as ± standard deviation.

Universiti Malaya

CHAPTER 4 RESULTS AND DISCUSSION

4.1 Rational design of peptide-based inhibitors

The peptide sequence DN58opt, TWWCFYFCRRHHPFWFFYRHN (Amir-Hassan et al., 2017; Xu et al., 2012) has been previously reported by Prof. Noorsaadah's team as a potent inhibitor of DV2 E protein. To identify the effective inhibitory sequence of DN58opt, the peptide sequence 'WCFYFC' was selected and served as 'core' for the design of new peptide inhibitors. Therefore, by varying the selection length at the N- and C-termini of DN58opt, 12 peptides sequence were designed using Autodock Vina version 1.5.6 (Trott & Olson, 2010) as shown in **Table 4.1**.

Table 4.1: Binding affinity value of 12 designed peptides.

No	Peptide ID	Peptide sequence	Length (aa)	Binding affinity (kcal/mol)
1	AC 001	WCFYFCRRH*	9	-7.0
2	AC 002	WCFYFC*	6	-6.1
3	AC 003	WWCFYFC*	7	-6.1
4	AC 004	TWWCFYFC*	8	-6.3
5	AC 005	WWCFYFCRR	9	-6.1
6	AC 006	WCFYFCRR	8	-6.0
7	AC 007	WWCFYFCRRH	10	-6.0
8	AC 008	WWCFYFCR	8	-5.9
9	AC 009	WWCFYFCR	8	-5.9
10	AC 010	WCFYFCR	7	-5.8
11	AC 011	WCFYFCRRHH	10	-5.8
12	AC 012	TWWCFYFCRR	10	-5.5

*****_Chosen peptide candidates for synthesis, biological screening and further docking analysis._

University Malaya

The 3D structures of the designed peptides were prepared using peptide tertiary structure prediction server (Kaur et al., 2007) and minimized using Discovery Studio version 2.5.5 (Dassault Systèmes BIOVIA, 2017). The potential binding pocket of DV2 E protein and its key residues were initially identified using blind docking of several peptides towards DV2 E protein crystal structure model (PDB ID: 1OAN) (Berman et al., 2000) using the software, Autodock Vina. Analysis of the blind docking results, particularly the binding poses, and affinities permitted to identify a small pocket in the DI/DIII hinge region as the peptides' potential binding site.

Subsequently, the MetaPocket 2.0 server was used to verify the validity of DV2 E protein binding pocket that was identified during blind docking. All available predictors namely, POCASA, ConCavity, GHECOM, Fpocket, SURFNET, Q-SiteFinder, PASS and LIGSITEcs were run in parallel by the MetaPocket 2.0 server to calculate the z-scores of all possible pockets on the protein surface and rank them (Huang, 2009). The results obtained from MetaPocket 2.0 server and the eight (8) other predictors confirmed that the potential binding site selected during the blind docking is DI/DIII hinge region of DV2 E protein.

This reflects the origin of DN58opt peptide sequence which is an optimized peptide sequence that was generated from wild type peptide, DN58wt. These two coded peptide sequences (DN58wt and DN58opt) are located at the DIII region of DV E protein (Xu et al., 2012). Besides, in the mid of findings of inhibitors against DV E protein, DI/DIII hinge region was previously reported, as one of the favorable binding sites for non-peptide inhibitors, particularly (5-(3-chlorophenyl)-N-(2-phenyl-2Hbenzo[d][1,2,3]triazol-6-yl) furan-2-carboxamide) (Dubey et al., 2017). Therefore, based on the binding energy and binding site at DI/DIII region, four (4) peptides (**Table 4.2**) were selected, synthetized, and screened against DV using plaque formation assay.

Universiti Malaya

Table 4.2: Docking binding energy of the 4 chosen peptides towards DV2 E protein at DI/DIII hinge region.

No	Peptide ID	Peptide sequence	Length (aa)	Binding energy (kcal/mol)
1	AC 001	$W_1C_2F_3Y_4F_5C_6R_7R_8H_9$	9	-7.0
2	AC 002	$W_1C_2F_3Y_4F_5C_6$	6	-6.1
3	AC 003	$W_1W_2C_3F_4Y_5F_6C_7$	7	-6.1
4	AC 004	$T_1W_2W_3C_4F_5Y_6F_7C_8$	8	-6.3

The estimated binding free energy obtained from AutoDock Vina for AC 001, AC 002, AC 003 and AC 004 ranges from – 7.0 kcal/mol to – 6.1 kcal/mol (**Table 4.2**). A lower estimated binding energy indicates stronger interactions between the peptides and the protein and vice versa. Consequently, AC 001 is predicted to inhibit the viral activity more efficiently than AC 004 followed by AC 002 and AC 003. Analyses of the plausible binding mode of the four peptides (**Figure 4.1** and **Figure 4.2**) showed that they bind in a similar fashion, i.e., into the binding pocket, with AC 001 being the nearest and occupying the pocket fully in comparison with the others.

Universiti Malaya

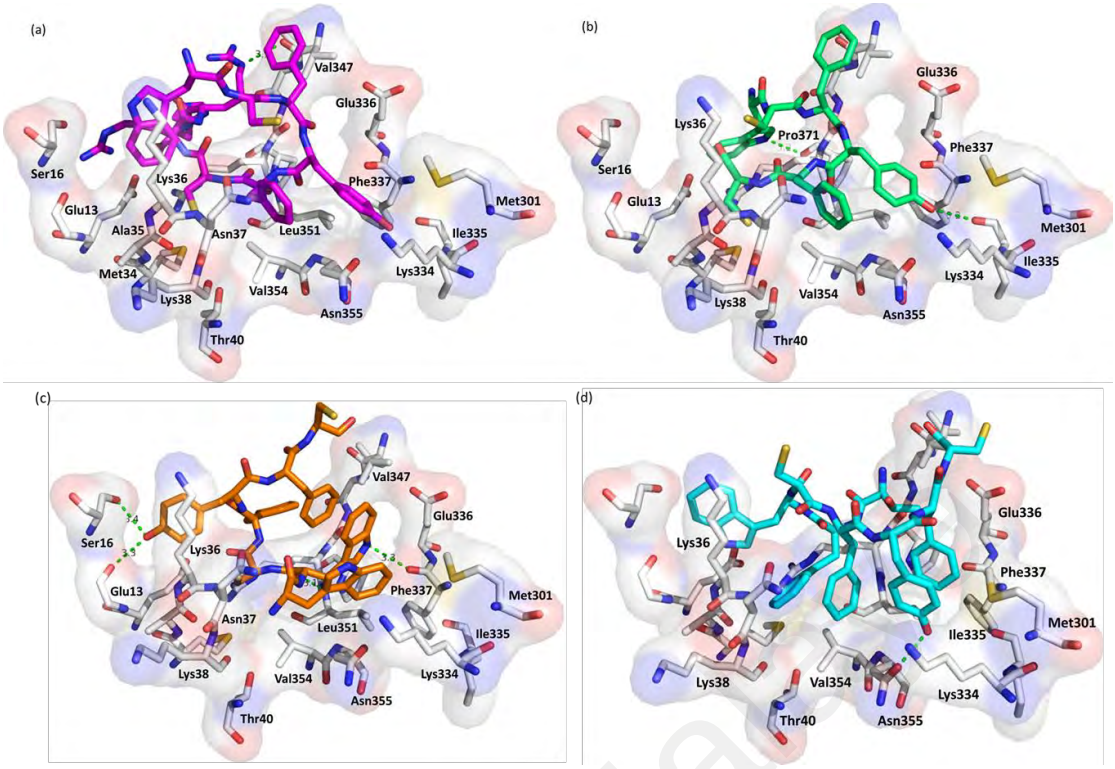

Figure 4.1: Binding poses of four chosen peptides into the binding pocket of the protein after docking analysis using Autodock Vina are shown separately. The surface represents the binding pocket of E protein while the peptides are shown in sticks. (a) AC 001, (b) AC 002, (c) AC 003 and (d) AC 004. The green dotted line shows the hydrogen bonding between the peptides and protein residues. The neighboring peptide residues which forms the binding pocket are labelled in blank font. The figure was created using PyMOL 1.6.

Universiti Ma

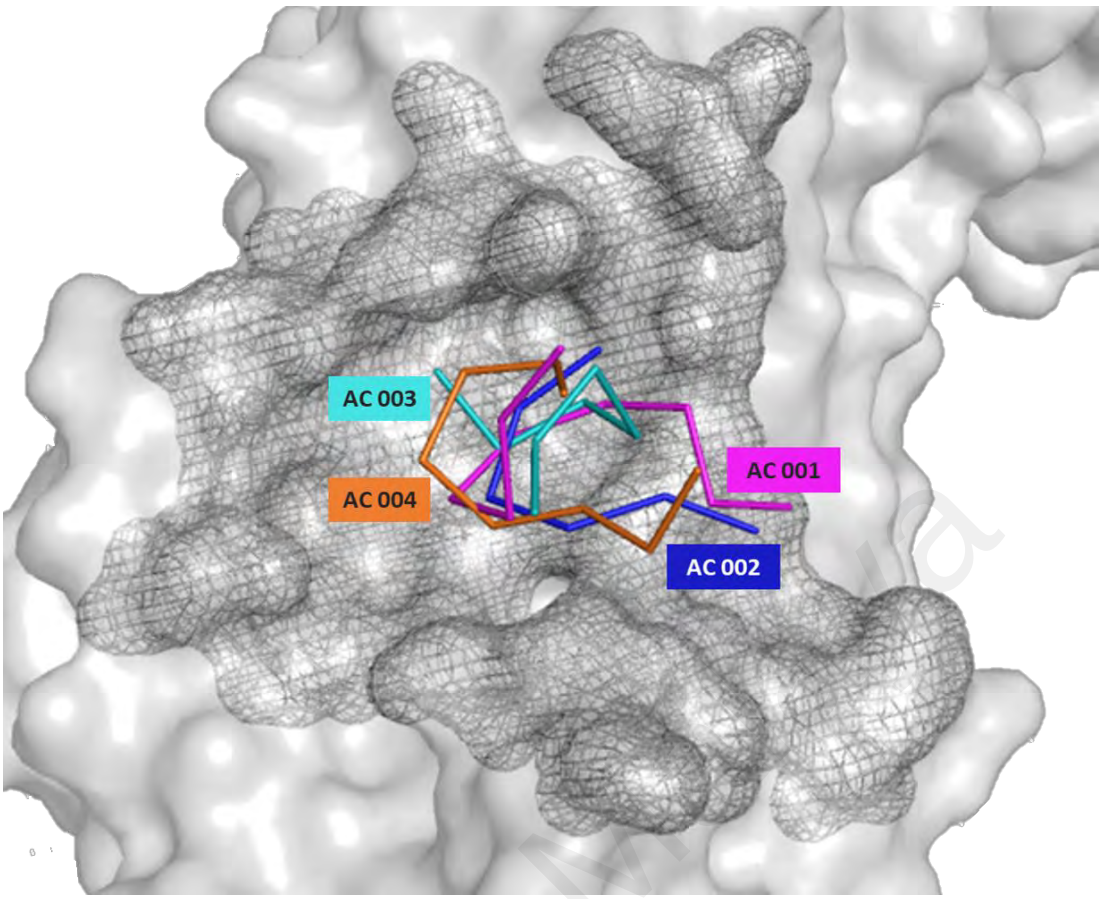

Figure 4.2: Superimposition of the best (lowest energy) binding poses of the 4 selected peptides into the binding pocket surface. Protein is presented in grey while the binding pocket is in mesh grey. The peptides are shown as ribbons: AC 001 (magneta), AC 002 (blue), AC 003 (cyan) and AC 004 (orange). The figure was created using PyMOL 1.6.

4.2 Peptide synthesis

The four designed peptides were manually synthesized using SPPS in a scale of 0.05 mmol. Since, the technique of preparing peptides is new for the current working laboratory, I start to synthesize the desired peptides from scratch. Therefore, the synthesis was optimized after facing many obstacles and failures.

4.2.1 Resin selection

Three of our peptide sequences have cysteine at carboxyl-terminal. For the first trial, the preloaded H-Cys (Acm)-2-CTC resin (resin loading: 0.62 mmol/g) was utilized to extend the peptide. About 75% of the desired peptide sequence was quantified by LCMS. Even though the peptide synthesis using the preloaded H-Cys (Acm)-2-CTC resin gave a satisfactory yield, yet the synthesis resulted to other byproducts. Additionally, the similar yield could not be reproduced for the next round. Therefore, it was concluded that using preloaded H-Cys(Acm)-2-CTC resin is not reliable.

Wang resin (substitution: 0.65 mmol/g) also was tried in the attempt to synthesis the same peptide sequence. In this case, some significant peaks were observed at 214 nm and 280 nm in the HPLC, which indicated the presence of peptide formed. Unfortunately, the peptides were not observed when analyzed with LCMS.

The peptide synthesis was revisited using new batch of 2-CTC resin (substitution: 1.47 mmol/g). Unfortunately, the synthesis still did not go well for the peptide sequence which had cysteine carboxyl-terminal because truncated peptides were obtained. Switching to rink amide resin from 2-CTC resin led to the desired peptides with cysteine at carboxyl-terminal. Rink amide resin worked very well for this where the desired peptides were synthesized without any byproducts.

Meanwhile, the Wang resin (substitution: 0.65 mmol/g) and preloaded Fmoc-His (trt) wang resin (substitution: 0.58 mmol/g) were also used to build the peptide with histidine at carboxyl-terminal. Unfortunately, both the resin did not lead to a reasonable peptide yield. However, the 2-CTC resin was utilized to synthesize the peptide and led to a satisfactory outcome with less by product. Therefore, 2-CTC resin for AC 001 and rink amide for AC 002, AC 003, and AC 004 were used.

Universiti Malaya

4.2.2 Optimization of deprotection step

Water is one of the factors behind the failure synthesis. Therefore, for optimum output, solvents were distilled, and the amino acids were freeze dried to remove excessive water content as the peptide synthesis are highly sensitive towards presence of water. Yet, the synthesis kept failing. Therefore, each step that are essential for peptide synthesis were optimized.

The Fmoc group is necessary to protect the amino group in an amino acid. Exposure of free amine group may lead to degradation of the amino acid. Therefore, Fmoc-protecting group is always preferable for a longer-term storage of peptide due to the high stability of Fmoc group. Piperidine, being basic in nature plays a major role in the deprotection of Fmoc group. Thus, with piperidine in the reaction mixture, the Fmoc group is deprotected to expose the free amino group in an amino acid.

For the synthesis in this project, 5% piperidine was used as a first trial during deprotection step. The peptide yield was low and truncated peptides were also formed. Hence, the percentage of piperidine was increased to 20% as reported in the literature. However, the deprotection of Fmoc group from the amine group was incomplete. This was verified using LCMS where, a peak with +222.5 Da ion was observed. This implies that the Fmoc group is intact with the amine group of the amino acid and lead to formation of truncated peptides. Subsequently, the combination of 1,8-Diazabicyclo [5.4.0] undec-7-ene (DBU) and piperidine were tried.

Both DBU and piperidine are basic but DBU is more basic in comparison with piperidine. Yet, only piperidine can capture the Fmoc group during deprotection step. DBU is only used to enhance the deprotection step which later brings the coupling step into completion. Therefore, several percentages of DBU and piperidine were tested for effective deprotection step. For instance, 1%DBU:20%piperidine,

Universiti Malaya

2%DBU:20%piperidine, and 3%DBU:20% piperidine which resulted in peptide yield of 35%, 22% and 18% respectively.

Unfortunately, having DBU in the reaction mixture created another challenge. We observed the formation of 3-(1-piperidinyl)alanine adduct as the side product at a higher percentage nearly, double the amount of desired peptide. This was verified when a peak with +51 Da ion at higher intensity was observed in LCMS spectrum. The +51 Da ion was only found on the cysteine at C-terminal of the peptide sequence. This side reaction is affected by many factors. In current synthesis, it might be due to DBU, which act as a strong base. The side reaction took place during the coupling of second amino acid next to cysteine and resulted in amide bond formation in which permitting for a base-catalyzed elimination and piperidine addition to occur (Lukszo et al., 1996). The mechanism for 3-(1-piperidinyl)alanine adduct formation is shown in **Scheme 4.1**.

As mentioned earlier, this side product is a huge trouble for my peptide research because there are three sequences with cysteine at the C-terminal in the chosen peptides. Therefore, to circumvent this problem, only 20% piperidine was used to deprotect the Fmoc instead of using DBU/piperidine mixture and fortunately, the side product has reduced with the absence of DBU.

Universiti Malaya

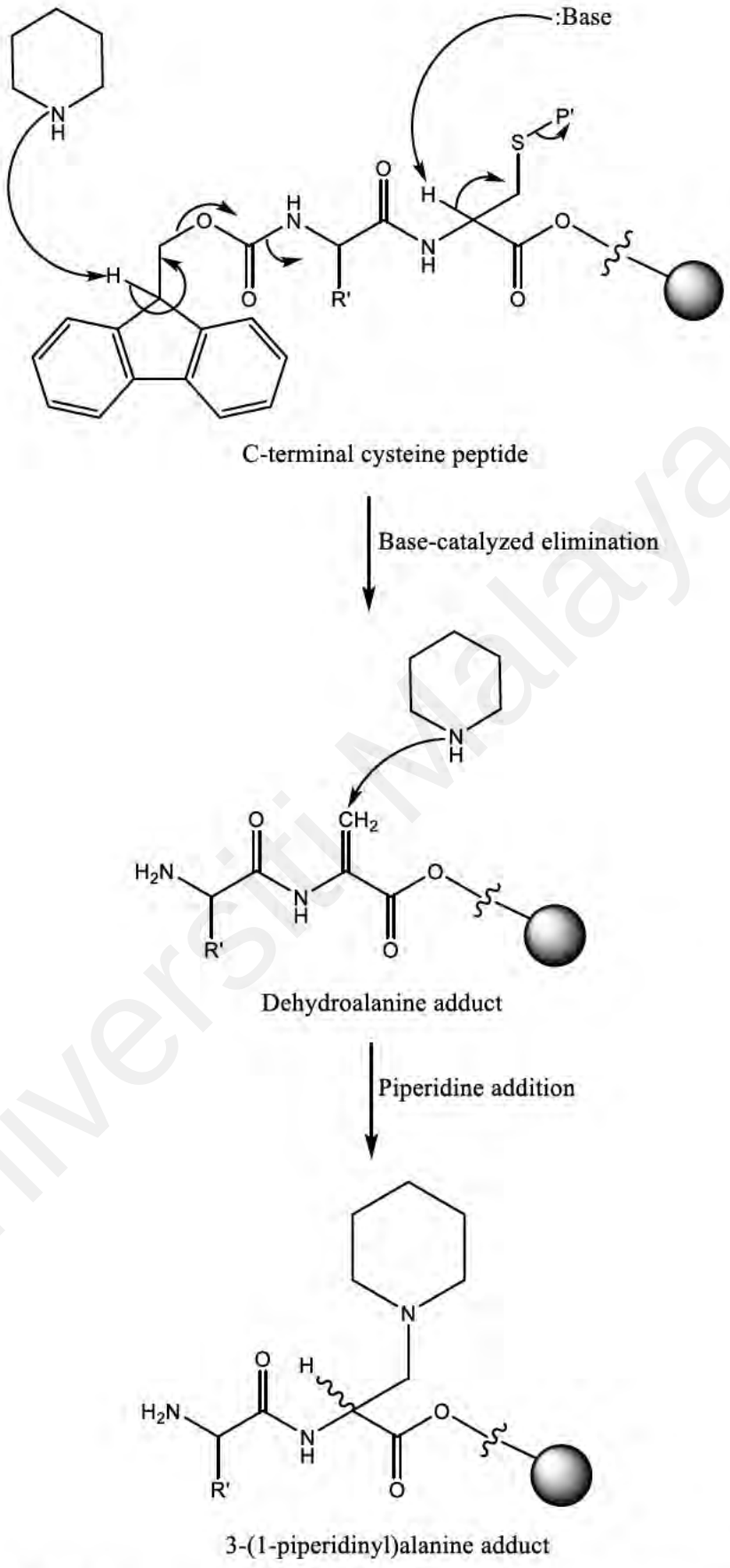

Scheme 4.1: Mechanism of 3-(1-piperidinyl)alanine adduct formation. (P'= Side chain protecting group, R'= Side chain).

Universiti Malaya

4.2.3 Optimization of amino acid coupling step

Coupling step needs a combination of reagents. HCTU, DIPEA, amino acids and DMF as solvent were utilized for the peptide synthesis. HCTU is a coupling reagent that is most often used since it has a reasonable price, high reactivity, and ability to reduce racemization. While DIPEA act as a base in the coupling reaction.

For optimization of the coupling step, the reaction duration time and number of couplings for each amino acid were studied, since each amino acid comes with different structure and nature. Some coupling steps were easier and required a shorter time to complete. While there were few coupling reactions which required more time due to the presence of bulky amino acids such as phenylalanine and tyrosine. In our peptide synthesis, the coupling of -FYF- sequence was very challenging as they are highly hydrophobic and bulky. Thus, it took more time and energy to optimize the -FYF- sequence. The formation of truncated peptides was the only recurring problem that was encountered along the peptide synthesis.

The occurrence of truncated peptides could be avoided by introducing additional acetylation step after each coupling step. Yet, the acetylation step was not effective for tyrosine coupling due to bulkiness issue/steric hinderance. This steric issue was verified when other less bulky amino acids like glycine, alanine, lysine, isoleucine, and phenylalanine were used to replace tyrosine in the peptide synthesis. Therefore, the acetylation step was introduced to all amino acids during their coupling step except when tyrosine is involved in the coupling reactions.

Moreover, the sequence of adding reagents that are required for coupling step is also one of the reasons for unsuccessful synthesis of the peptide. The sequence for addition of the reagents for optimized output is as shown below.

Add amino acid + HCTU → Add DMF → Sonicate (2-5) min → Transfer the mixture to reaction vessel

Universiti Malaya

The crude synthesized peptide was analyzed with LCMS and purified using reverse phase HPLC. The yield of the synthetized peptides is summarized in **Table 4.3**.

Table 4.3: The calculated yields of crude peptide after cleavage from resin and lyophilization (synthesis scale: 0.05 mmol).

Linear Peptide ID	Peptide sequence	Yield of crude peptide after lyophilization (mg)	Yield of semi purified peptide linear peptide (mg)
AC 001	WCFYFCRRH	30	5
AC 002	WCFYFC	20	18
AC 003	WWCFYFC	35	30
AC 004	TWWCFYFC	37	30

The experimental parameters of the peptides are also shown below:

Universiti Malaya

AC 001 Yield: 44.5%. Molecular weight: 1316.57. ESI-MS $[M+2H^+]^{2+}$ *m/z* 659.2937 (calculated 659.2850), $[M+3H^+]^{3+}$ *m/z* 439.8638 (calculated 439.8567), $[M+4H^+]^{4+}$ *m/z* 330.1498 (calculated 330.1425). R_t 19.0 min (0-100% ACN; C18 column), purity ≥ 85%.

(a)

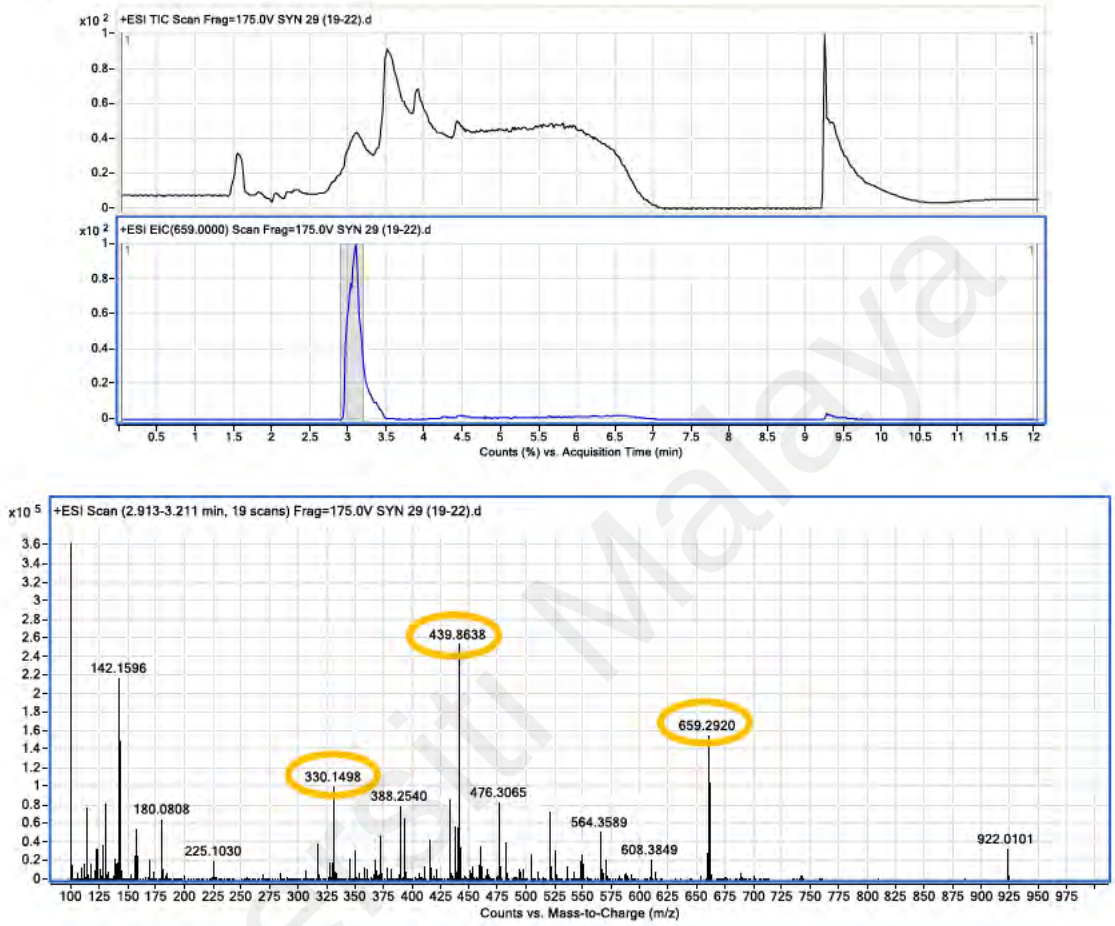

(b) (i) Crude

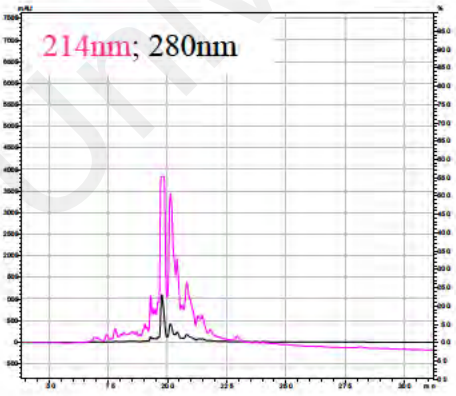

(ii) Purified

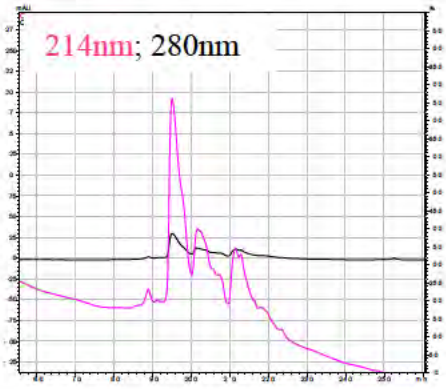

Figure 4.3: (a) MS data of AC 001; ESI-MS $[M+2H^+]^{2+}$ *m/z* 659.2937, $[M+3H^+]^{3+}$ *m/z* 439.8638, and $[M+4H^+]^{4+}$ *m/z* 330.1498; (b) (i) HPLC spectrum of crude AC 001, wavelength absorbance at 214nm and 280nm; R_t at 19.0 min. (ii) HPLC spectrum of purified AC 001, wavelength absorbance at 214nm and 280nm; R_t at 19.0 min.

Universiti Malaya

AC 002 Yield: 46.0%. Molecular weight: 866.32. ESI-MS $[M+H^+]^+$ *m/z* 867.3319 (calculated 867.3200), $[M+2H^+]^{2+}$ *m/z* 434.1684 (calculated 434.1600), $[M+4H^+]^{4+}$ *m/z* 218.2107 (calculated 217.5800). R_t 23.0 min (0-100% ACN; C18 column), purity ≥ 85%.

(a)

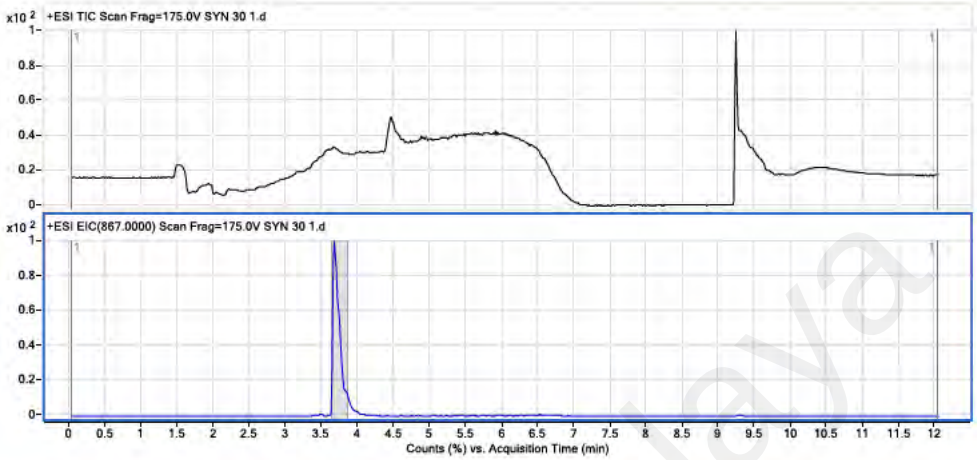

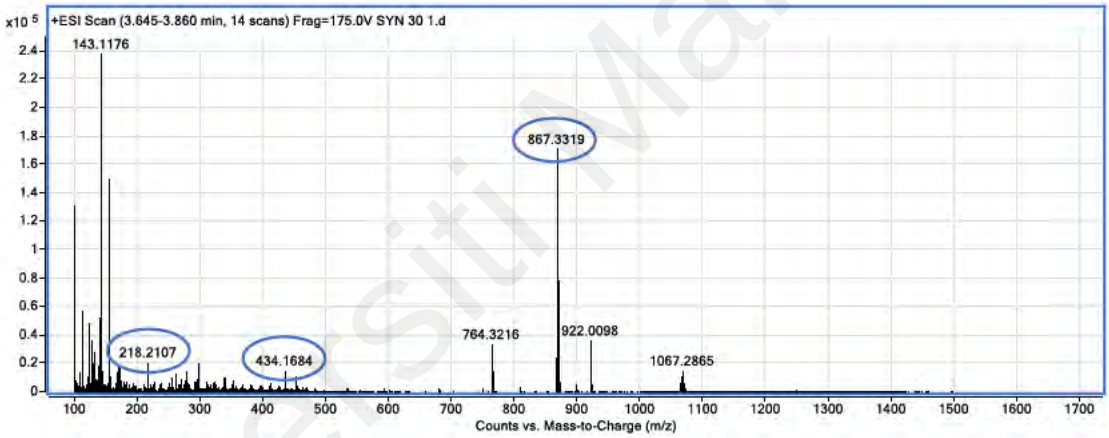

(b) (i) Crude

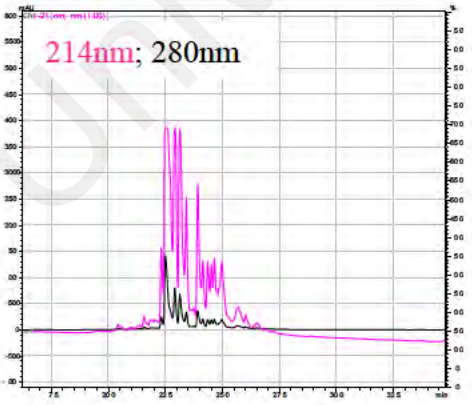

(ii) Purified

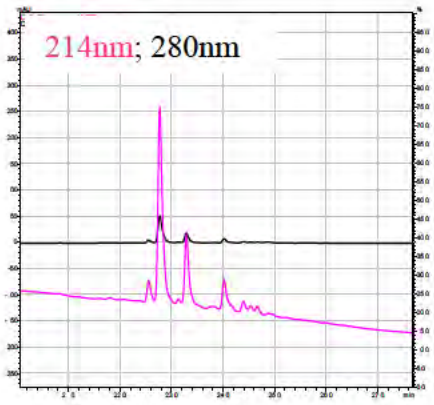

Figure 4.4: (a) MS data of AC 002; ESI-MS $[M+H+]^+$ m/z 867.3319, $[M+2H+]^{2+}$ m/z 434.1684, $[M+4H+]^{4+}$ m/z 218.2107. (b) (i) HPLC spectrum of crude AC 002; wavelength absorbance at 214nm and 280nm; R_t at 23.0 min. (ii) HPLC spectrum of purified AC 002; wavelength absorbance at 214nm and 280nm; R_t at 23.0 min.

Universiti Malaya

AC 003 Yield: 66.5%. Molecular weight: 1052.40. ESI-MS $[M+H^+]^+$ *m/z* 1053.4804 (calculated 1053.4000). R_t 24.0 min (0-100% ACN; C18 column), purity ≥ 85%.

(a)

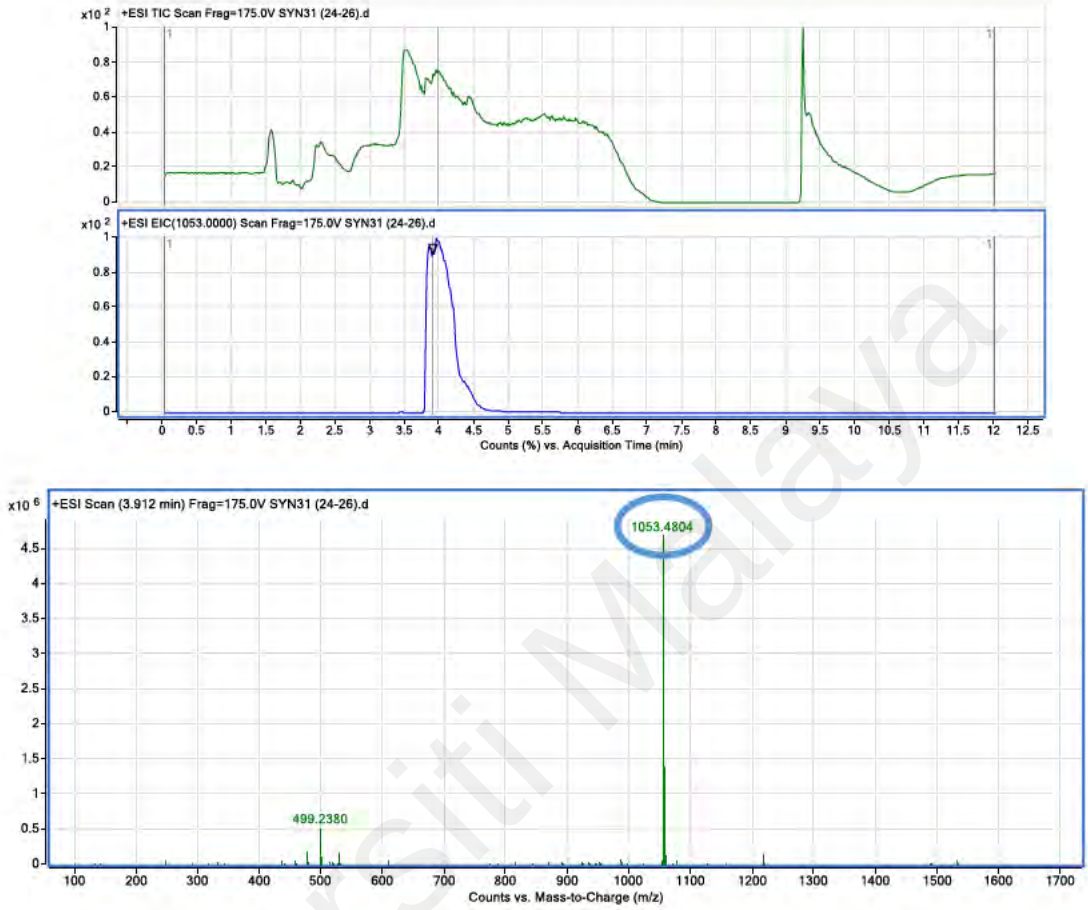

(b) (i) Crude

(ii) Purified

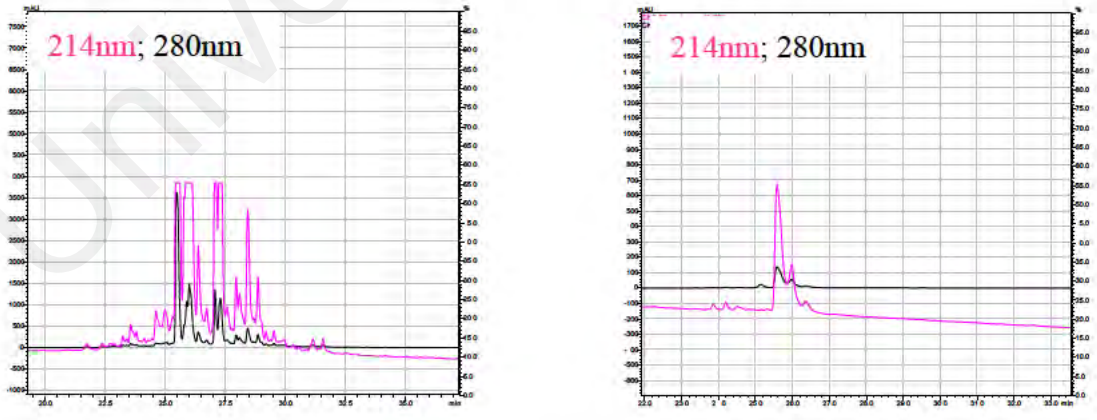

Figure 4.5: (a) MS data of AC 003; ESI-MS $[M+H^+]^+$ *m/z* 1053.4804. (b) (i) HPLC spectrum of crude AC 003; wavelength absorbance at 214nm and 280nm; R_t at 24.0 min. (ii) HPLC spectrum of purified AC 003; wavelength absorbance at 214nm and 280nm; R_t at 24.0 min.

Universiti Malaya

AC 004 Yield: 64.2%. Molecular weight: 1153.45. ESI-MS $[M+H^+]^+$ *m/z* 1154.4592 (calculated 1154.4500). R_t 25.0 min (0-100% ACN; C18 column), purity ≥ 85%.

(a)

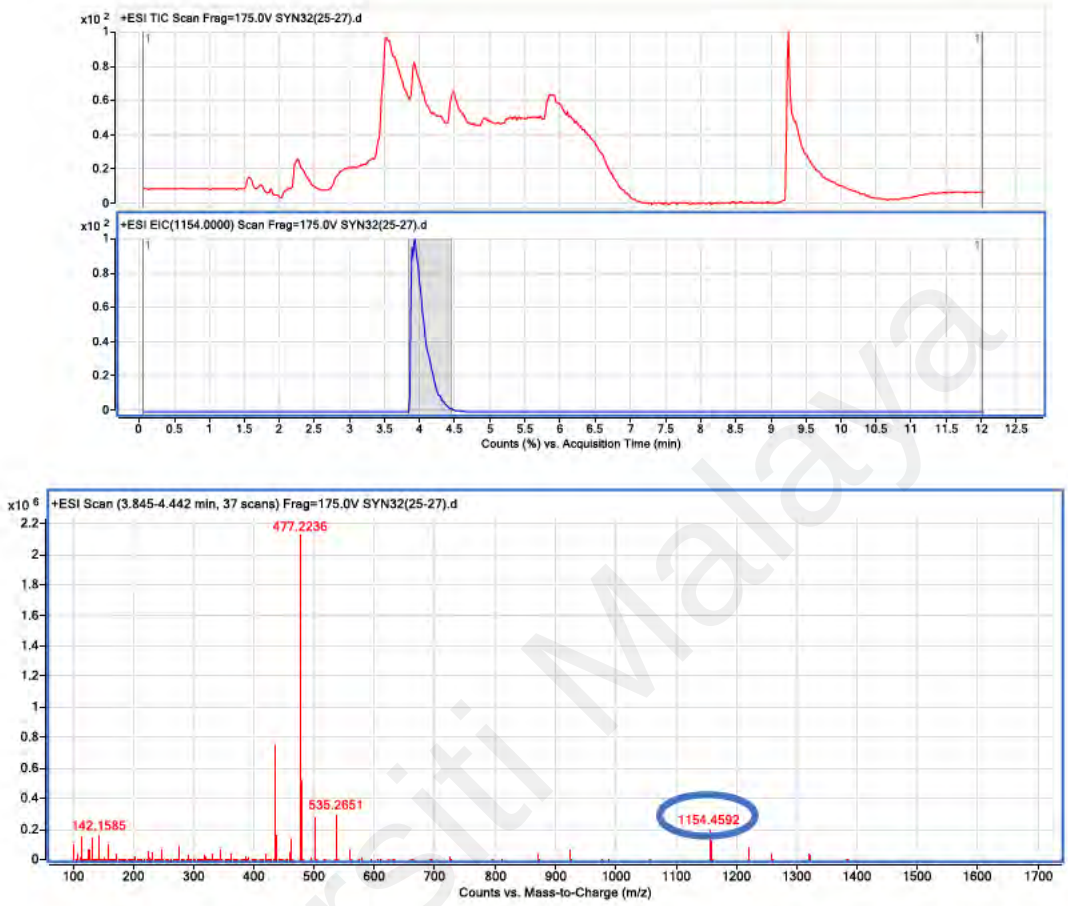

(b) (i) Crude

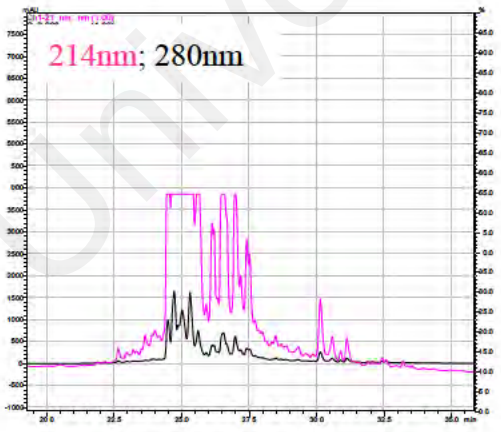

(ii) Purified

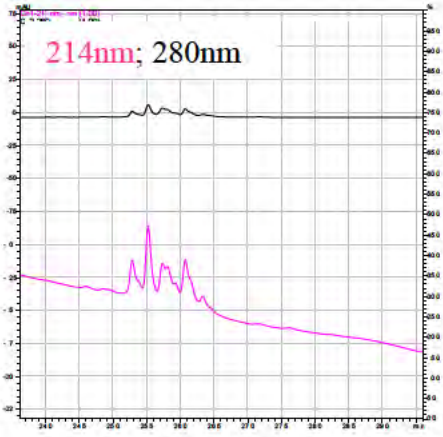

Figure 4.6: (a) MS data of AC 004; ESI-MS $[M+H^+]^+$ *m/z* 1154.4592. (b) (i) HPLC spectrum of crude AC 004; wavelength absorbance at 214nm and 280nm; R_t at 25.0 min. (ii) HPLC spectrum of purified AC 004; wavelength absorbance at 214nm and 280nm; R_t at 25.0 min.

Universiti Malaya

4.3 Screening of peptides with dengue virus using Vero cells

4.3.1 MTS cytotoxicity assay

In vitro analysis was performed for all four synthesized peptides which includes cytotoxicity assay and plaque formation assay. The cytotoxicity of the AC peptides on Vero cells was determined using MTS assay prior to the analysis of peptide antiviral activity against DV2. Cytotoxicity analysis is crucial to avoid false interpretation during the analysis of the antiviral activity. The Vero cells were exposed to different concentration of the designed peptides ranging from 0 to 100 µM (0, 25, 50, and 100 µM) in a 96-well culture plate for 48h. The cytotoxic effects of the peptides on the viability of the Vero cells are presented as percent cell viability compared to the control DMSO/media group (**Figure 4.7**). The peptides showed more than 97% viability at the tested concentrations with no significant difference compared to the control group. Therefore the peptides are considered non-cytotoxic.

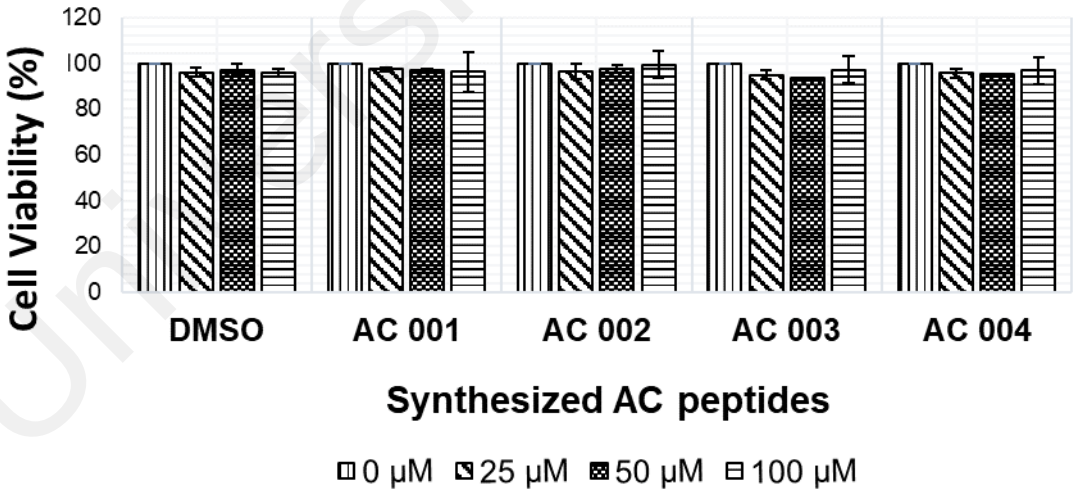

Figure 4.7: Cell viability of Vero cells after exposure to different concentrations of the AC peptides assessed by MTS assay in vitro.The Vero cells were treated with different concentrations of peptides (0, 25, 50, and 100) µM and DMSO served as a control. Cell viability analysis was done after 48 hours of treatment and absorbance was obtained at OD_{515nm}. The error bars represent ± standard deviations.

Universiti Malaya

4.3.2 Plaque formation assay

The synthetized peptides were screened *in vitro* to evaluate their potential inhibitory activity against DV2 using pre-treatment plaque formation assay. This assay is typically used to assess viral entry inhibition or viricidal activity (Aoki-Utsubo et al., 2018). All four AC peptides were evaluated for their antiviral activity at 100 µM. AC 001 showed significant inhibitory activity by reducing the plaque formation by 40.34% ± 5.9% followed by AC 004 (28.15% ± 5.6%), AC 002 (24.63% ± 8.9%), and AC 003 (22.28% ± 6.2%) as shown in **Figure 4.8**. Ribavirin, the positive control, inhibited plaque formation by about 33% ± 6%. Ribavirin is a guanosine analogue that blocks viral replication mainly by interfering with guanosine triphosphate (GTP) synthesis (Te et al., 2007).

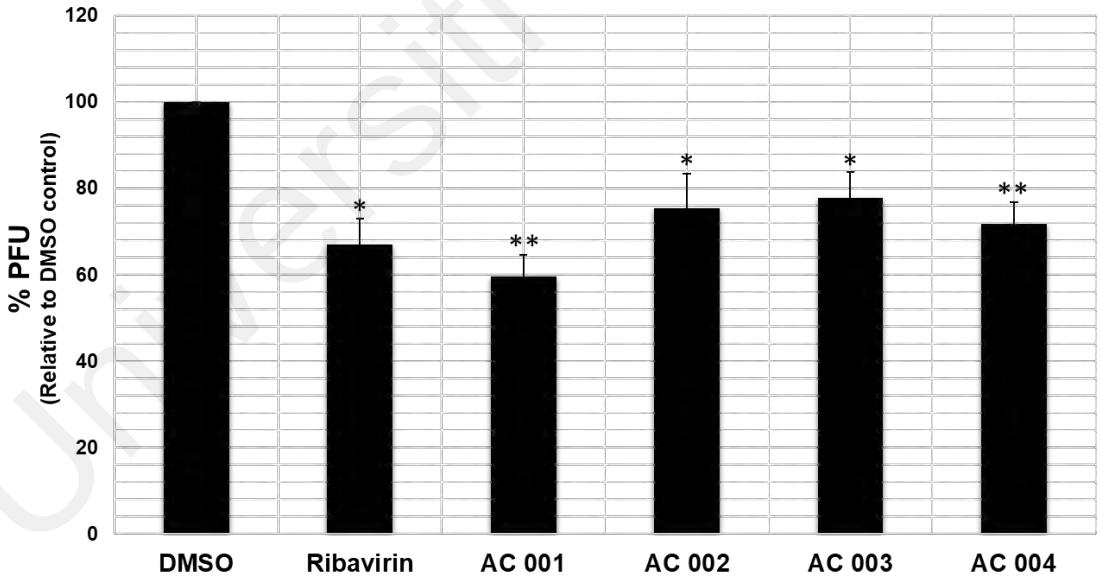

Figure 4.8: Antiviral activity of synthesized peptides against DV2 using plaque formation assay. The antiviral activity was performed by infecting the Vero cells with DV2 pre-incubated with AC peptide (200 PFU DV2 and 100 µM of peptide). AC 001 inhibited DV2 formation by 40.34% ± 5.9%. DMSO served as negative control while ribavirin as positive control. Each bar represents the mean with standard error of the means as the error bars. N=3. Asterisk denotes statistically significant difference (Paired T-test, **$p < 0.01$; *$p < 0.05$) from the negative control.

Universiti Malaya

Apart from direct inhibition on viral genome replication, ribavirin has also been shown to exert its antiviral activities via several different modes such inhibition of inosine monophosphate dehydrogenase, induction of RNA mutagenesis and immunomodulation (Te, H. S et al., 2007). Previously, it was reported that pre-treatment of viral inoculum with ribavirin reduced virus infection by about 40% (Rothan et al., 2015; de la Guardia et al., 2017). The partial inhibition was expected since the main mode of action for ribavirin is viral RNA replication. Importantly, we also observed a result similar to the previous report using ribavirin as the positive control in the present assay.

Based on the biological assay result, AC 001 showed a better inhibitory effect on DV2 while AC 003 being the least active inhibitor. This result confirms the binding affinity calculation depicted in **Table 4.2.** However, as biological system resolves around dynamics (fluid) interactions, a detailed molecular dynamics simulations studies were performed to find out the movement of complex atoms during a period of 60 ns. Molecular dynamics stimulations permit flexibility (fluid movement) to the peptide and protein receptor, therefore, facilitate the relaxation of the complete system and accounting the induced fit effects.

4.4 Molecular dynamics (MD)

4.4.1 Binding free energy calculation

The binding affinities ($\Delta E_{binding}$) were estimated by averaging snapshots taken from the molecular dynamics' trajectories using the molecular mechanics Poisson–Boltzmann surface area (MM-PBSA) method and are reported in **Table 4.4**.

Universiti Malaya

Table 4.4: Relative binding free energies of complexes estimated using MM-PBSA.

Peptide	vdW	EEL	EPB	EN POLAR	$\Delta E_{binding}$ (kcal/mol)*
AC 001	-46.85 ± 3.68	-177.91 ± 19.51	198.94 ± 20.37	-7.71 ± 0.39	-33.51 ± 5.11
AC 002	-18.49 ± 8.32	-103.55 ± 55.28	110.70 ± 52.92	-4.16 ± 1.43	-15.50 ± 7.11
AC 003	-38.17 ± 3.62	-32.99 ± 10.33	1.58 ± 8.54	-6.10 ± 0.32	-12.85 ± 4.98
AC 004	-59.60 ± 3.18	-78.82 ± 20.25	126.47 ± 18.24	-8.23 ± 0.32	-20.19 ± 6.14

Note: The vdW and EEL represent the van der Waals and electrostatic contributions from MM-PBSA, respectively. EPB stands for PB electrostatic contribution to the solvation free energy, and EN POLAR correspond to the nonpolar contribution to the solvation free energy. ΔE binding is the final estimated binding free energy. * - the low $\Delta E_{binding}$ might be due to entropic attributes were not included in a MM-PBSA calculation.

Universiti Malaya

By comparing, the binding free energies obtained from MM-PBSA calculation, AC 001 is predicted to be the most potent peptide of the series (-33.51± 5.11 Kcal/mol) followed by AC 004 (-20.19 ± 6.14 Kcal/mol), AC 002 (-15.50 ± 7.11 Kcal/mol) and then AC 003 (-12.85 ± 4.98 Kcal/mol). The computational data demonstrated a good correlation with the experimental results, where the inhibition activity of AC 001 is higher than AC 004, followed by AC 002 and AC 003 (**Figure 4.8**).

The van der Waals (vdW) interactions and non-polar parts of the solvation free energy contributes positively to the binding, as opposed to the unfavourable total electrostatic contributions (EEL+EPB) (**Table 4.4**). Each energy term (vdW, ENPOLAR, EEL+ EPB) was found to be more favourable upon binding of AC 001 in comparison with the other peptides in a correlated manner. To understand the obtained results, further studies, including system stability and flexibility and hydrogen bonds analysis were performed for the most active peptide AC 001 (40.34% ± 5.9%) and the least active peptide AC 003 (22.28% ± 6.2%).

4.4.2 System stability and flexibility

To evaluate the structural stability of the systems, root mean square deviations (RMSD) method was used to measure the difference between the backbones of DV2 E protein from its initial structural conformation till its final position (Law et al., 2005). The stability of the protein relative to its conformation can be determined by the deviations produced during its simulation. The lesser the deviations, the more stable is the peptide bound structure.

Universiti Malaya

RMSD value for the C-alpha backbone were calculated for 60 ns simulation for both AC001- and AC003- protein complex and are shown in **Figure 4.9**.

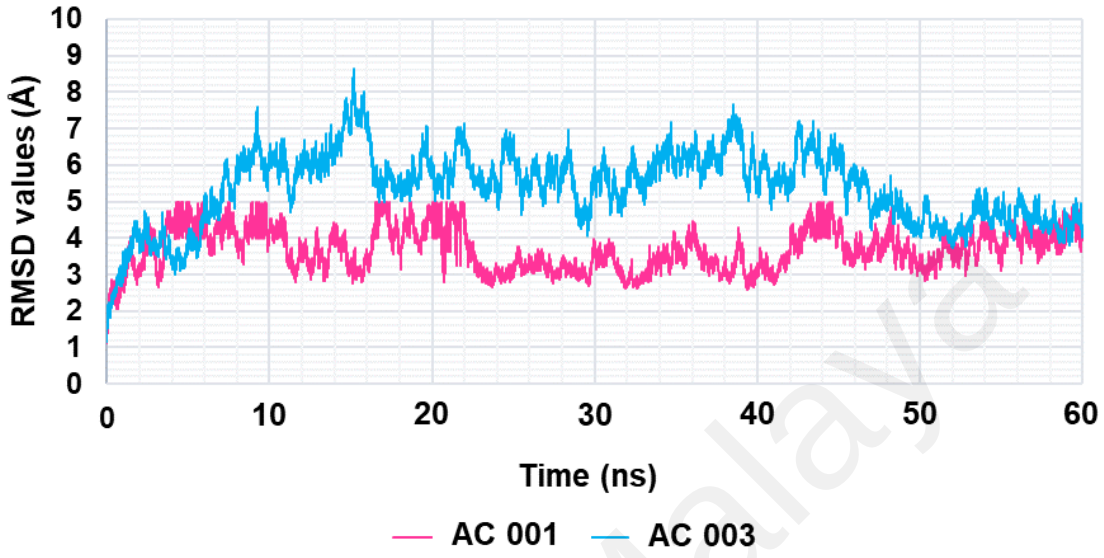

Figure 4.9: Plot of RMSD of all C_α-atoms of AC 001-protein complex (magneta) and AC 003-protein complex (Cyan) over 60 ns of simulation.

From the RMSD values, it was observed that AC 001-DV2 protein system (**Figure 4.9**, in magenta) displayed a sudden increase in the RMSD value of 4 Å with less fluctuation up to 4 ns. Besides, the system equilibration was obtained after 5 ns and remained stable after 10 ns at an average of 4.3 Å till the end of the simulation. On the contrary, the RMSD values of AC 003-protein system (**Figure 4.9**, in cyan) gradually increased to reach 8.0 Å. The system stabilized after 15 ns; however, fluctuations were visible over the course of simulation with the structure maintaining an RMSD value averaging 5.3 Å.

The analysis of RMSD trajectories showed that the AC 001-protein complex maintained an overall stability throughout 60 ns of simulation while the AC 003-protein complex displayed more fluctuations. The RMSD values suggests AC 001-protein complex to be more stable and undergoes lesser conformational changes within the simulated

Universiti Malaya

timescale. Moreover, peptide AC 001 has the ability remain intact in the protein binding pocket compared to AC 003. This may validate of AC 001 being a better antiviral towards DV2 and AC 003 being the least in inhibiting DV2.

In order to gain further insights into the dynamic stability of the binding, snapshots of the peptide-protein complex conformation of AC 001 at different timescales (0, 30, 60 ns) were extracted and superimposed (**Figure 4.10**). It was observed that AC 001 bound closer and remained in the binding site throughout the simulations, as compared to AC 003 which left the site shortly after simulation started (dynamics figure not shown).

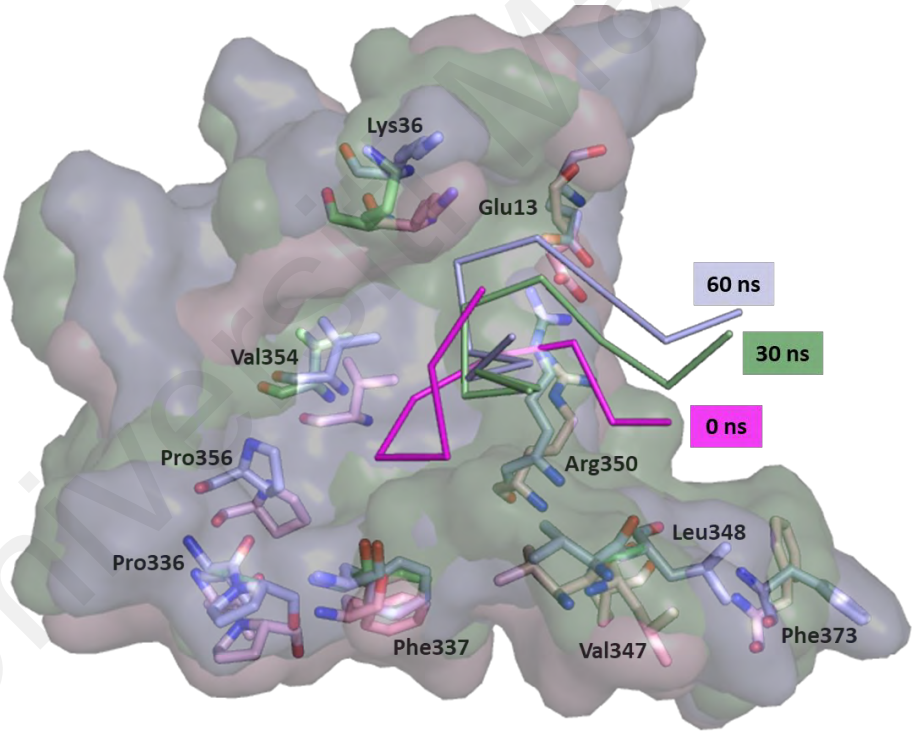

Figure 4.10: Superimposition of the AC 001-protein complexes during molecular dynamics simulations (pre- (0 ns), mid- (30 ns) and post- (60 ns) MD). Protein binding pocket is presented at different timescales as light blue surface at 0 ns, light green surface at 30 ns and light pink surface at 60 ns. AC 001 is shown as blue ribbon at 0 ns, green ribbon at 30 ns and magenta ribbon at 60 ns. Key amino acid residues surrounding the pocket are displayed. The figure was created using PyMOL.

University of Malaya

4.4.3 Hydrogen bonds analysis

Pairwise energy decomposition was calculated for AC 001 and AC 003-protein complexes to identify the main amino acids involved in the binding affinity. **Figure 4.11** shows the decomposed energies on a per residue basis for the peptide AC 001 and AC 003. The values indicated unfavorable and favorable contributions for the binding.

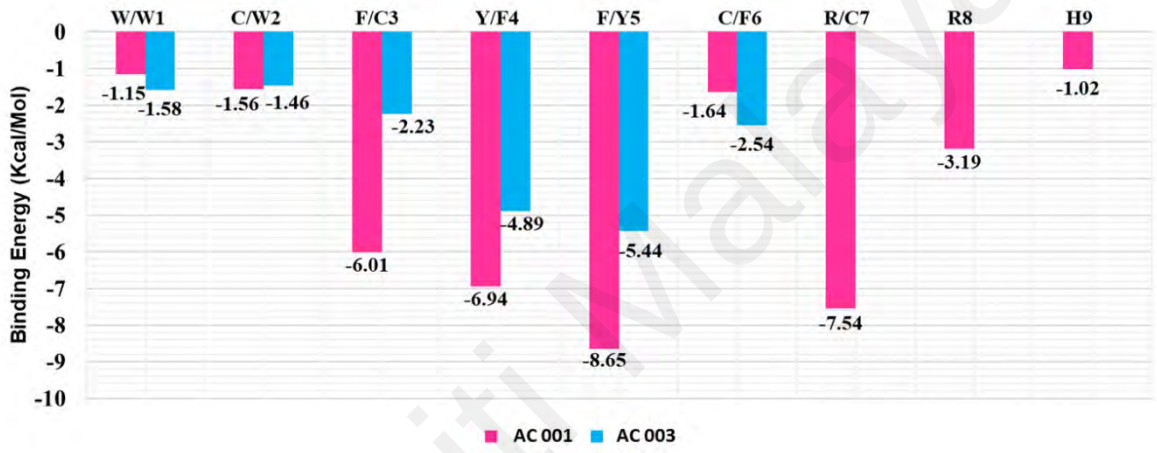

Figure 4.11: Decomposed binding free energy (kcal/mol) of AC 001 (magneta) and AC 003 (cyan) on a per-residue basis. All the residues of AC 001 contribute significantly to the binding.

All the residues of AC 001 peptide sequence are positively implicated in the binding, particularly, F3, Y4, F5, R7 and R8. The binding energy values were ranging from -7.54 kcal/mol to -6.01 kcal/mol. Among these peptide residues, F5 and R7 involved in stronger binding interaction with the lowest energy value of -8.65 kcal/mol and -7.54 kcal/mol respectively. After F5 and R7, F3 and Y4 contributed better binding interactions with the value of -6.94 and -6.01 respectively. Consequently, AC 001 has more residues involved in holding the peptide in binding pocket site via favorable peptide–protein interactions. By contrast, the residues of the peptide sequence AC 003 are contributing less to its interaction

Universiti Malaya

into the binding pocket, in the exception of F4 and Y5, thus affecting the stability of the complex. Therefore, justifying both the lower inhibition activity and the higher binding energy obtained (**Table 4.4**).

The per-residue decomposed binding energy of AC 001 and AC 003 permitted to highlight the overall importance of the FYF sequence in the peptide–protein interaction. Additionally, the R7 and R8 in AC 001 peptide sequence were also involved in the maintenance of the complex stability which the AC 003 do not have.

Further hydrogen bond analyses were carried out to highlight the protein key residues implicated in the binding and to understand the behavior of AC 001 in the binding site. **Figure 4.12** and **Figure 4.13** show the likely binding mode of AC 001 and AC 003, respectively, into the binding pocket before the stimulation starts.

Universiti Malaya

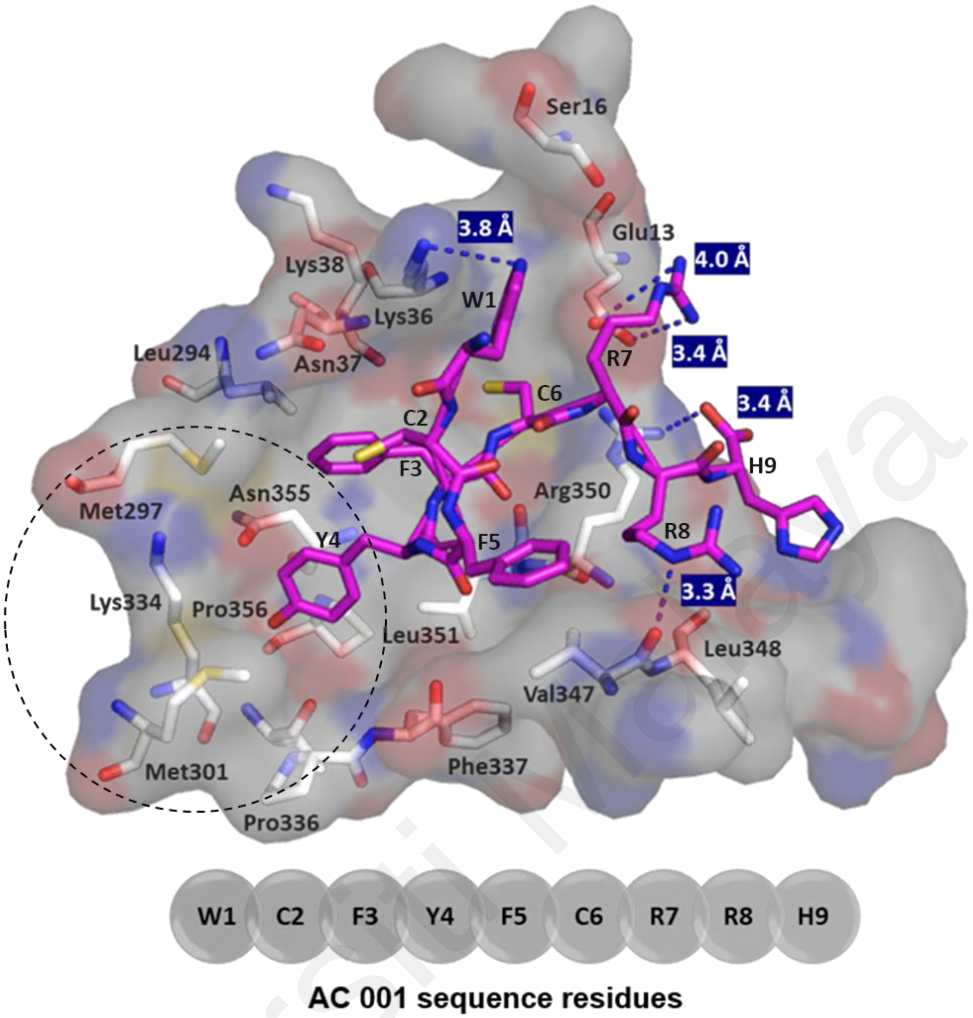

Figure 4.12: The plausible binding mode of AC 001 into the binding pocket. AC 001 residues are presented in a single-letter code while binding pocket key amino acids are shown in three letter codes. Hydrogen bonds are presented in blue dotted lines as well as their distance during MD simulations. Hydrophobic pocket is shown in dotted circle. The figure was created using PyMOL.

The hydrogen bond analysis of AC 001 prior to molecular dynamics simulations showed that the indole group of W1 is forming a hydrogen bond with the backbone of Lys36, while, the phenol ring of Y4 is housed into the hydrophobic cavity formed by Met301, Lys334, Phe337, Asn355 and Pro356. Not far by, the phenyl ring of F5 is accommodated at upper the surface formed by Asn37, Lys38, Leu294 and Met297. The imino and amino

groups of R7 are involved in 2 hydrogen bonds with the carbocylic acid of Glu13 while the NH group of R8 is formed a hydrogen bonding with the carbonyl group of Val347. Finally, H9 is observed to engage in a supplimentary hydrogen bonding with the backbone of Arg350 (**Figure 4.12**).

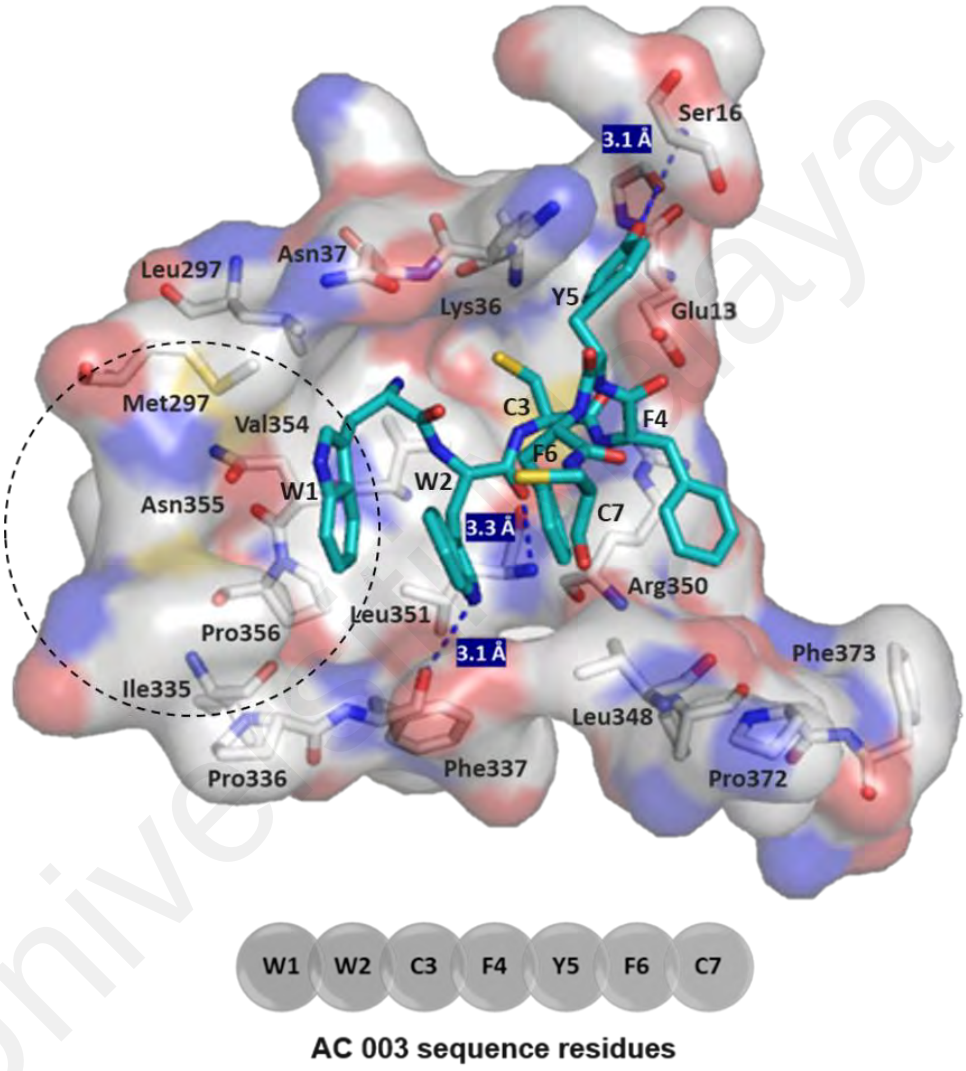

Figure 4.13: The plausible binding mode of AC 003 into the binding pocket. AC 003 residues are presented in a single-letter code while binding pocket key amino acids are shown in three letter codes. Hydrogen bonds are shown in blue dotted lines as well as their distance during MD simulations. Hydrophobic pocket is shown in dotted circle. The figure was created using PyMOL.

Universiti Malaya

Meanwhile, AC 003 displays four hydrogen bonds (**Figure 4.13**) with the binding site of the DV2 E protein. The oxygen of the phenol ring Y5 formed hydrogen bond with the backbone of Ser16 and Glu14 (not shown in **Figure 4.13**). In addition, the W2 indole-NH is hydrogen bonded to the oxygen of Phe337 while its oxygen formed another hydrogen bond with Leu351. W1 is accommodated into the hydrophobic pocket formed by Met297, Ile335, ASN355 and Pro356 and is involved in van der Waals interactions with Met301 and Asn37.

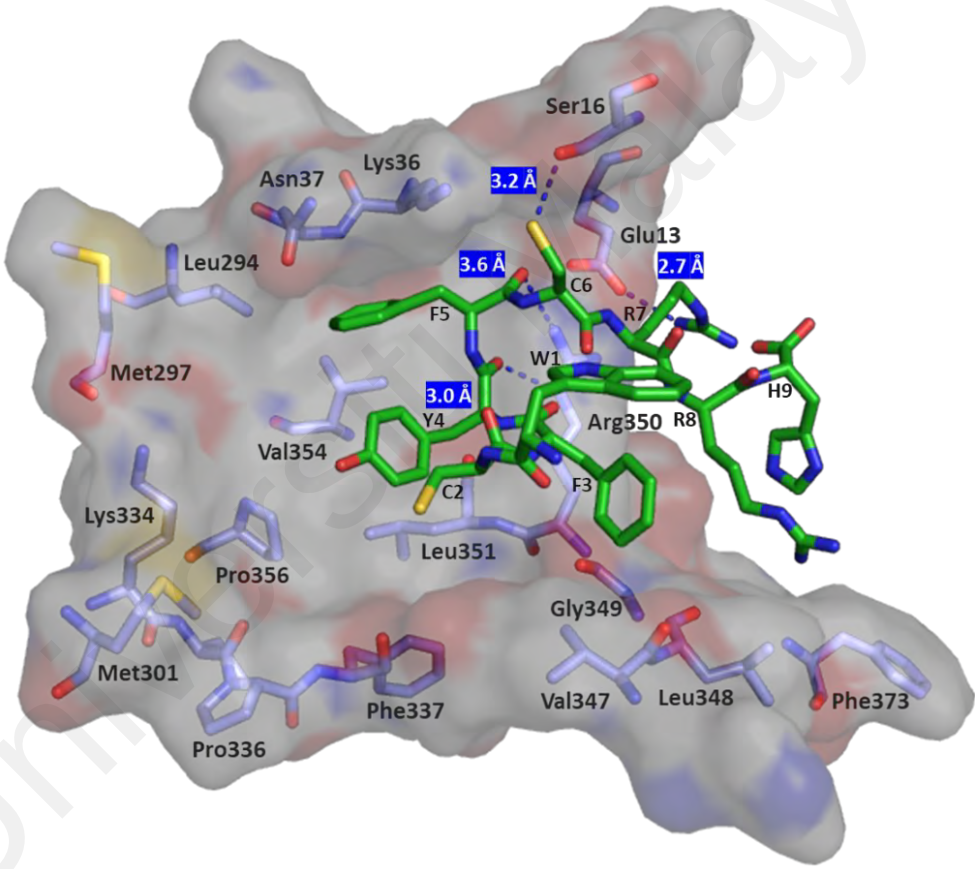

Figure 4.14: The plausible binding mode of AC 001 into the binding pocket post molecular dynamics simulations. Hydrogen bonds are showed by dotted lines as well as their distance during MD simulations. The figure was created using PyMOL.

Throughout the 60 ns molecular dynamics simulations, AC 001 remained stable and anchored on the upper and deeper in the protein binding pocket (**Figure 4.10**). **Figure 4.14**

illustrates AC 001 interactions with the binding pocket residues after dynamics simulations. It was observed that AC 001 key residue R7 amino group kept its hydrogen bond interaction with the carboxylic group of Glu13 while W2, R8 and H9, due to their upper and deeper shifting, having lost their hydrogen bonds with the backbones of Lys36, Val347 and Arg350 respectively compared to pre-MD stimulation structure (**Figure 4.12**).

On the contrary, Y4 and F5 have established hydrogen bonds through their hydroxyl group with Arg350. Moreover, the phenol group of Y4 and the phenyl group of F5 are projected into the hydrophobic pocket limited by Lys36, Asn37, Leu294, Val354, Pro356, Pro336 and Phe337, thus are involved in hydrophobic interactions. Additionally, a new hydrogen bond was observed between C6 and the backbone of Ser16 through its sulfur group after the MD stimulations (**Figure 4.14**).

This study proposed that these AC peptides were able to inhibit DV infection by blocking DV E protein, which plays a major role in viral host membrane fusion. This was analyzed by conducting plaque formation assay where the DV2 and AC peptide were pre-incubated before introducing to the Vero cells. Through the biological assay, it was noticed that AC 001 (inhibition % = 40.34% ± 5.9%) has the highest potential to reduce the viral infection compared to other four peptides while AC 003 being the least active towards DV2. The selected four AC peptide candidates out of 12 were chosen based on their binding possess and lower binding energy at the binding pocket of DV2 E protein. The molecular dynamic studies well supported the biological result obtained in **Figure 4.8**. AC 001 had the binding free energy value of -33.51 ± 5.11 kcal/mol **(Table 4.4)** which is the lowest energy among all, and this was justified by performing additional analysis for instance, system stability and flexibility and hydrogen bond analysis.

It is quite noticeable that AC 001 possess more stable peptide bound structure towards the binding pocket of DV2 as the RMSD value displayed less fluctuations and lowest value

Universiti Malaya

about 4.3Å on average throughout the 60 ns stimulations **(Figure 4.9)**. Furthermore, hydrogen bond analysis revealed that AC 001 has more residues which are contributing to stronger binding interactions towards DV binding site with lower binding energy values **(Figure 4.11).** Additionally, other interactions were also observed during the 60 ns stimulations such as van der Waals and hydrophobic interaction within the binding site.

Meanwhile, higher binding free energy **(Table 4.4)**, lack of interactions of peptide residues with protein binding site **(Figure 4.11)** and **(Figure 4.13)** and unstable conformations with more fluctuations in the RMSD values **(Figure 4.9)** were observed for AC 003 peptide. Due to this, it left the binding site shortly after stimulation started (dynamic figure not shown). These could be the reasons for AC 003 being least active compound towards DV2 **(Figure 4.8)**.

These results are supported by previous studies in which DET4 being the most active and DET2 for being least active peptide towards DV. The reason behind their respective activities towards DV were verified using computational approach. DET4 being the active peptide, reduced the plaque formation by 84.6% ± 5.6% with the binding energy value of - 39.85 ± 8.97 kcal/mol. Meanwhile, DET2 being the least active peptide reduced the plaque formation by 40.6% ± 24.8% with the binding energy value of - 19.51 ± 6.61 kcal/mol (Isa et al., 2019; Alhoot et al., 2013).

Besides that, there are several other peptide inhibitors were reported previously. The antiviral studies of peptides were initiated by Hrobowski et. al. (2005), who reported DN59, correspond to the stem domain of DV2 to confer an inhibition percentage of 93 ± 2% and IC_{50} value of 10µM which was analyzed via *in silico* and *in vitro* studies. This research was inspired by the human immunodeficiency virus (HIV) T20 drug which mimics part of the HIV's envelope protein to cater inhibition. Furthermore, DN57opt (Costin et al., 2010) and 1OAN1 (Costin et al., 2010), were discovered to be active peptides towards DV2 E protein.

Universiti Malaya

These two peptides showed higher inhibitory activity interfere by causing structural changes on dengue virion surface during virus-cell binding with IC_{50} value of 8μM and 7μM, respectively. Peptide $DV2^{419-447}$ (Schmidt et al., 2010) was derived from the stem of DV E protein, which models a conformational intermediate. This peptide showed an inhibitory activity against DV by binding specifically at the DV E protein at its trimeric post fusion conformation with the lowest K_d value of 150nM.

Additionally, peptide gg-ww (Chew et al., 2015), showed a promising outcome by having highest binding affinity towards DV2. Further biological studies were conducted to validate the obtained results in which, it was known to have antiviral activity with 96% inhibition rate with IC_{50} value of 77 $umol^{-1}$. To add on with, P4 and P7 peptides (Cui et al., 2018), were synthesized and screened towards DV2 E protein mainly at DIII region with IC_{50} values of 19.08 ± 2.52 μM and 12.86 ± 5.96 μM, respectively. Lately in 2019, three peptides (Pep 1, Pep 2, and Pep 3) (John et al., 2019) were designed, synthesized, and antiviral activity was evaluated towards all serotypes of DV. Pep 2 showed a higher inhibitory activity with IC_{50} value of below 20uM towards all DV serotypes compared to rest of them. Apart from these, EF (Panya et al., 2014) are LL-37 (Alagarasu et al., 2017) has also been reported as peptide inhibitors against DV.

However, compared to these known DV2 inhibitors, AC 001 showed moderate activity against DV2 E protein **(Figure 4.8)**. This could be due to the bulky side chains of R8, and H9 of AC 001 were hanging away from protein atoms which might cause a very high entropy cost that could have impact its binding adversely (as shown in **Figure 4.14**). These binding interaction studies between peptide and protein residues can be served as a knowledge for future peptide-based drug designing with desired qualities. Therefore, in summary for this work, molecular dynamic analysis seemed to correlate well with the

Universiti Malaya

biological results (**Figure 4.8**) as well as the docking results that was obtained earlier (**Table 4.2**) and **(Table 4.4)**.

Universiti Malaya

CHAPTER 5 CONCLUSION AND FUTURE STUDIES

5.1 Conclusion

In conclusion, based on the results obtained from biological assays and molecular dynamics, AC 001 showed the best inhibitory activity towards DV2 (inhibition % = 40.34% ± 5.9%), displayed a lower binding energy (-33.51 ± 5.11 kcal/mol) and determinate the key residues involved in the binding, mainly, Glu13, Arg350 and Leu351 for the protein and Y4, F5 and R7 for AC 001. Due to the presence of stronger protein-ligand interaction of AC 001 at the binding site, AC 001 gained more stability during the MD simulations and remained in the binding cavity throughout the 60 ns simulations. Overall, the correlation between computational and biological results supported our hypothesis in that the designed peptides target the DV2 E protein and permitted to identify the minimal peptide sequence required to inhibit DV2 replication. Herein, the findings of this study will be used for the development of future compounds.

5.2 Future studies

The active peptides and the parent sequence could be modified in terms of mutating the sequence, scramble the amino acid sequence and peptide cyclisation to study their antiviral activity towards DV. Besides that, a detailed computational study also can be done on the most active peptide candidate with different sequence to view the favorable interactions between the dengue protein and ligand.

Universiti Malaya

REFERENCES

Abe, T., Sando, A., Teraoka, F., Otsubo, T., Morita, K., Tokiwa, H., . . . Hidari, K. I. (2014). Computational design of a sulfoglucuronide derivative fitting into a hydrophobic pocket of dengue virus E protein. *Biochemical and Biophysical Research Communications, 449*(1), 32-37.

Aguilar, M. I. (2004). HPLC of Peptides and Proteins. *In HPLC of Peptides and Proteins* (pp. 3-8). Springer, Totowa, NJ.

Alagarasu, K., Patil, P. S., Shil, P., Seervi, M., Kakade, M. B., Tillu, H., & Salunke, A. (2017). In-vitro effect of human cathelicidin antimicrobial peptide LL-37 on dengue virus type 2. *Peptides, 92*, 23-30.

Alhoot, M. A., Rathinam, A. K., Wang, S. M., Manikam, R., & Sekaran, S. D. (2013). Inhibition of dengue virus entry into target cells using synthetic antiviral peptides. *International Journal of Medical Sciences, 10*(6), 719-729.

Amir-Hassan, A., Lee, V. S., Baharuddin, A., Othman, S., Xu, Y., Huang, M., . . . Othman, R. (2017). Conformational and energy evaluations of novel peptides binding to dengue virus envelope protein. *Journal of Molecular Graphics and Modelling, 74*, 273-287.

Antes, I. (2010). DynaDock: A new molecular dynamics-based algorithm for protein–peptide docking including receptor flexibility. *Proteins: Structure, Function, and Bioinformatics, 78*(5), 1084-1104.

Aoki-Utsubo, C., Chen, M., & Hotta, H. (2018). Time-of-addition and temperature-shift assays to determine particular step (s) in the viral life cycle that is blocked by antiviral substance (s). *Bio-protocol, 8*(9), Article#e2830.

Berman, H. M., Westbrook, J., Feng, Z., Gilliland, G., Bhat, T. N., Weissig, H., Shindyalov, I. N., & Bourne, P. E. (2000). The Protein Data bank. *Nucleic Acids Research, 28*(1), 235-242.

Bodenreider, C., Beer, D., Keller, T. H., Sonntag, S., Wen, D., Yap, L., . . . Zhou, T. (2009). A fluorescence quenching assay to discriminate between specific and nonspecific inhibitors of dengue virus protease. *Analytical Biochemistry, 395*(2), 195-204.

Universiti Malaya

Case, D. A., Babin, V., Berryman, J., Betz, R. M., Cai, Q., Cerutti, D. S. Cheatham III,.… Kollman, P. A. (2014). AMBER 14. University of California, San Fransisco.

Carolina De La Guardia , R. L. (2014). Progress in the Identification of Dengue Virus Entry/Fusion Inhibitors. *BioMed Research International*, *2014,* Article#825039.

Champagne, K., Shishido, A., & Root, M. J. J. J. o. B. C. (2009). Interactions of HIV-1 inhibitory peptide T20 with the gp41 N-HR coiled coil. *Journal of Biological Chemistry, 284*(6), 3619-3627.

Chen, Y., Maguire, T., Hileman, R. E., Fromm, J. R., Esko, J. D., Linhardt, R. J., & Marks, R. M. (1997). Dengue virus infectivity depends on envelope protein binding to target cell heparan sulfate. *Nature Medicine, 3*(8), 866-871.

Cheng, G., Liu, Y., Wang, P., & Xiao, X. (2016). Mosquito defense strategies against viral infection. *Trends in Parasitology, 32*(3), 177-186.

Chew, M.-F., Poh, K.-S., & Poh, C.-L. (2017). Peptides as therapeutic agents for dengue virus. *International Journal of Medical Sciences, 14*(13), 1342-1359.

Chew, M. F., Tham, H. W., Rajik, M., & Sharifah, S. (2015). Anti-dengue virus serotype 2 activity and mode of action of a novel peptide. *Journal of Applied Microbiology, 119*(4), 1170-1180.

Costin, J. M., Jenwitheesuk, E., Lok, S. M., Hunsperger, E., Conrads, K. A., Fontaine, K. A., . . . Michael, S. F. (2010). Structural optimization and de novo design of dengue virus entry inhibitory peptides. *PLoS Negected Tropical Disease, 4*(6), Article#e721.

Creighton, T. E. (1993). *Proteins: structures and molecular properties*. Macmillan.

Cui, X., Wu, Y., Fan, D., Gao, N., Ming, Y., Wang, P., & An, J. (2018). Peptides P4 and P7 derived from E protein inhibit entry of dengue virus serotype 2 via interacting with beta3 integrin. *Antiviral Res, 155*, 20-27.

Darden, T., York, D., & Pedersen, L. J. T. (1993). Particle mesh Ewald: An N log (N) method for Ewald sums in large systems. *The Journal of Chemical Physics, 98*(12), 10089–10092.

Darwish, N. T., Alias, Y. B., & Khor, S. M. (2015). An introduction to dengue-disease diagnostics. *TrAC Trends in Analytical Chemistry, 67*, 45-55.

Universiti Malaya

Dassault Systèmes BIOVIA, (2017) . Discovery Studio Modeling Environment, Release 2017. *Dassault Systèmes*; San Diego, CA, USA.

Davis, T. (2018, October 15). Amino acid usesin industry. *NEWS Medical*. Retreived from https://www.news-medical.net

DeLano, W.L. (2002). Pymol: An open-source molecular graphics tool. *CCP4 Newsletter On Protein Crystallography, 40*, 82-92.

de la Guardia, C., Quijada, M., & Lleonart, R. (2017). Phage-Displayed Peptides Selected to Bind Envelope Glycoprotein Show Antiviral Activity against Dengue Virus Serotype 2. *Advances in Virology*, *2017*, Article#1827341.

Drauz, Karlheinz; Grayson, Ian; Kleemann, Axel; Krimmer, Hans-Peter; Leuchtenberger, Wolfgang; Weckbecker, Christoph (2006). "Amino Acids". *Ullmann's Encyclopedia of Industrial Chemistry*. Weinheim: Wiley-VCH.

Dubey, K. D., Tiwari, G., & Ojha, R. P. (2017). Targeting domain-III hinging of dengue envelope (DENV-2) protein by MD simulations, docking and free energy calculations. *Journel of Molecular Modeling, 23*(4), 102.

El-Faham, A., & Albericio, F. (2011). Peptide coupling reagents, more than a letter soup. *Chemical Reviews*, *111*(11), 6557-6602.

Essman, U., Perera, L., Berkowitz, M., Darden, T., Lee, H., & Pedersen, L. J. J. C. P. (1995). A smooth particle mesh ewald potential. *The Journal of Chemical Physics*, *103*, 8577–8592.

Fuaad, A. A. A., Skwarczynski, M., & Toth, I. (2016). The use of microwave-assisted solid-phase peptide synthesis and click chemistry for the synthesis of vaccine candidates against hookworm infection. *Methods in Molecular Biology (Clifton, N.J.), 1403*, 639–653.

Fuaad, A. A. H. A., Pearson, M. S., Pickering, D. A., Becker, L., Zhao, G., Loukas, A. C., Skwarczynski, M., & Toth, I. (2015). Lipopeptide nanoparticles: Development of vaccines against hookworm Parasite. *ChemMedChem., 10*(10), 1647–1654.

Genheden, S., & Ryde, U. (2015). The MM/PBSA and MM/GBSA methods to estimate ligand-binding affinities. *Expert Opinion on Drug Discovery*, *10*(5), 449-461.

Universiti Malaya

Gotz, A. W., Williamson, M. J., Xu, D., Poole, D., Le Grand, S., & Walker, R. C. (2012). Routine microsecond molecular dynamics simulations with AMBER on GPUs. 1. Generalized born. *Journal of Chemical Theory and Computation, 8*(5), 1542–1555.

Fatima, K., & Syed, N. I. (2018). Dengvaxia controversy: impact on vaccine hesitancy. *Journal of Global Health, 8*(2).

Flipse, J., Wilschut, J., & Smit, J. M. (2013). Molecular Mechanisms Involved in Antibody-Dependent Enhancement of Dengue Virus Infection in Humans. *Traffic, 14*(1), 25-35.

Hassandarvish, P., Rothan, H. A., Rezaei, S., Yusof, R., Abubakar, S., & Zandi, K. (2016). In silico study on baicalein and baicalin as inhibitors of dengue virus replication. *RSC Advances, 6*(37), 31235-31247.

Hrobowski, Y. M., Garry, R. F., & Michael, S. F. (2005). Peptide inhibitors of dengue virus and West Nile virus infectivity. *Virology Journal, 2*(1), 1-10.

Huang, B. (2009). MetaPocket: a meta approach to improve protein ligand binding site prediction. *OMICS A Journal of Integrative Biology*, *13*(4), 325-330.

Isa, D. M., Chin, S. P., Chong, W. L., Zain, S. M., Rahman, N. A., & Lee, V. S. (2019). Dynamics and binding interactions of peptide inhibitors of dengue virus entry. *Journal of Biological Physics, 45*(1), 63-76.

Isidro-Llobet, A., Alvarez, M., & Albericio, F. (2009). Amino acid-protecting groups. *Chemical Reviews*, *109*(6), 2455-2504.

Ismail, N. A., & Jusoh, S. A. (2017). Molecular Docking and Molecular Dynamics Simulation Studies to Predict Flavonoid Binding on the Surface of DENV2 E Protein. *Journal-Interdisciplinary Sciences, 9*(4), 499-511.

Jadav, S. S., Kaptein, S., Timiri, A., De Burghgraeve, T., Badavath, V. N., Ganesan, R., . . . Jayaprakash, V. (2015). Design, synthesis, optimization and antiviral activity of a class of hybrid dengue virus E protein inhibitors. *Bioorganic & Medical Chemistry Letters, 25*(8), 1747-1752.

John, A. M., Jittmittraphap, A., Chattanadee, S., Anand, A. A. P., Shenbagarathai, R., & Leaungwutiwong, P. J. V. r. (2019). In vitro analysis of synthetic peptides in blocking the entry of dengue virus. *Virus Research, 260*, 142-150.

Universiti Malaya

Kampmann, T., Yennamalli, R., Campbell, P., Stoermer, M. J., Fairlie, D. P., Kobe, B., & Young, P. R. (2009). In silico screening of small molecule libraries using the dengue virus envelope E protein has identified compounds with antiviral activity against multiple flaviviruses. *Antiviral Research, 84*(3), 234-241.

Katzelnick, L. C., Coloma, J., & Harris, E. (2017). Dengue: knowledge gaps, unmet needs, and research priorities. *The Lancet Infectious Diseases, 17*(3), e88-e100.

Kaur, H., Garg, A., Raghava, G. J. P., & letters, p. (2007). PEPstr: a de novo method for tertiary structure prediction of small bioactive peptides. *Protein & Peptide Letters, 14*(7), 626-631.

Keramagi, A. R., & Skariyachan, S. (2018). Prediction of binding potential of natural leads against the prioritized drug targets of chikungunya and dengue viruses by computational screening. *3 Biotech, 8*(6), Article#274.

Kim, S. J., & McAlpine, S. R. (2013). Solid phase versus solution phase synthesis of heterocyclic macrocycles. *Molecules*, *18*(1), 1111-1121.

Kreutzer, A. G., Salveson, P. J., & Yang, H. (2018). *Standard Practices for Fmoc-Based Solid-Phase Peptide Synthesis in the Nowick Laboratory* (Version 1.6. 3).

Kumar, A. P., & Lukman, S. (2018). Allosteric binding sites in Rab11 for potential drug candidates. *PLoS One, 13*(6), Article#e0198632.

Law, R. J., Capener, C., Baaden, M., Bond, P. J., Campbell, J., Patargias, G., . . . Modelling. (2005). Membrane protein structure quality in molecular dynamics simulation. *Journal of Molecular Graphics and Modelling, 24*(2), 157-165.

Leal, E. S., Aucar, M. G., Gebhard, L. G., Iglesias, N. G., Pascual, M. J., Casal, J. J., . . . Bollini, M. (2017). Discovery of novel dengue virus entry inhibitors via a structure-based approach. *Bioorg Med Chem Lett, 27*(16), 3851-3855.

Lee, A. C.-L., Harris, J. L., Khanna, K. K., & Hong, J.-H. (2019). A comprehensive review on current advances in peptide drug development and design. *International Journal of Molecular Sciences, 20*(10), Article#2383.

Ieronymaki, M., Androutsou, M. E., Pantelia, A., Friligou, I., Crisp, M., High, K., ... & Tselios, T. (2015). Use of the 2-chlorotrityl chloride resin for microwave-assisted solid phase peptide synthesis. *Peptide Science*, *104*(5), 506-514.

Universiti Malaya

Lescar, J., Luo, D., Xu, T., Sampath, A., Lim, S. P., Canard, B., & Vasudevan, S. G. (2008). Towards the design of antiviral inhibitors against flaviviruses: the case for the multifunctional NS3 protein from Dengue virus as a target. *Antiviral Research, 80*(2), 94-101.

Leung, D., Schroder, K., White, H., Fang, N. X., Stoermer, M. J., Abbenante, G., . . . Fairlie, D. P. (2001). Activity of recombinant dengue 2 virus NS3 protease in the presence of a truncated NS2B co-factor, small peptide substrates, and inhibitors. *Journal of Biological Chemistry, 276*(49), 45762-45771.

Lukszo, J., Patterson, D., Albericio, F., & Kates, S. A. (1996). 3-(1-Piperidinyl) alanine formation during the preparation ofC-terminal cysteine peptides with the Fmoc/t-Bu strategy. *Letters in Peptide Science, 3*(3), 157-166.

Meng, X.-Y., Zhang, H.-X., Mezei, M., & Cui, M. (2011). Molecular docking: a powerful approach for structure-based drug discovery. *Current Computer-aided Drug Design, 7*(2), 146-157.

Merrifield, R. B. (1963). Solid phase peptide synthesis. I. The synthesis of a tetrapeptide. *Journal of the American Chemical Society*, *85*(14), 2149-2154.

Miceli, L. A., Teixeira, V. L., Castro, H. C., Rodrigues, C. R., Mello, J. F., Albuquerque, M. G., . . . De Souza, A. M. (2013). Molecular docking studies of marine diterpenes as inhibitors of wild-type and mutants HIV-1 reverse transcriptase. *Marine drugs, 11*(11), 4127-4143.

Mir, A., Ismatullah, H., Rauf, S., & Niazi, U. H. (2016). Identification of bioflavonoid as fusion inhibitor of dengue virus using molecular docking approach. *Informatics in Medicine Unlocked, 3*, 1-6.

Modis, Y., Ogata, S., Clements, D., & Harrison, S. C. (2003). A ligand-binding pocket in the dengue virus envelope glycoprotein. *Proc Natl Acad Sci U S A, 100*(12), 6986-6991.

Mondotte, J. A., Lozach, P.-Y., Amara, A., & Gamarnik, A. V. (2007). Essential Role of Dengue Virus Envelope Protein N Glycosylation at Asparagine-67 during Viral Propagation. *Journal of Virology, 81*(13), 7136-7148.

Mustafa, M., Rasotgi, V., Jain, S., & Gupta, V. J. M. J. A. F. I. (2015). Discovery of fifth serotype of dengue virus (DENV-5): A new public health dilemma in dengue control. *Medical Journal Arned Forces India, 71*(1), 67-70.

Universiti Malaya

Nelson, D. L., & Cox, M. M. (2005). *Lehninger's principles of biochemistry*. Revised edition, 21-45.

Noble, C. G. (2010). Strategies for development of dengue virus inhibitors. *Anitiviral Research, 85*, 450-462.

Okamoto, T., Suzuki, T., Kusakabe, S., Tokunaga, M., Hirano, J., Miyata, Y., & Matsuura, Y. (2017). Regulation of apoptosis during flavivirus infection. *Viruses, 9*(9), Article#243.

Palomo, J. M. (2014). Solid-phase peptide synthesis: an overview focused on the preparation of biologically relevant peptides. *The Royal Society of Chemistry Advances*, *4*(62), 32658-32672.

Panya, A., Bangphoomi, K., Choowongkomon, K., & Yenchitsomanus, P. T. (2014). Peptide inhibitors against dengue virus infection. *Chemical Biology & Drug Design, 84*(2), 148-157.

Poh, M. K., Yip, A., Zhang, S., Priestle, J. P., Ma, N. L., Smit, J. M., . . . Schul, W. (2009). A small molecule fusion inhibitor of dengue virus. *Antiviral Res, 84*(3), 260-266.

Popova, N., Deyev, I., & Petrenko, A. (2013). Clathrin-mediated endocytosis and adaptor proteins. *Acta Naturae, 5*(3), 62-73.

Prusis, P. (2013). Design and evaluation of substrate-based octapeptide and non substrate-based tetrapeptide inhibitors of dengue virus NS2B–NS3 proteases. *Biochemical and Biophysical Research Communications, 434*, 767-772.

Rey, F. A., Stiasny, K., Vaney, M. C., Dellarole, M., & Heinz, F. X. J. E. r. (2018). The bright and the dark side of human antibody responses to flaviviruses: lessons for vaccine design. *EMBO Reports, 19*(2), 206-224.

Roe, D. R., & Cheatham III, T. E. (2013). PTRAJ and CPPTRAJ: software for processing and analysis of molecular dynamics trajectory data. Journal of chemical theory and *computation*, *9*(7), 3084-3095.

Rothan, H. A., Bahrani, H., Mohamed, Z., Teoh, T. C., Shankar, E. M., Rahman, N. A., & Yusof, R. (2015). A combination of doxycycline and ribavirin alleviated chikungunya infection. *PLoS One*, *10*(5), Article#e0126360.

Universiti Malaya

Salazar, M. I., del Angel, R. M., Lanz-Mendoza, H., Ludert, J. E., & Pando-Robles, V. (2014). The role of cell proteins in dengue virus infection. *Journal of proteomics, 111*, 6-15.

Schmidt, A. G., Lee, K., Yang, P. L., & Harrison, S. C. (2012). Small-molecule inhibitors of dengue-virus entry. *PLoS Pathog, 8*(4), Article#e1002627.

Schmidt, A. G., Yang, P. L., & Harrison, S. C. (2010). Peptide inhibitors of dengue-virus entry target a late-stage fusion intermediate. *PLoS Pathog, 6*(4), Article#e1000851.

Screaton, G., Mongkolsapaya, J., Yacoub, S., & Roberts, C. (2015). New insights into the immunopathology and control of dengue virus infection. *Nature Reviews Immunology, 15*(12), 745-759.

Srivarangkul, P., Yuttithamnon, W., Suroengrit, A., Pankaew, S., Hengphasatporn, K., Rungrotmongkol, T., . . . Boonyasuppayakorn, S. (2018). A novel flavanone derivative inhibits dengue virus fusion and infectivity. *Antiviral Research, 151*, 27-38.

Synthesis of Amino Acids. (2020, August 11). Retrieved June 30, 2021, from https://chem.libretexts.org/@go/page/36469.

Tambunan, U. S., Zahroh, H., Parikesit, A. A., Idrus, S., & Kerami, D. J. D. t. i. (2015). Screening analogs of β-OG pocket binder as fusion inhibitor of dengue virus 2. *Drug Target Insights, 9*, 33-39.

Te, H. S., Randall, G., & Jensen, D. M. (2007). Mechanism of action of ribavirin in the treatment of chronic hepatitis C. *Gastroenterology & Hepatology, 3*(3), 218-225.

Tomlinson, S. M., & Watowich, S. J. (2011). Anthracene-based inhibitors of dengue virus NS2B–NS3 protease. *Antiviral Research, 89*(2), 127-135.

Tourdot, R. R. R. (2013). Clathrin Mediated Endocytosis, its Role in Viral Entry. *Atlas Genet Cytogenet Oncol Haematol, 17*(8), 583-588.

Trott, O., & Olson, A. J. (2010). AutoDock Vina: improving the speed and accuracy of docking with a new scoring function, efficient optimization, and multithreading. *Journal of Computational Chemistry, 31*(2), 455-461.

Universiti Malaya

Valderrama, A., Díaz, Y., & López-Vergès, S. (2017). Interaction of Flavivirus with their mosquito vectors and their impact on the human health in the Americas. *Biochemical and Biophysical Research Communications, 492*(4), 541-547.

Wang, Q.-Y. (2008). A Small-Molecule Dengue Virus Entry Inhibitor. *Antimicrobial Agents and Chemotheraphy, 53*(5), 1823-1831.

Ward, T., Samuel, M., Maoz, D., Runge-Ranzinger, S., Boyce, R., Toledo, J., . . . Horstick, O. (2017). Dengue data and surveillance in Tanzania: A systematic literature review. *Tropical Medicine & International Health, 22*(8), 960-970.

WHO. (2019). Dengue and Severe dengue. Retrieved from https://www.who.int/news-room/fact-sheets/detail/dengue-and-severe-dengue.

Xu, Y., Rahman, N. A., Othman, R., Hu, P., & Huang, M. (2012). Computational identification of self-inhibitory peptides from envelope proteins. *Proteins, 80*(9), 2154-2168.

Yang, J. M., Chen, Y. F., Tu, Y. Y., Yen, K. R., & Yang, Y. L. (2007). Combinatorial computational approaches to identify tetracycline derivatives as flavivirus inhibitors. *PLoS One, 2*(5), Article#e428.

Yang, T., Li, H., Tai, Y. et al. (2020). Transcriptional regulation of amino acid metabolism in response to nitrogen deficiency and nitrogen forms in tea plant root (Camellia sinensis L.). *Scientific Reports 10*, Article#6868.

Yennamalli, R., Subbarao, N., Kampmann, T., McGeary, R. P., Young, P. R., & Kobe, B. (2009). Identification of novel target sites and an inhibitor of the dengue virus E protein. *Journal of Computer- Aided Molecular Design, 23*(6), 333-341.

Young V.R. (2000) Protein and Amino Acids. In: Gershwin M.E., German J.B., Keen C.L. (Eds.), *Nutrition and Immunology* (pp. 49-64). Humana Press, Totowa, NJ.

Zhou, Z., Khaliq, M., Suk, J.-E., Patkar, C., Li, L., Kuhn, R. J., & Post, C. B. J. A. c. b. (2008). Antiviral Compounds Discovered by Virtual Screening of Small− Molecule Libraries against Dengue Virus E Protein. *ACS Chemical Biology, 3*(12), 765-775.

Zhang, Z., Li, Y., Lin, B., Schroeder, M., & Huang, B. (2011). Identification of cavities on protein surface using multiple computational approaches for drug binding site prediction. *Bioinformatics*, *27*(15), 2083-2088.

Universiti Malaya

LIST OF PUBLICATIONS AND PAPERS PRESENTED

List of publications

1. **Arumugam, A. C.**, Agharbaoui, F. E., Khazali, A. S., Yusof, R., Abd Rahman, N., & Ahmad Fuaad, A. A. H. (2020). Computational-aided design: minimal peptide sequence to block dengue virus transmission into cells. *Journal of Biomolecular Structure and Dynamics*, 1-10.

Papers presented

1. **Arumugam, A. C.**, Agharbaoui, F. E., Khazali, A. S., Yusof, R., Abd Rahman, N., & Ahmad Fuaad, A. A. H. (2018). *Design and synthesis of peptides as Dengue Envelope Protein inhibitors.* Paper presented at the ASEAN Emerging Researchers Conference, 3-4 December 2018, Sunway University, Selangor, Malaysia.

Universiti Malaya